I.O.S.

SIZEWELL-DUNWICH BANKS FIELD STUDY
TOPIC REPORT 4

A D HEATHERSHAW and B J LEES

Tidal currents: observed tidal and residual circulations

Report No 104

1980

NATURAL ENVIRONMENT RESEARCH COUNCIL

INSTITUTE OF OCEANOGRAPHIC SCIENCES

INSTITUTE OF OCEANOGRAPHIC SCIENCES

Wormley, Godalming,
Surrey, GU8 5UB.
(0428 - 79 - 4141)

(Director: Dr. A.S. Laughton)

Bidston Observatory,
Birkenhead,
Merseyside, L43 7RA.
(051 - 653 - 8633)

(Assistant Director: Dr. D.E. Cartwright)

Crossway,
Taunton,
Somerset, TA1 2DW.
(0823 - 86211)

(Assistant Director: M.J. Tucker)

SIZEWELL-DUNWICH BANKS FIELD STUDY

TOPIC REPORT 4

A D HEATHERSHAW and B J LEES

Tidal currents: Observed tidal and residual circulations

Report No 104

1980

This project was supported financially by the Department of the Environment

Institute of Oceanographic Sciences
Crossway
Taunton
Somerset

CONTENTS

SUMMARY

This is the fourth in the Topic Report series concerning the Sizewell-Dunwich Bank area.

Recording current meter data, tidal elevations and meteorological data have been used to examine the tidal and residual circulations in the area and their response to meteorological forcing.

Current meter data have confirmed that the tidal currents are essentially rectilinear with ellipticities of the order of 5% and less and with tidal stream maxima of the order of 100 cm s^{-1}.

The residual flow pattern in the area is complex although there is evidence of an anti-clockwise eddy in the mean circulation, which is situated over the Sizewell Bank and possibly extends to cover the Dunwich Bank. Current measurements from a long term current meter mooring have confirmed that the residual circulation is likely to be influenced by meteorological forcing. In particular the alongshore component of the residual flow and wind stress are well correlated during storm periods.

Analysis of current meter and tidal elevation data has shown that the tides in this area may be considered as a mixture of standing wave and progressive wave oscillations, consistent with the proximity of the study area to an amphidrome. For both the M_2 and S_2 tides the standing wave component is dominant.

1 INTRODUCTION

The primary objective of the present study (Lees, 1980a) has been to investigate nearshore sediment transport processes in the Sizewell–Dunwich Bank area off the East Anglian coast of the British Isles (Figure 1). These investigations parallel those of a similar study carried out in the Swansea Bay area of the Bristol Channel (Heathershaw and Hammond, 1979).

Sediment is moved by tidal currents and to a lesser extent by the oscillatory currents and mass transport effects due to surface gravity waves. The object of this report is to describe the tidal and residual current circulation patterns in the Sizewell–Dunwich Bank area and in particular to determine the role they play in transporting sediment. However a complete description of the current system in the area should include a consideration of wind driven currents and surge currents. Therefore the effects of meteorological forcing on the water circulation are also evaluated.

The tidal dynamics of the Sizewell–Dunwich Bank area are essentially those of the southern North Sea with flow patterns and magnitudes being influenced by bathymetry and coastline geometry. It is beyond the scope of this report to review in full the physical oceanography of this area and reference should therefore be made to the work of Proudman and Doodson (1924), Kagan (1966), Lee and Ramster (1968), Pitt et al (1973) and the Admiralty Tidal Stream Atlas, North Sea, Southern Portion (1976). More detailed accounts of recent work are given in Nihoul (1975), Caston (1976), Maier-Reimer (1977), McCave (1979) and in the Sizewell area in particular by Macqueen and Parker (1979).

The area under study is characterised by a low tidal range (springs 1.9 m neaps 1.1 m) and maximum surface currents of the order of 100 cm s^{-1}. The seabed slopes gently from the shore to a depth of 15 m below Chart Datum over a distance of 5 km. It comprises alluvial clay in the N and shelly sands in the S, with the mainly fine to very fine sand of the Sizewell–Dunwich Bank lying on this platform, parallel to the coastline.

2 THEORETICAL CONSIDERATIONS

2.1 Tidal dynamics

The tides in the North Sea are dominated by the principal lunar (M_2) tide which enters the area from the North Atlantic (Figure 2) and is reflected from the coasts as it propagates southwards. In the absence of coastlines or variable seafloor topography the tide would travel as a progressive wave at a speed determined by the earth's rotation and the latitude. The surface elevation of

such a wave is in phase with the current, so that maximum current velocities occur at the times of maximum or minimum elevations. However, the North Sea is effectively closed at its southern end and the resulting standing wave pattern of tides is modified by the earth's rotation to produce a series of amphidromic points, the southernmost of which is shown in Figure 2. At an amphidrome the tidal range is zero. In a standing wave the elevation and current are 90° out of phase, that is the current is zero at the times of maximum and minimum elevation.

The Sizewell-Dunwich tidal pattern lies between these two extremes and slack water, or more accurately the turn of the tide, occurs typically 1.0-1.5 hours after high and low waters, an approximate phase difference of 30°-45°. Thus the tidal wave is a combination of both progressive and standing forms and the aim of part of the work has been to separate and quantify these two components.

2.2 Meteorological forcing

Meteorological factors may affect the water circulation in two ways:

(a) directly by the application of a wind stress to the sea's surface, leading to a surface drift, and

(b) indirectly from changes in sea level which may occur as a result of the wind piling up water against a coast, or as a result of changes in atmospheric pressure.

A useful parameter for determining the response of the water column to an applied wind stress is the depth of frictional influence D, given by

$$D = \pi \left(\frac{2 N_z}{f} \right)^{\frac{1}{2}} \qquad (1)$$

where N_z is the vertical eddy viscosity coefficient and f is the Coriolis parameter. In particular the ratio h/D, where h is the water depth, is useful in determining how much of the water column is likely to be influenced by the wind. The depth of frictional influence (Heathershaw and Hammond, 1979) is that depth at which for most practical purposes the wind driven current has fallen to an insignificant level (about 5% of its value at the surface). Heathershaw and Hammond have found that in the Swansea Bay area of the Bristol Channel ($h \simeq$ 20m) the ratio h/D, for representative values of N_z, approaches unity at wind speeds of the order 8-10 m s^{-1}. These figures may be applied to the Sizewell-Dunwich Bank area, the difference in latitude giving rise to an error in D of the order of 1% and less, which is probably much less than the error in D due to the uncertainty in N_z.

For the Swansea Bay area ($h \simeq$ 20m) Heathershaw and Hammond have shown that

wind driven currents near the surface may be as large as 10 cm s^{-1} at wind speeds of 20 m s^{-1} and for the generally shallower waters of the Sizewell–Dunwich Bank area wind driven currents are likely to be of this order and will probably have a more pronounced effect throughout the water column.

Where a wind driven current impinges on a coast the resultant current system is modified by the presence of slope currents which occur as a result of the wind piling up water against the coast leading to horizontal pressure gradients and seaward flowing (slope) currents near the seabed. For water depths of 20 m and wind speeds of 20 m s^{-1} the slope currents are typically 5 cm s^{-1} (Heathershaw and Hammond, 1979). The exact values of both the wind driven currents and the slope currents are critically dependent upon the choice of a suitable eddy viscosity (N_z) parameterisation, which, for combinations of flow in wind driven shear layers and tidal currents, is by no means clear.

The term 'storm surge' applies to a raising or lowering of sea level produced by the wind, and by changes in atmospheric pressure over the sea associated with a storm. The precise combination of meteorological conditions which leads to the occurrence of a storm surge in the North Sea have been described elsewhere (eg Heaps, 1967). Suffice it to say that in general when a depression moves over a sea area there is usually a rise in sea level followed by a fall. However, the change in sea level at any one location may be due partly to changes in atmospheric pressure and partly due to the action of the wind on the sea's surface. The change in sea level Δz due to a change in pressure is given by the statical law

$$\Delta z = \Delta p_a / \rho g \qquad (2)$$

where Δp_a is the change in atmospheric pressure p_a relative to some ambient level, ρ the fluid density and g the acceleration due to gravity. A decrease in atmospheric pressure of one millibar leads to an increase in sea level of approximately one centimetre (this effect being known as the inverted barometer effect). The change in sea level due to wind piling up water against a coast is given by

$$\Delta z = \frac{M \tau}{\rho g h} \Delta x \qquad (3)$$

where M is a coefficient which decreases with increasing depth from 3/2 to 1, and τ is the wind stress resulting from a steady wind blowing over a distance Δx in an enclosed sea (Heathershaw and Hammond, 1979).

When a depression is particularly small, deep, and fast moving, changes in sea level due to the pressure effect (Equation 2) are generally small when compared with the changes which are brought about by wind stress (Equation 3). In general a raising of sea level by wind stress and/or pressure effects is usually referred to as a positive surge whereas a decrease is referred to as a negative surge. Where these effects are due to wind stress alone they may also be called 'set up' or 'set down' respectively.

In a later section of this report we present direct evidence of the effect of wind driven currents and storm surges on the circulation and sea level in the Sizewell–Dunwich Bank area.

3 METHODS AND OBSERVATIONS

Recording current meter observations were carried out in the Sizewell–Dunwich Bank area (Figure 3) between February 1975 and April 1979. The criteria for locating the current meters were to some extent determined by the requirements of a finite difference numerical model (Lees, 1980a), the aims of which were firstly to model the water circulation and secondly, at a later stage, to incorporate terms which would enable prediction of sediment movement to be made.

The water flow model uses depth averaged equations of motion (Heaps, 1978) which, in this particular case, required mid–depth current measurements for calibration. The bulk of the current measurements described in this report have, therefore, been made at mid–depth using Aanderaa (Figure 4) and Plessey (Figure 5) recording current meters mounted on conventional 'U'–shape moorings (Figure 6). The exact relationship between mid–depth and depth–mean currents could be examined using velocity profile data obtained from the Marconi current meter system (Figure 7) which was located just inshore of the Banks from 5–7 September 1976 (Figure 3). Soulsby (1978) has also examined the errors which are introduced into sediment transport predictions by the use of depth averaged equations. These and other aspects of the Marconi current meter data are discussed later.

The locations at which current measurements were made (Figure 3) were therefore chosen to provide as much useful information as possible on the water circulation pattern, both for the model and for later sediment transport studies.

The earliest measurements (1975) were made with Aanderaa recording current meters at stations B, L, R and T (Figure 3). However, due to the Savonius rotor's (Figure 4) poor response in shallow wave influenced tidal flows (McCullough, 1977), the succeeding measurements were all made with Plessey current meters. The

mid-depth levels were typically 5-6 m above the seabed.

Details of the locations, instrument types, elevations, record dates and durations are given in Table 1. One current meter location (Station A, Figure 3) was occupied continuously for 32 months by changing the mooring every 2 months. Unfortunately, one of the few meter losses during the study occurred during the major storm surge of February 1979. However, data are available for the smaller surges which occurred during the study period. The remaining stations were occupied for periods ranging from 2 weeks in 1975 and 1976 to 2 months in 1977 and 1978. In all cases current speed and direction were recorded every 10 minutes.

Approximately 23,766 hours of useful recording current meter data have been collected and analysed and these, together with tidal elevation data supplied by the Institute of Oceanographic Sciences, Bidston, and meteorological data supplied by the Meteorological Office, form the basis of this report.

4 TIDAL CURRENTS

4.1 Harmonic analysis

In order to examine the tidal dynamics of the Sizewell-Dunwich area, and in particular the phase relationship between currents and elevations, current meter records were harmonically analysed using the IOS Bidston computer program TIRA (Tidal Institute Recursive Analysis). This program, which employs a least squares regression technique, was used to analyse, where possible, 29 day data sets, the optimum length for separating the tidal constituents (Doodson, 1928), to produce information on the amplitudes and phases of the tidal constituents in current meter records. As only 11 records proved to be of adequate length and quality, further analyses were carried out on 13-15 day data sets, similar to work undertaken by Robinson (1979), but the results from these should be treated with some caution.

The 29 day records were analysed for 26 major plus 8 related constituents (Table 2). The related constituents are those which cannot be separated in a 29 day record. For the 13-15 day records there were 16 major plus 14 related constituents (Table 3), the latter taken from a Lowestoft data analysis carried out by IOS Bidston. They had been used successfully by Vassie for a similar type of analysis in the area (personal communication).

Edited current meter records with timing adjusted to GMT were corrected for any timing errors. These are indicated in Table 4, and were made by a linear interpolation procedure which amounts to stretching or contracting the record to fit the relevant optimum 29 or 13-15 day period.

The results of the harmonic analyses of the current meter data are shown in Tables 5 and 6. At Station A (Figure 3), the long term mooring where 7 29-day and 3 shorter records suitable for analysis with TIRA were obtained, it has been possible to examine the variability of the amplitude and phase estimates. Thus in Table 5 the means, standard deviations and standard errors of the amplitude and phase values are given for the principal tidal constituents in the resolved N-S and E-W components of the currents. At the remaining stations where fewer records were available, the amplitude and phase values for the principal semi-diurnal constituents (M_2 and S_2) only are given. These results are shown in Table 6.

The amplitudes and phases of the same constituents in the elevations at Lowestoft are also shown in Table 7. These were obtained from an analysis of 1 year's records centred on 1 July 1965 and carried out by IOS Bidston.

Comparison of the amplitudes and phases of the M_2 tidal constituents, shown in Tables 5-7, show a phase difference of about 125° between elevations and currents which confirms that the wave is a combination of progressive and standing components, as discussed above.

4.2 Rotary analysis

The amplitude and phase of the principal tidal constituents in the measured currents, resolved into N-S and E-W components, have been used to construct tidal ellipses using a rotary analysis method (Gonella, 1972, Godin, 1972) which is described in full in Heathershaw and Hammond (1979). These analyses give the orientation of the ellipse, its semi-major and semi-minor axes, (a and b respectively), and the phase of current vector describing the ellipse.

Typical tidal ellipse characteristics from Station A are shown in Figures 8a and 8b. Figure 8a shows the semi-diurnal constituents, M_2, S_2, N_2 and K_2 and Figure 8b the quarter diurnal constituents M_4 and MS_4. These diagrams give a good indication of the rectilinearity of the currents, with M_2 ellipticities, ie the ratio b/a expressed as a percentage, of the order of 5% or less. Figures 9a and 9b summarise the M_2 tidal ellipse data for the mid-depth currents in the area. In particular Figure 9a shows the phase lags in degrees, relative to the equilibrium tide at Greenwich, and the ellipse orientations. The arrows indicate the directions of maximum tidal streaming corresponding to the given phases. For comparison, phase information at similar locations is also shown in Figure 10. This is for the N-S component of the M_2 tidal current only and is taken from Macqueen and Parker (1979). Figure 9b shows the amplitudes of the M_2 tidal currents and their ellipticity, at each location. The amplitudes are in general less in the shallower water towards the coast and on the Banks and the phase lags are also

less in shallow water indicating that maximum tidal streaming occurs earlier near the coast and on the Banks where the effects of bottom friction are more pronounced. These features are consistent with the findings of Macqueen and Parker (1979).

Over the area as a whole it has been found that the M_2 and S_2 currents rotate in an anticlockwise direction similar to those at the Inner Dowsing (Pugh and Vassie, 1976) with clockwise rotation at two of the most southerly stations only (Figure 9b).

4.3 Non-linear effects

Heathershaw and Hammond (1979) have examined the effects of the non-linear terms in the equations of motion for the tidal currents in Swansea Bay. Their results show that in general the contribution from higher harmonics due to non-linear effects, in particular the M_4 tidal constituent, increases in the shallower water towards the coast. On an exposed, near-linear coastline such as that of the Sizewell-Dunwich Bank area the effects are not expected to be as apparent. Shallowing of the water nearshore and on the banks reduces the amplitudes of the M_2, S_2 and M_4, although there is no consistent pattern shown by the M_4/M_2 amplitude ratio (Figure 11a).

The distribution of currents over the neap-spring cycle can also be deduced from the tidal ellipse information. Since sediment transport varies at high transport rates as u_*^3 where u_* is the friction velocity, and tidal mixing as u_o^3/h where u_o is the tidal stream amplitude (Robinson, 1979) then it is helpful to look at the distribution of the currents as

$$(M_2 - S_2)^3 \qquad \text{Neaps}$$

and $$(M_2 + S_2)^3 \qquad \text{Springs}$$

Figure 11b shows that at any one location tidal mixing or sediment transport is likely to undergo a 6-fold change during the neap-spring cycle.

4.4 Progressive and standing wave calculations

Observations in the Sizewell-Dunwich Bank area show that the flood current maxima occur typically 1½–2 hours before the maximum elevation, an approximate phase difference of 45°–60°. Some insight into this behaviour can be gained by representing at least the two major diurnal constituents, the M_2 and S_2, as sums of a progressive wave component and a standing wave component. A suitable technique for separating these components has been described by Pugh and Vassie (1976) and is briefly outlined below. The notation used is almost identical to

that of Macqueen and Parker (1979). Pugh and Vassie carried out their analysis on current and tidal elevation measurements at the Inner Dowsing light tower in the North Sea, whereas Macqueen and Parker used observations made near the Sizewell Nuclear Power Station (Figure 3).

The analysis for the M_2 constituent is considered first. That for the S_2 and other constituents would follow a similar pattern. Because the region under study is small compared with a tidal wavelength, the difference in high water times over the area is small compared with a tidal period.

The currents in a progressive wave are given by $W_p \cos nt$ where W_p is the amplitude of the current, n the frequency and t the time in hours, relative to local high water (t = 0 is the time of maximum elevation). The wave propagates in a direction λ , measured clockwise from true N. Resolution into N–S and E–W components then gives

N–S: $W_p \cos nt \cos\lambda$ and E–W: $W_p \cos nt \sin\lambda$

Similarly for the standing wave propagating in a direction ϕ , the currents are given by: $W_s \sin nt$ which has components:

N–S: $W_s \sin nt \cos\phi$ and E–W: $W_s \sin nt \sin\phi$

From the harmonic (TIRA) analysis of the current meter records we have the amplitudes (H_u , H_v) and phases (g_u , g_v), of the N–S and E–W components of the M_2 tide relative to the equilibrium tide at Greenwich. The phases relative to local high water, using the value given by Macqueen and Parker (1979) for Sizewell, are then g_u' and g_v' .

It follows that the N–S component

$$W_p \cos nt \cos\lambda + W_s \sin nt \cos\phi = H_v \cos(nt - g_v') \qquad (4)$$

and for the E–W component

$$W_p \cos nt \sin\lambda + W_s \sin nt \sin\phi = H_u \cos(nt - g_u') \qquad (5)$$

Equating the progressive and standing components in these equations gives:

$$\left.\begin{aligned} W_p \cos\lambda &= H_v \cos g_v' \\ W_p \sin\lambda &= H_u \cos g_u' \end{aligned}\right\} \qquad (6)$$

and

$$\left.\begin{aligned} W_S \cos\phi &= H_V \sin g_V' \\ W_S \sin\phi &= H_U \sin g_U' \end{aligned}\right\} \tag{7}$$

Solving these two sets of equations gives

$$W_P = \left[(H_V \cos g_V')^2 + (H_U \cos g_U')^2\right]^{\frac{1}{2}} \tag{8}$$

$$W_S = \left[(H_V \sin g_V')^2 + (H_U \sin g_U')^2\right]^{\frac{1}{2}} \tag{9}$$

$$\lambda = \arctan\left(\frac{H_U \cos g_U'}{H_V \cos g_V'}\right) \tag{10}$$

where λ represents the direction of flow between mid-flood and the following mid-ebb in the progressive wave and

$$\phi = \arctan\left(\frac{H_U \sin g_U'}{H_V \sin g_V'}\right) \tag{11}$$

where ϕ represents the direction of flow of the standing wave during a falling tide.

The resulting values for the amplitudes and directions of M_2 propagation are given in Table 8 while values for the S_2, O_1, K_1 and N_2 constituents of the tidal wave are given in Tables 9–12.

In all cases but one (Record 560K8, Station A), the standing wave amplitude in the M_2 constituent exceeds that of the progressive wave. The progressive wave propagates southwards and the standing wave northwards. These findings are all consistent with those of Macqueen and Parker (1979). As these authors also noted, there is a tendency for the standing wave dominance to be greatest at stations nearer the shore (Stations D, S and X, Figure 3). However, at Station A (long term) the records show a variation from apparent progressive wave dominance in one data set (560K8, October 1978) to dominance by the standing wave shown at its maximum in the June 1978 data set.

In the case of S_2 constituent also, the standing wave appears to dominate over the progressive component (Table 9). Although Macqueen and Parker (1979) only carried out an analysis of the M_2 constituent, Pugh and Vassie (1976) found a difference in dominance for the two constituents at the Inner Dowsing Station, with $W_P > W_S$ for the M_2 and for the S_2, $W_P < W_S$.

4.5 Velocity profiles

Profile measurements were made with the Marconi current meter system (Figure 7) at the locations shown in Figure 3 on the 5, 6 and 7 September 1976. Simultaneous current measurements were made at heights of 1.2, 3.2, 4.2 and 6.2 m above the sea-bed, only limited data being available from the sensors at 2.2 m and 5.2 m due to instrument failure.

Figure 12 shows that while the velocity structure of the bottom half of the flow is complex it appears to vary systematically over the tidal cycle. A characteristic of the ebb and flood patterns is the layer of high velocity fluid moving at a height of 4-5 m above the bed. On the rising flood tide this is displaced to a higher level (Figure 12) and only the bottom of the layer is sampled by the current meters.

Figures 13 and 14 also illustrate these features and show typical ebb and flood velocity profiles for accelerating and decelerating phases of the tidal cycle.

The Marconi current measurements were made in a comparatively narrow channel between the Sizewell-Dunwich Banks and the coast (Figure 3) and it is likely that they will have been considerably influenced by bathymetry. In particular on the falling ebb tide, currents are more likely to be constrained to flow in this channel whereas on the rising flood tide currents are able to flow out of the channel and over the banks.

Near the sea-bed, in the lowest 2 m of the flow say, the velocity distribution in a steady neutrally stable flow may be represented by a logarithmic velocity profile of the form

$$u = \frac{u_*}{k} \ln \frac{z}{z_0} \qquad (12)$$

where u is now the velocity at a height z, u_* is the friction velocity, k is von Karman's constant and z_0 is the roughness length. Above the logarithmic layer, and over the rest of the water column, the velocity profile may be represented by a power law (eg Dyer, 1970) of the form

$$\frac{u}{u_1} = \left(\frac{z}{z_1}\right)^p \qquad (13)$$

where u is the velocity at height z and u_1 is the velocity at the reference height z_1, p is normally considered to be between 1/7 and 1/10 (Dyer, 1970). However, immediately above the logarithmic layer the flow may equally well be described by Cole's wake law (see Soulsby, 1978) which gives

$$u(z) = \frac{u_*}{k} \ln\left(\frac{z}{z_o}\right) + \frac{u_* \Pi}{k}\left(1 - \cos\frac{\pi z}{\delta}\right) \qquad (14)$$

for $z_o \leq z \leq \delta$ where δ is the boundary layer thickness, Π is an experimentally determined constant found to be 0.55 and where the other terms have their usual meanings.

Measurements near the sea-bed in the Sizewell-Dunwich Bank area (Lees, 1980b) have confirmed that in the lower 2 m of the flow the velocity profile may be logarithmic (Equation 12) for up to 94% of the time at the 95% confidence level. However, Figures 13 and 14 show that above the logarithmic layer the velocity distribution varies considerably over the tidal cycle and Figure 15 shows that it is poorly represented by a power law distribution (Equation 13). Figure 15 shows power law profiles with values of p = 0.1, 0.2, 0.3, and a logarithmic velocity profile for a z_o value of 0.5 cm. These clearly give even poorer representation of the velocity distribution above 2 m, but would probably give reasonable agreement below this. Also shown in Figure 15 is a Cole's wake law profile for z_o = 0.5 cm.

The forms of the velocity profiles shown in Figures 13 and 14 may represent an adjustment to boundary roughness (Dyer, 1970). In particular retarded velocities near the bed may represent an adjustment to increased upstream roughness whereas increased velocities near the bed may correspond to decreased upstream roughness.

Further analyses of the velocity profile data by Soulsby (1978) have shown only weak veering in the bottom 6 m of the flow, some 2-3°, and that the phase difference between the bed shear stress (calculated from the profiles) and the depth mean flow is variable.

5 RESIDUAL CURRENTS

5.1 Residual circulation

Eulerian residuals were obtained from the current meter data using Doodson's X_o filter which is described by Heathershaw and Hammond (1979). They found, as did Hill and Ramster (1972), that this yields similar residual flow estimates to those obtained by averaging over two tidal cycles, Hill and Ramster using a 25 hour mean and Heathershaw and Hammond taking their average over a 24 hour 50 minute period. Doodson's X_o filter is preferred since its tidal suppresion characteristics are well determined (Pugh and Vassie, 1976). However, it has not been possible to use it on the earliest data collected in 1975, and in those cases

the daily mean residuals have been obtained from running 24 hour 50 minute averages. It should be noted that these residuals are not synoptic.

The magnitudes and directions of the measured residuals are summarised in Table 13 and Figure 16. It is emphasised that these are Eulerian residuals and relate only to the net flow of water through the point at which the current was measured, in contrast to Lagrangian measurements which would be given by drifters. Macqueen and Parker (1979) made estimates of the residual flows using both techniques at Sizewell, in light wind conditions. They found good agreement between the two.

The strongest residuals, 10.0 cm s^{-1} and 12.9 cm s^{-1}, occur between the Sizewell-Dunwich Bank and the shore. They are parallel to the coastline and bank and flow towards the S, ie in the flood direction. Ebb, or northward residuals are shown on the seaward side of the banks with values ranging from 5.8 cm s^{-1} to 8.0 cm s^{-1}. Stations still on the seaward side of the banks, but closer to them, give residuals towards the crests of the banks. An anticlockwise eddy is present over the Sizewell Bank, and its apparent limits cover the area of the 'col' between the banks, and the channel between Thorpe Ness and the Sizewell Bank. There are possible indications of smaller anticlockwise eddies in the residual circulation at the northern end of both the Sizewell-Dunwich Bank and of the Aldeburgh Ridge.

5.2 Variability in measured residual currents

Figure 17 and Table 13 show how the residual flow direction estimates can vary throughout the year at Station A. They lie within an arc extending from 191° to 290°. The January/February 1977 residual, with a bearing of 290°, shows large standard errors on the speed values, but a direction steadiness factor (Ramster et al, 1978; Heathershaw and Hammond, 1979) of 83%.

At the remaining stations, occupied for two month periods or less, the largest standard errors are shown in the late summer months at Stations C, E and N. At Stations C and X the steadiness factor is only about 26%, indicative of small overall residual flows. These stations are both situated in possible "eddy" areas, which could be consistent with conditions of variable flow. At all other stations the steadiness factor is above 71%. The part played in these variations by meteorological conditions will be examined in greater detail below. Smoothed progressive vector diagrams corresponding to the records in Table 13 and Figure 16 are shown in Appendix A together with their steadiness factors.

All these features have important implications for sediment transport, and for the structure and maintenance of the banks.

6 METEOROLOGICAL FORCING

We have shown previously that the water movements in shallow coastal waters, such as the Sizewell-Dunwich Bank area, are likely to be influenced by meteorological forcing. From calculations in similar water depths Heathershaw and Hammond (1979) were able to show that wind driven currents of the order of 10 cm s^{-1} were possible during strong winds and that wind induced "set-up" might lead to slope currents of the order of 5 cm s^{-1}.

In this section of the report we examine current and sea surface elevation measurements made during storms to determine the actual response of the water column to meteorological forcing.

6.1 Residual currents and sea surface elevations

During the study it was not possible, due to instrument failure or loss, to make current measurements during a particularly severe storm surge. However, a data set, for the period September to December 1976, has been examined which shows clearly the effect of the wind on water movements in the study area. In addition some data are presented which illustrate the changes in sea level which occurred during two particularly large storm surges in January 1976 and January 1978. The residual flow regime at Station A, for the period September-November 1976 is illustrated in Figures 18a, b. These show that at times the quiescent flow, in a S to SW direction, may be completely reversed and that residual flows in a N direction may persist for periods of up to 6-7 days during strong S winds.

The effects of storms on the sea surface elevations are illustrated in Figure 19 which shows observed and predicted tides at Lowestoft for the periods 3-4 January 1976 and 11-12 January 1978. Figure 19a shows a positive surge of the order of 2 m which persists over two tidal cycles while Figure 19b shows a smaller surge of about 1.5 m. Weather charts for these periods show the usual pattern (eg Heaps, 1967) of events with particularly deep depressions tracking S into the North Sea from the Atlantic. The increases in sea level which are illustrated in Figure 19 are due in part to the decrease in atmospheric pressure ("inverted barometer effect", Equation 2) as the depressions move through the area and also due to winds driving water down into the southern North Sea ("wind set-up", Equation 3).

An analysis of the differences between observed and predicted tides at Lowestoft, for the period 1975-1979 (Figure 20) has shown that the most probable difference is slightly less than zero (a longer record would give the most probable value as zero) with the standard deviation of the difference equal to

0.22m. As an approximate rule Pugh (1980) has suggested that a surge of at least 5 times the standard deviation of the differences, will occur on average once a year. This gives reasonable agreement with the hourly tide differences at Lowestoft assuming that a surge of 5 times the standard deviation, or greater, has a duration of the order of 10 hours. This duration is similar to that of the surge shown in Figure 19a.

Although current measurements were not available during these two periods it is likely that the surges will have had a considerable effect on the water circulation in the area.

6.2 Correlation analyses

To examine in more detail the relation between currents and the wind, currents were resolved into E-W and N-S components and filtered, using a Doodson X_0 filter (Heathershaw and Hammond, 1979), to give estimates of the alongshore and offshore-onshore components of the mean flow, centred on 1200 GMT each day. Similarly, the wind was resolved into E-W and N-S components and daily means of the wind speed squared taken to parameterise wind stress. Thus the following parameters were considered:

$\overline{u_x}$, $\overline{u_y}$ the E-W and N-S components of the residual flow at Station A calculated using Doodson's X_0 filter

$\overline{W_x|\underset{\sim}{W}|}$ and $\overline{W_y|\underset{\sim}{W}|}$ the E-W and N-S components of the wind speed squared. $\underset{\sim}{W}$ is the wind velocity (W_x, W_y) measured at Gorleston.

In addition daily mean values of the following parameters have been examined:

$\overline{H_s}$ the significant wave height measured at Dunwich

$\overline{\zeta_R}$ the residual tidal elevation at Lowestoft

$\overline{P}$ the atmospheric pressure measured at Gorleston

Figure 21 shows these parameters plotted as a function of time and illustrates a high degree of correlation between the alongshore components of the residual current (u_y) and the wind stress (W_y $\underset{\sim}{W}$). These variations are also shown in Figure 22, which shows the two time series overlapped, and examined in more detail below.

The data sets in Figure 21 were subjected to correlation analyses. The results of these calculations are shown in Table 14. Due to a gap in the middle of the current meter records when the instruments were being changed over, the

analysis was carried out in two parts, the first on a 53 day data set and the second on a 42 day data set.

Table 14a confirms the observation made in Figure 22 and shows that during the first 53 days of the record, the alongshore component of the residual flow ($\overline{u_y}$) is significantly correlated, at the 5% level, with the alongshore component of the wind stress ($\overline{W_y|W_y|}$). In fact the correlation remains significant, even at the 0.1% level. Table 14a also shows that the onshore–offshore component of the residual flow ($\overline{u_x}$) is significantly correlated with the alongshore wind stress ($\overline{W_y|W_y|}$) although due to scaling differences this dependence is not apparent in Figure 21.

Table 14b shows that in the second part of the record the alongshore components of the residual flow ($\overline{u_y}$) and the wind stress ($\overline{W_y|W_y|}$) remain significantly correlated, and that there is some dependence of the onshore–offshore component of the residual flow ($\overline{u_x}$) on the onshore–offshore wind stress ($\overline{W_x|W_x|}$). The negative correlation might suggest a compensatory flow in response to wind set-up or set-down near the coast although this conclusion is not supported by the negative correlation between the residual elevation, ζ_R , and $\overline{u_x}$. However the tidal elevation data are for Lowestoft and may not be entirely representative of processes in the Sizewell–Dunwich Bank area.

With current measurements made in shallow water it is not possible to eliminate entirely the effects of waves. While the use of conventional propeller rotor current meters overcomes some of the difficulties associated with Savonius rotor meters, the response of complete rotor–vane systems in combined wave and tidal current velocity fields is not known. It is also possible that mooring motion due to wave action on subsurface buoyancy (Figure 6) will influence current measurements. In fact Table 14a shows that in the first data set the alongshore component of the residual flow ($\overline{u_y}$) is, apparently, significantly correlated with the wave height ($\overline{H_s}$). However, since the wind generates both currents and waves, this correlation might be expected and need not imply any mechanism linking the two processes. This conclusion is supported to some extent by Figure 21 which shows (Event A) high waves occurring during a period of low winds and having no effect on the residual currents. The second data set, which exhibits weaker but significant correlations between residual flow and wind stress, shows no significant correlations between residual currents and wave height.

7 CONCLUSIONS

Analysis of current meter and tidal elevation data has shown that the tides in the Sizewell-Dunwich Bank area may be considered as a mixture of standing and progressive wave oscillations. For the M_2 and S_2 currents, standing wave tides are dominant with a standing wave/progressive wave ratio of about 3:2. Maximum tidal streaming ($M_2 + S_2$) at mid depth is of the order 100 cm s^{-1} over the area as a whole.

Harmonic and rotary analysis of the tidal currents confirms that the principal semi-diurnal constituents are essentially rectilinear (Figures 8 and 9), with ellipticities of the order of 5% and less, and that the M_2 phase lags are in general smaller towards the coast indicating that maximum tidal streaming occurs here before it does offshore. Non-linear effects in the currents are less apparent than in a similar study in Swansea Bay on the South Wales coast (Heathershaw and Hammond, 1979) the current amplitude ratio M_4/M_2 varying from 0.016 to 0.072 with some tendency towards larger values in shallow water.

The mean tidal or residual circulation in the area is complex (Figure 16). Close inshore and landward of the Banks, strong southerly residuals, of the order of 13 cm s^{-1} have been measured while offshore from, and to the N of, the Banks residual flows are somewhat weaker. Taken as a whole the residual current measurements indicate an anticlockwise eddy which is situated to the N of Thorpe Ness and over the Sizewell Bank, and which possibly extends to cover the Dunwich Bank. This feature of the circulation may have some significance in terms of processes which are capable of maintaining the Banks in their present positions.

Current measurements at the long term mooring (Figure 17) show that the residual circulation is variable both in strength and direction although the variability is unlikely to bring about any major change in the overall circulation pattern. Comparisons of the residual currents at the long term mooring with meteorological data show that the circulation is likely to be influenced by the wind and in particular we have found that during periods of strong southerly winds there is a high degree of correlation between the alongshore components of the residual flow and the wind stress (Figure 22). During these periods the quiescent flow direction may be completely reversed for periods of 6-7 days.

In terms of sediment transport and coastal erosion processes the sensitivity of the mean tidal circulation and sea surface elevation in the Sizewell-Dunwich

Bank area to meteorological forcing may be of special significance. In particular, periods of strong alongshore winds may modify the residual circulation which could influence the directions of net sediment movement as bedload and in suspension. Furthermore, storm surges which on the basis of evidence presented in this report may increase tidal levels by as much as 2 m (Figure 19a) could, in conjunction with waves, result in overtopping or breaching of the beach crest on the coast adjacent to the Sizewell–Dunwich Banks area.

From the point of view of numerical modelling the complex vertical structure of the currents in the vicinity of the banks (Figures 12, 13 and 14) may lead to difficulty with 2–dimensional representations of the flow and lead to some uncertainty in predicted bed shear stress values.

8 ACKNOWLEDGEMENTS

We would like to acknowledge the support and co–operation of our colleagues at the Institute of Oceanographic Sciences' Taunton and Bidston Laboratories. Recording current meters were supplied by the NERC Research Vessel Services, Barry, who also deployed and recovered the instruments. Meteorological data were supplied by the Meteorological Office, Bracknell.

This work was supported financially by the Department of the Environment.

REFERENCES

CASTON, V.N.D., 1976. A wind-driven near-bottom current in the southern North Sea. Estuarine and Coastal Marine Science, 4, 23-32.

DOODSON, A.T., 1928. The analysis of tidal observations. Philosophical Transactions of the Royal Society of London, A, 227, 223-279.

DYER, K.R., 1970. Current velocity profiles in a tidal channel. Geophysical Journal Royal Astronomical Society, 22, 153-161.

GODIN, G., 1972. The Analysis of Tides. Liverpool University Press. 264 pp.

GONELLA, J., 1972. A rotary-component method for analysing meteorological and oceanographic vector time series. Deep Sea Research, 19, 833-846.

HEAPS, N.S., 1967. Storm Surges. In H. Barnes (Ed). Oceanography and Marine Biology. An Annual Review, 5, 11-47.

HEAPS, N.S., 1978. Linearized vertically-integrated equations for residual circulations in coastal seas. Deutsche Hydrographische Zeitschrift, 31, 147-169.

HEATHERSHAW, A.D. and HAMMOND, F.D.C., 1979. Swansea Bay (Sker) Project. Topic Report: 4. Tidal currents: Observed tidal and residual circulations and their response to meteorological conditions. Institute of Oceanographic Sciences Report, No. 92, pp 154.

HILL, H.W. and RAMSTER, J.W., 1972. Variability in current meter records in the Irish Sea. Rapports et Procès-Verbaux des Reunions, Conseil Permanent International pour L'Exploration de la Mer, 162, 232-247.

HYDROGRAPHIC DEPARTMENT, TAUNTON, 1976. Tidal Stream Atlas. North Sea. Southern Portion. NP 251. Edition 3.

KAGAN, B.A., 1966. Tides and tidal currents of the principal lunar semidiurnal wave M_2 in the North Sea. Izvestiya, Atmospheric and Oceanic Physics, 2, 423-433, English translation by P.A. Keehn.

LEE, A. and RAMSTER, J., 1968. The hydrography of the North Sea - a review of our knowledge in relation to pollution problems. Heligolander wiss Meeresunters, 17, 44.

LEES, B.J., 1980a. Sizewell - Dunwich Banks Field Study. Topic Report: 1. a) Introduction b) Geological background. Institute of Oceanographic Sciences Report, No 88, pp 29.

LEES, B.J., 1980b. Sediment transport measurements in the Sizewell - Dunwich Banks area, East Anglia, U.K. International Association of Sedimentologists Special Publication (in press).

MACQUEEN, J.F. and PARKER, G.C.C., 1979. Tidal currents measured near a British coastal power station. Advances in Water Resources, 2, 113-122.

MAIER-REIMER, E., 1977. Residual circulation in the North Sea due to the M_2-tide and mean annual wind stress. Deutsche Hydrographische Zeitschrift, 30, 69-80.

McCAVE, I.N., 1979. Tidal currents at the North Hinder lightship, southern North Sea: flow directions and turbulence in relation to maintenance of sand banks. Marine Geology, 31, 101-114.

McCULLOUGH, J.R., 1977. Problems in measuring currents near the ocean surface. Marine Technology Society and Institute of Electrical and Electronic Engineers. Oceans' 77 Conference Record, 2, 1-7.

NIHOUL, J.C.J., 1975. Effect of the tidal stress on residual circulation and mud deposition in the Southern Bight of the North Sea. Pure and Applied Geophysics, 113, 577-581.

PITT, E.G., CARSON, R.M. and TUCKER, M.J., 1973. The current system around the British Isles as it relates to offshore structures. National Institute of Oceanography Internal Report, No. A.62, pp 25.

PROUDMAN, J. and DOODSON, A.T., 1924. The principal constituents of the tides of the North Sea. Philosophical Transactions of the Royal Society of London, A, 224, 185-219.

PUGH, D.T., 1980. Sea Level Variability and Extremes. MIAS News Bulletin, No. 3, 6-10.

PUGH, D.T. and VASSIE, J.M., 1976. Tide and surge propagation off-shore in the Dowsing region of the North Sea. Deutsche Hydrographische Zeitschrift, 29, 163-213.

RAMSTER, J.W., HUGHES, D.G. and FURNES, G.K., 1978. A 'Steadiness' factor for estimating the variability of residual drift in current meter records. Deutsche Hydrographische Zeitschrift, 31, 230-236.

ROBINSON, I.S., 1979. The tidal dynamics of the Irish and Celtic Seas. Geophysical Journal Royal Astronomical Society, 56, 159-197.

SOULSBY, R.L., 1978. The use of depth-averaged currents to estimate bed shear stress, as applied to a numerical model of the Sizewell - Dunwich Bank area. Institute of Oceanographic Sciences Internal Document, No 26, pp 40.

TABLE 1

Details of current meter records described in this report

Record (Plessey M021 meter)	Station	Height above seabed (m)	Useful data (Hrs mins)
238 H6	A	6	1392 20
232 K6	A	6	1236 30
238 A7	A	6	148 10
260 E7	A	6	502 50
238 G7	A	6	1509 30
629 J7	A	6	1651 50
534 D8	A	6	1479 00
560 F8	A	6	1488 10
260 H8	A	6	654 40
560 K8	A	6	517 20
534 D9	A	6	1215 40

Coding of records:

Letter refers to month of deployment eg A = January, B = February etc.

Number refers to year of deployment eg 6 to 1976, 7 to 1977 etc.

TABLE 1 (CONT)

Record (Plessey M021 meter)	Station	Height above seabed (m)	Useful data (Hrs mins)
*B39-2 B5	B	6	c320 00
532 H6	C	6	332 50
669 H8	D	6	880 40
669 K8			222 30
667 H6	E	7	336 30
232 G7	F	8	1322 10
534 D5	G	6	279 30
680 D5	H	6	281 00
626 H6	J	5	311 20
556 D5	K	6	293 40
*295-C B5	L	6	c320 00
267 H6	M	6	311 30
594 J6	N	3	307 30
534 J6	P	2	307 40
629 D5	Q	6	282 20
*567-5 B5	R	6	c335 00
232 H6	S	5	304 40
*570-6 B5	T	6	c340 00
663 D5	V	6	336 00
534 H8	W	8	1614 20
560 G7	X	6	1484 50
265 G7	Y	6	115 40
237 G7	Z	8	1343 30

* Aanderaa meter

TABLE 2

Harmonic analysis of tidal currents (29 day records)

Constituents analysed using TIRA

Major constituent (26)	Speed (degrees per mean solar hour)	Related constituent (8)	Major constituent to which related
MM	0.54	P1	K1
MSF	1.02	PI1	K1
Q1	13.40	PSI1	K1
O1	13.94	PHI1	K1
M1	14.49	K2	IS_2
K1	15.04	T2	S_2
J1	15.59	NU_2	N_2
OO1	16.14	$2N_2$	N_2
MU_2	27.97		
N_2	28.44		
M_2	28.98		
L_2	29.53		
S_2	30.00		
$2SM_2$	31.02		
MO_3	42.93		
M_3	43.48		
MK_3	44.03		
MN_4	57.42		
M_4	57.97		
SN_4	58.44		
MS_4	58.98		
$2MN_6$	86.41		
M_6	86.95		
MSN_6	87.42		
$2MS_6$	87.97		
$2SM_6$	88.98		

TABLE 3

Harmonic analysis of tidal currents (13 - 15 day records)
Constituents analysed using TIRA

Major Constituent (16)	Speed (degrees mean solar hour^{-1})	Related Constituents (14)	Major Constituent to which related
Z0	00.00	SIG1	2Q1
MSF	1.02	Q1	O1
2Q1	12.85	RHO1	O1
O1	13.94	PI1	K1
K1	15.04	P1	K1
OO1	16.14	S1	K1
M2	28.98	PSI1	K1
S2	30.00	J1	OO1
MU2	27.97	2N2	MU2
M3	43.48	N2	M2
M4	57.97	NU2	M2
MS4	58.98	L2	M2
S4	60.00	T2	S2
M6	86.95	K2	S2
2MS6	87.97		
2SM6	88.98		

TABLE 4

Records analysed with TIRA

Record	Station	Length of data analysed (days)	Timing error ($s\ day^{-1}$)
238 H6	A	29	-223.21
232 K6	A	29	*
260 E7	A	14.5	*
238 G7	A	29	+118.51
629 J7	A	29	+298.56
534 D8	A	29	+59.77
560 F8	A	29	+9.66
260 H8	A	14.5	*
560 K8	A	14.5	*
534 D9	A	29	+441.04
669 H8	D	29	-16.83
667 H6	E	14	+336.02
232 G7	F	29	*
626 H6	J	13	0.00
267 H6	M	13	0.00
534 J6	P	13	0.00
232 H6	S	13	0.00
534 H8	W	29	*
560 G7	X	29	+6.67
237 G7	Z	29	*

* Timing correction not possible as meter ceased recording before recovery, usually because tape was full

TABLE 5

Amplitudes and phases of the principal tidal constituents in the currents Station A (long-term mooring) at mid-water level

		Amplitudes, H_u, H_v (cm s^{-1})			Phases, g_u, g_v (^{o})		
		Mean	σ Standard deviation	$\sigma/N^{\frac{1}{2}}$ Standard error	Mean	σ Standard deviation	$\sigma/N^{\frac{1}{2}}$ Standard error
O_1	U	0.36	0.27	0.10	298.81	52.22	19.74
	V	2.27	0.40	0.15	297.41	16.72	6.32
K_1	U	0.59	0.37	0.14	99.27	23.58	8.91
	V	2.15	0.31	0.12	123.62	13.66	5.16
N_2	U	2.26	1.13	0.43	18.78	42.49	16.06
	V	11.00	4.67	1.77	31.67	44.92	16.98
M_2	U	15.06	3.00	1.14	42.67	5.00	1.89
	V	72.25	5.36	2.03	56.17	5.12	1.94
S_2	U	4.12	1.40	0.53	87.69	28.81	10.89
	V	20.25	3.38	1.28	98.76	24.57	9.29
M_4	U	1.21	0.68	0.26	15.16	42.18	15.94
	V	3.95	0.80	0.30	8.41	10.34	3.91
MS_4	U	0.80	0.54	0.20	82.26	48.00	18.14
	V	1.53	0.56	0.21	66.08	25.79	9.75
M_6	U	1.10	0.28	0.11	2.20	23.00	8.69
	V	2.95	0.78	0.30	41.08	17.76	6.71

Number of monthly analyses (N) = 7

U = EW component of current in cm s^{-1}

V = NS component of current in cm s^{-1}

Phases are in degrees relative to the equilibrium tide at Greenwich.
Mean values are vector means

TABLE 6

Amplitudes and phases of the principal semi-diurnal constituents in the tidal currents at Stations D, E, F, J, M, S, X and Z

Station	Constituent	Amplitudes (H)(cms^{-1})		Phases (g) (°)	
		H_u	H_v	g_u	g_v
D	M_2	34.43	77.55	39.81	43.30
	S_2	10.37	22.34	84.87	92.54
E *	M_2	31.68	74.45	54.58	58.48
	S_2	10.15	24.71	100.39	104.73
F	M_2	34.31	81.05	55.49	57.50
	S_2	10.02	24.22	104.52	106.99
J *	M_2	10.41	72.99	27.90	50.50
	S_2	2.42	21.41	69.92	91.71
M *	M_2	10.50	71.97	41.39	49.80
	S_2	3.09	19.85	68.18	88.88
S *	M_2	9.88	61.52	34.89	43.46
	S_2	2.80	17.52	77.19	83.93
X	M_2	25.81	61.84	37.56	36.62
	S_2	7.25	16.97	87.94	86.55
Z	M_2	42.27	76.55	58.17	55.07
	S_2	13.02	23.03	110.35	107.03

* Refers to 13-15 day data base

U = E-W component of current in cm s^{-1}

V = N-S component of current in cm s^{-1}

TABLE 7

Amplitudes and phases of the principal constituents in the tidal elevations at Lowestoft. One year's data centred on 1 July 1965

Constituent	Amplitude (m)	Phase (°)
O_1	0.140	157.0
K_1	0.117	330.2
N_2	0.139	228.6
M_2	0.743	257.5
S_2	0.220	296.7
M_4	0.050	329.7
MS_4	0.039	23.8
M_6	0.041	118.9

Phases are in degrees relative to the equilibrium tide at Greenwich

TABLE 8

Progressive and standing wave amplitudes and directions for the M_2 constituent

Station	Record	Progressive wave		Standing wave	
		Amplitude W_p (m s^{-1})	Direction λ (degrees from true N)	Amplitude W_s (m s^{-1})	Direction ϕ (degrees from true N)
A	238 H6	.542	189	.573	15
A	232 K6	.370	186	.539	13
A	260 E7	.516	191	.626	16
A	534 D8	.419	187	.542	11
A	560 F8	.396	189	.595	13
A	260 H8	.483	186	.585	12
A	560 K8	.585	189	.506	17
D	669 H8	.379	202	.759	24
E	667 H6	.537	202	.606	24
F	232 G7	.584	202	.659	24
J	626 H6	.419	183	.607	30
M	267 H6	.405	186	.604	9
P	534 J6	.171	186	.429	12
S	232 H6	.281	187	.556	10
W	534 H8	.451	207	.687	30
X	560 G7	.242	204	.625	23
Z	237 G7	.559	210	.673	28

λ represents direction of flow in the progressive wave between mid-flood and following mid-ebb

ϕ represents direction of flow in the standing wave during a falling or ebb tide

TABLE 9

Progressive and standing wave amplitudes and directions for the S_2 constituent

Station	Record	Progressive wave		Standing wave	
		Amplitude W_p ($m\ s^{-1}$)	Direction λ (degrees from true N)	Amplitude W_s ($m\ s^{-1}$)	Direction ϕ (degrees from true N)
A	238 H6	.236	191	.054	26
A	232 K6	.014	97	.246	9
A	260 E7	.175	195	.206	15
A	534 D8	.043	178	.184	11
A	560 F8	.101	189	.178	13
A	260 H8	.107	180	.165	10
A	560 K8	.144	188	.174	15
D	669 H8	.110	199	.220	26
E	667 H6	.167	200	.208	23
F	232 G7	.175	201	.195	23
J	626 H6	.095	181	.194	7
M	267 H6	.079	181	.185	10
P	534 J6	.038	183	.118	15
S	232 H6	.055	186	.169	9
W	534 H8	.143	207	.195	30
X	560 G7	.069	204	.171	23
Z	237 G7	.181	211	.193	28

TABLE 10

Progressive and standing wave amplitudes and directions for the O_1 constituent

Station	Record	Progressive wave		Standing wave	
		Amplitude W_p (m s^{-1})	Direction λ (degrees from true N)	Amplitude W_s (m s^{-1})	Direction ϕ (degrees from true N)
A	238 H6	.020	195	.010	9
A	232 K6	.014	199	.019	1
A	260 E7	.020	183	.022	22
A	534 D8	.020	191	.008	347
A	560 F8	.019	188	.005	286
A	260 H8	.024	184	.018	22
A	560 K8	.019	186	.011	10
D	669 H8	.027	202	.028	31
E	667 H6	.034	208	.018	28
F	232 G7	.024	205	.017	29
J	626 H6	.029	208	.021	353
M	267 H6	.026	198	.014	13
P	534 J6	.005	205	.009	6
S	232 H6	.023	212	.015	28
W	534 H8	.016	209	.019	56
X	560 G7	.014	200	.012	47
Z	237 G7	.023	214	.014	27

TABLE 11

Progressive and standing wave amplitudes and directions for the K_1 constituent

Station	Record	Progressive wave		Standing wave	
		Amplitude W_p ($m\ s^{-1}$)	Direction λ (degrees from true N)	Amplitude W_s ($m\ s^{-1}$)	Direction ϕ (degrees from true N)
A	238 H6	.018	188	.008	84
A	232 K6	.021	182	.017	1
A	260 E7	.021	194	.001	4
A	534 D8	.018	193	.009	34
A	560 F8	.024	197	.006	40
A	260 H8	.023	203	.010	47
A	560 K8	.024	186	.002	36
D	669 H8	.045	198	.016	37
E	667 H6	.044	211	.009	321
F	232 G7	.040	201	.011	22
J	626 H6	.029	224	.022	270
M	267 H6	.016	197	.003	165
P	534 J6	.011	259	.004	256
S	232 H6	.028	274	.015	278
W	534 H8	.034	208	.014	37
X	560 G7	.021	205	.008	44
Z	237 G7	.036	210	.012	42

TABLE 12

Progressive and standing wave amplitudes and directions for the N_2 constituent

Station	Record	Progressive wave		Standing wave	
		Amplitude W_p ($m\ s^{-1}$)	Direction λ (degrees from true N)	Amplitude W_s ($m\ s^{-1}$)	Direction ϕ (degrees from true N)
A	238 H6	.015	193	.023	187
A	232 K6	.090	191	.015	30
A	260 E7	.103	191	.120	16
A	534 D8	.073	184	.126	8
A	560 F8	.066	190	.108	14
A	260 H8	.098	186	.111	12
A	560 K8	.116	189	.096	17
D	669 H8	.064	199	.123	28
E	667 H6	.108	201	.115	24
F	232 G7	.087	201	.116	24
J	626 H6	.084	183	.117	10
M	267 H6	.081	186	.116	9
P	534 J6	.036	186	.083	12
S	232 H6	.058	186	.107	10
W	534 H8	.075	207	.140	29
X	560 G7	.032	204	.099	22
Z	237 G7	.097	212	.113	29

TABLE 13

Summary of measured residual currents from current meter observations and variability in the direction and speed of residual flow estimates where Doodson's X_o filter was used.

Record	Station	Height above seabed (m)	Residual current					
			Speed			Direction		Length of record (days)
			Speed ($cm\ s^{-1}$)	Standard error of E-W component ($cm\ s^{-1}$)	Standard error of N-S component ($cm\ s^{-1}$)	Direction from true N (°)	Steadiness factor B (%)	
238 H6	A	6	5.29	0.21	0.95	264.36	66.95	54
232 K6	A	6	3.46	0.23	0.76	193.88	63.91	44
238 A7	A	6	8.62	1.23	2.59	289.89	83.44	5
260 E7	A	6	8.01	0.26	0.92	198.28	97.23	20
238 G7	A	6	4.13	0.11	0.53	229.74	76.91	62
629 J7	A	6	4.85	0.16	0.66	251.13	72.42	68
534 D8	A	6	7.31	0.14	0.37	203.38	97.67	58
560 F8	A	6	8.19	0.13	0.37	191.17	98.41	61
260 H8	A	6	5.91	0.25	0.44	197.60	95.69	26
560 K8	A	6	4.53	0.25	0.84	228.25	79.33	20
534 D9	A	6	3.82	0.21	0.62	225.19	73.04	45

Record	Station	Height above seabed (m)	Residual current					
			Speed			Direction		
			Speed ($cm\ s^{-1}$)	Standard error of E-W component ($cm\ s^{-1}$)	Standard error of N-S component ($cm\ s^{-1}$)	Direction from true N (^{o})	Steadiness factor B (%)	Length of record (days)
B39/2 B5*	B	10	5.08	-	-	32.70	97.00	13
532 H6	C	6	1.04	0.88	1.31	198.43	25.24	13
669 H8	D	6	4.28	0.31	0.49	242.77	84.45	35
669 K8	D	6	3.43	0.38	1.17	256.91	74.37	8
667 H6	E	7	5.80	0.34	1.26	10.97	91.43	13
232 G7	F	8	4.62	0.17	0.51	73.53	85.19	54
534 D5*	G	5	6.38	-	-	356.04	94.00	12
680 D5*	H	5	3.09	-	-	321.33	78.00	12
626 H6	J	4.5	6.76	0.36	1.05	210.80	88.96	12
556 D5*	K	5	8.02	-	-	249.83	97.00	12
295/C B5*	L	10	2.80	-	-	288.40	73.00	13

* Residual flow estimates made from progressive vector plots

TABLE 13 (cont)

Record	Station	Height above seabed (m)	Residual current					
			Speed			Direction		Length of record (days)
			Speed (cm s^{-1})	Standard error of E-W component (cm s^{-1})	Standard error of N-S component (cm s^{-1})	Direction from true N (°)	Steadiness factor B (%)	
267 H6	M	6	10.03	0.28	0.82	181.78	99.56	12
594 J6	N	3	6.66	0.49	0.61	227.91	95.36	11
534 J6	P	2	4.76	0.37	1.52	194.72	71.26	12
629 D5*	Q	5	9.08	-	-	216.68	99.00	12
567/5 B5*	R	10	7.95	-	-	338.50	94.00	14
232 H6	S	4.5	12.92	0.34	0.94	180.85	99.21	12
570/6 B5*	T	10	3.96	-	-	138.40	73.00	14
663 D5*	V	5	6.09	-	-	148.41	94.00	14
534 H8	W	8	5.25	0.20	0.29	198.81	95.29	66
560 G7	X	6	0.65	0.17	0.35	71.54	26.83	61
265 G7	Y	6	5.15	0.39	0.19	297.83	99.48	4
237 G7	Z	8	9.38	0.17	0.46	208.83	96.08	55

* Residual flow estimates made from progressive vector plots

TABLE 13 (cont)

TABLE 14

Meteorological forcing: correlation analyses of (a) 53 and (b) 42 day data sets using currents measured at Station A during the periods 1/9/76 - 23/10/76 and 30/10/76 - 10/12/76 respectively.

		Correlation coefficient r						
		$\bar{u}_x$	$\bar{u}_y$	$\overline{W_x\|\underset{\sim}{W}\|}$	$\overline{W_y\|\underset{\sim}{W}\|}$	$\bar{P}$	$\bar{H}_s$	$\bar{\zeta}_R$
(a)	$\bar{u}_x$	1	.63	.02	.49	-.26	.16	-.13
	$\bar{u}_y$		1	.02	.77	-.52	.52	-.25
	$\overline{W_x\|\underset{\sim}{W}\|}$			1	-.26	-.02	-.32	.03
	$\overline{W_y\|\underset{\sim}{W}\|}$				1	-.54	.66	-.05
	$\bar{P}$					1	-.54	-.15
	$\bar{H}_s$						1	.06
	$\bar{\zeta}_R$							1
(b)	$\bar{u}_x$	1	.42	-.27	.26	-.32	.09	-.30
	$\bar{u}_y$		1	.18	.35	-.28	-.06	-.21
	$\overline{W_x\|\underset{\sim}{W}\|}$			1	.43	-.14	.12	.14
	$\overline{W_y\|\underset{\sim}{W}\|}$				1	-.37	.63	-.35
	$\bar{P}$					1	-.23	-.40
	$\bar{H}_s$						1	-.21
	$\bar{\zeta}_R$							1

Level of significance	Correlation coefficient 5%	1%	.1%
Table a	.27	.35	.44
Table b	.30	.39	.49

Values of r underlined are significant at the 5% level. x and y denote onshore-offshore and alongshore directions respectively and the overbars denote daily mean values.

u_x, u_y denote x and y components of the residual current
W_x, W_y denote x and y components of the wind velocity $\underset{\sim}{W}$
H_s denotes significant wave height ζ_R denotes residual tidal elevation
P denotes atmosphere pressure

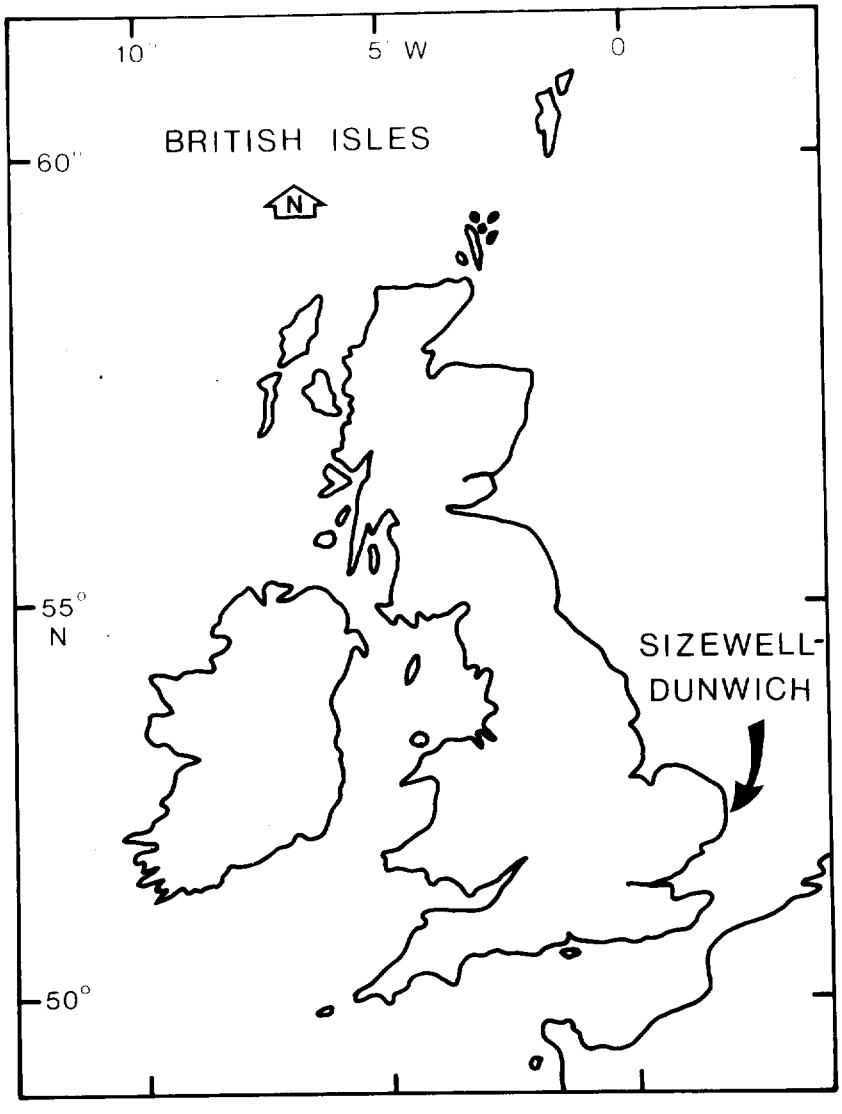

Figure 1 Location of study area

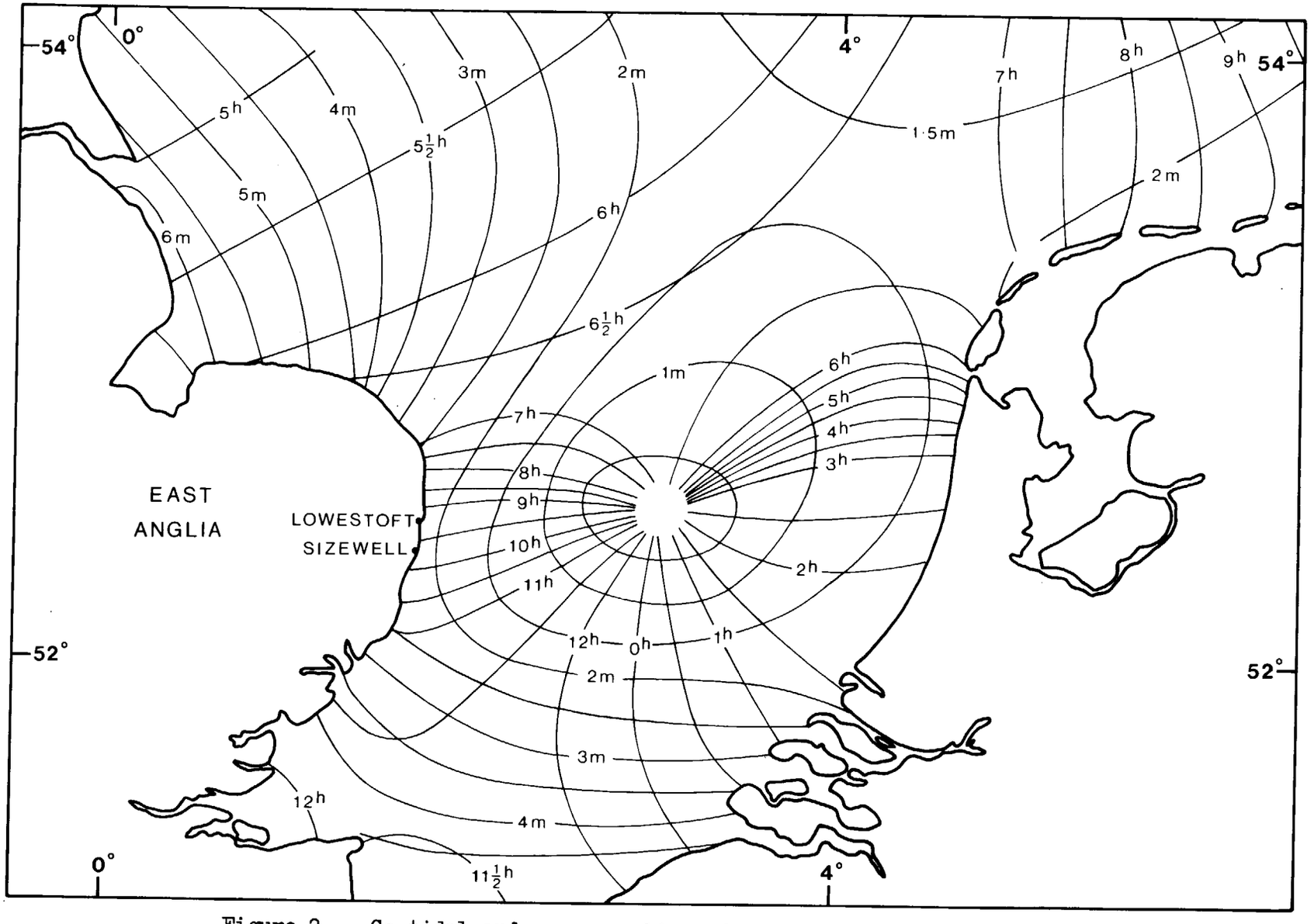

Figure 2 Co-tidal and co-range lines for the southern North Sea (mean High Water Time Interval and mean Spring Range). Reproduced courtesy of the Hydrographer of the Navy from Chart No 5059.

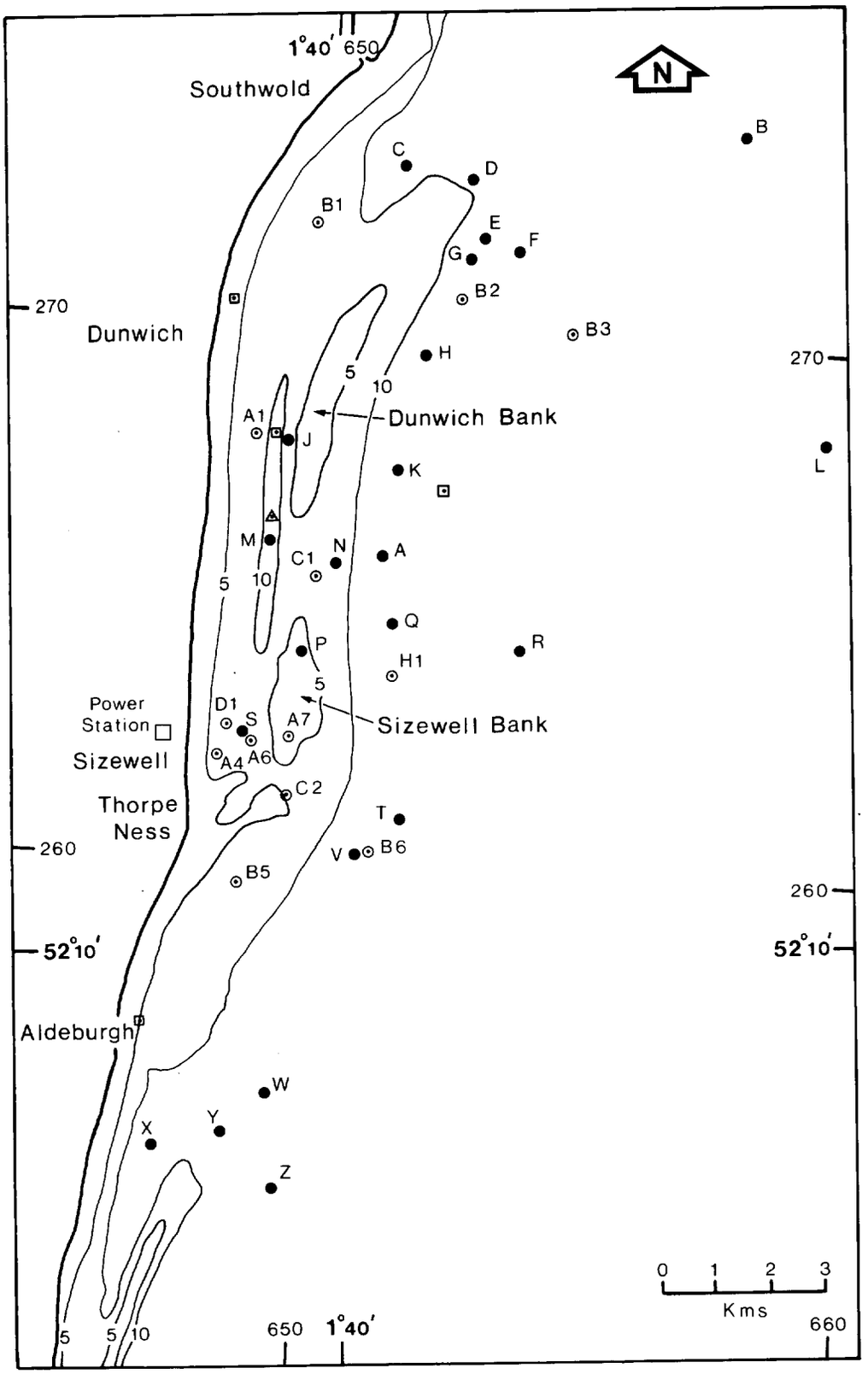

Figure 3 Location of IOS recording current meter moorings (●) in the Sizewell-Dunwich Banks area. Also shown are the positions of Waverider Buoy moorings (⊡), the Marconi current meter mooring (◬) and the CEGB moorings (⊙).

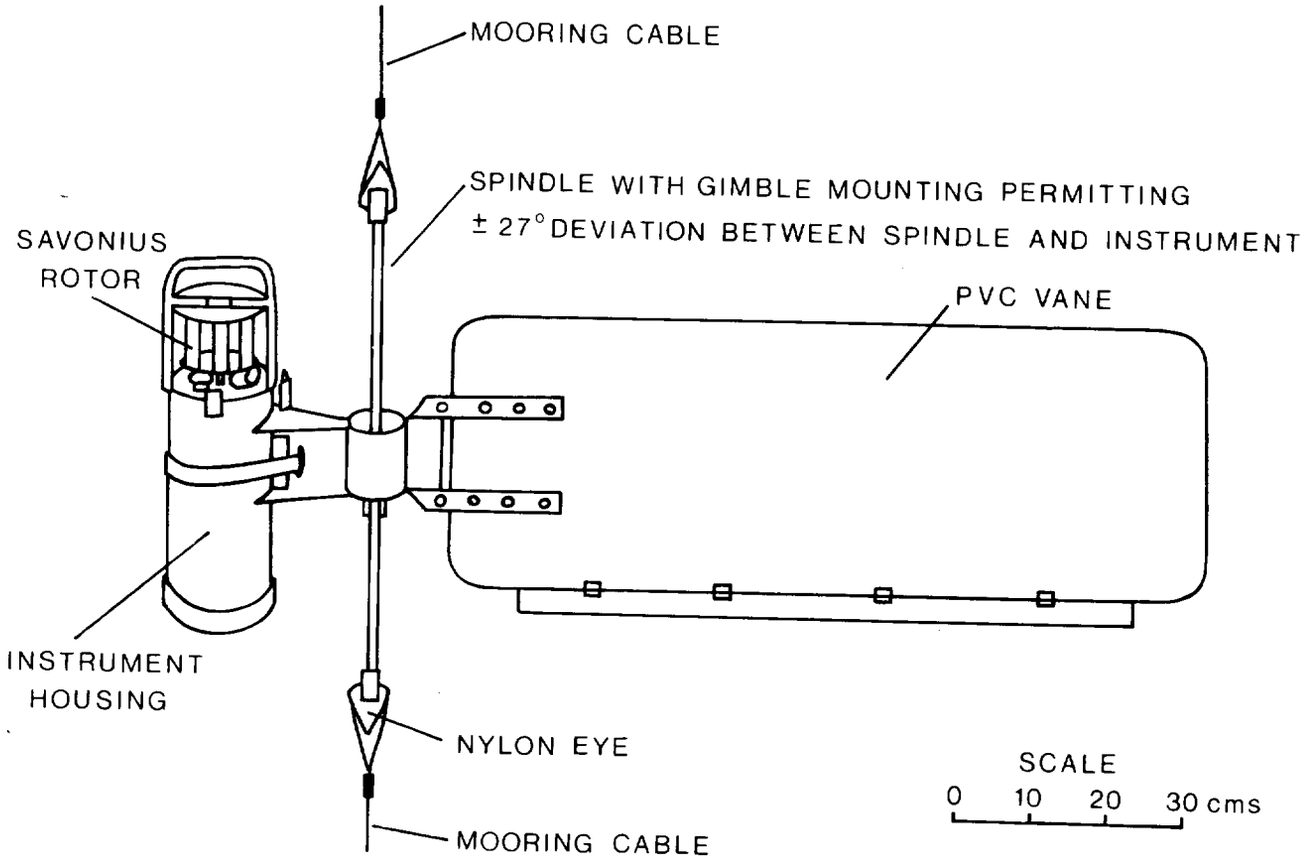

Figure 4 The Aanderaa recording current meter model RCM4.

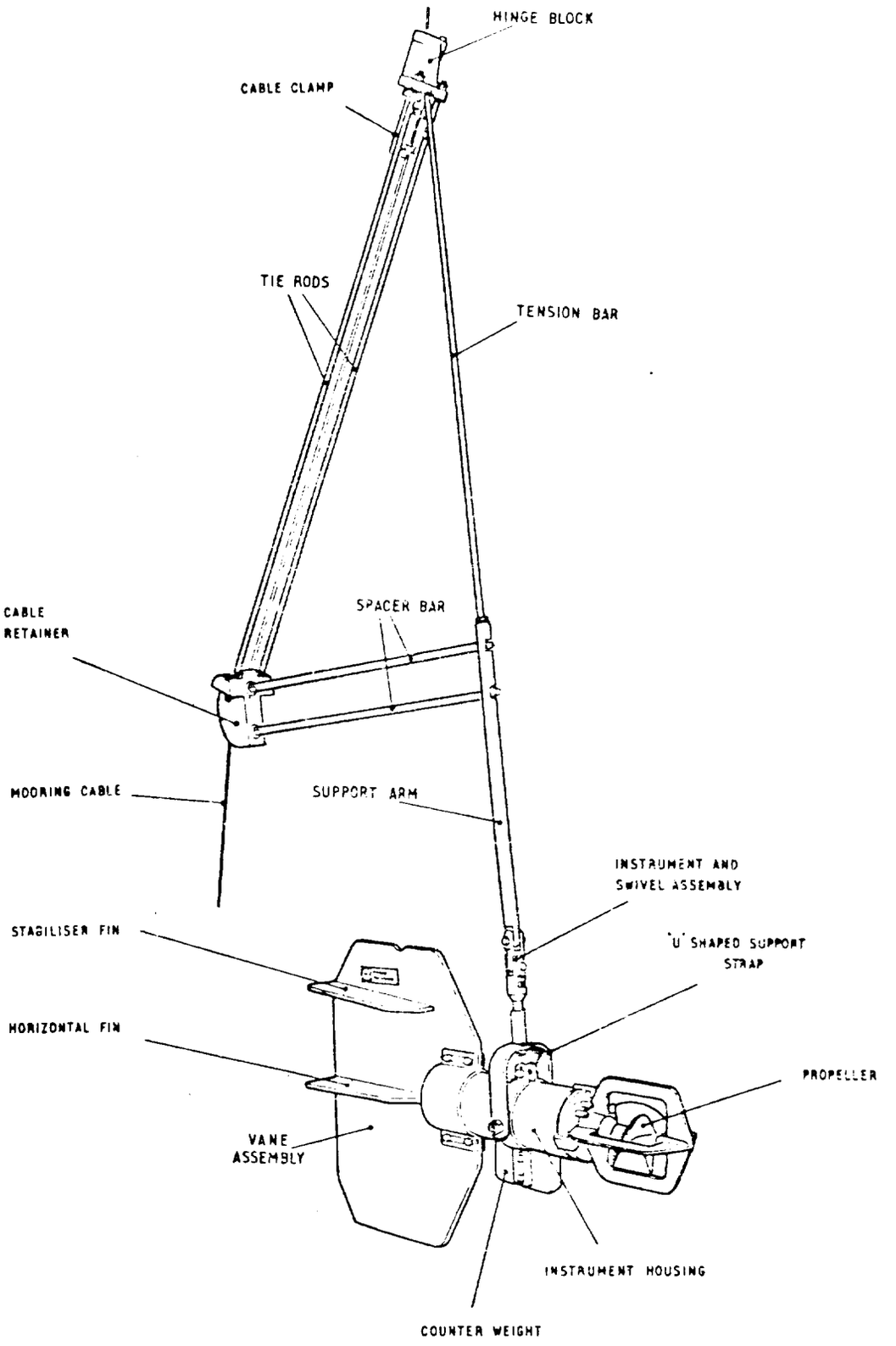

The Plessey recording current meter model M021

(Reproduced courtesy of the Plessey Company Ltd.)

Figure 5

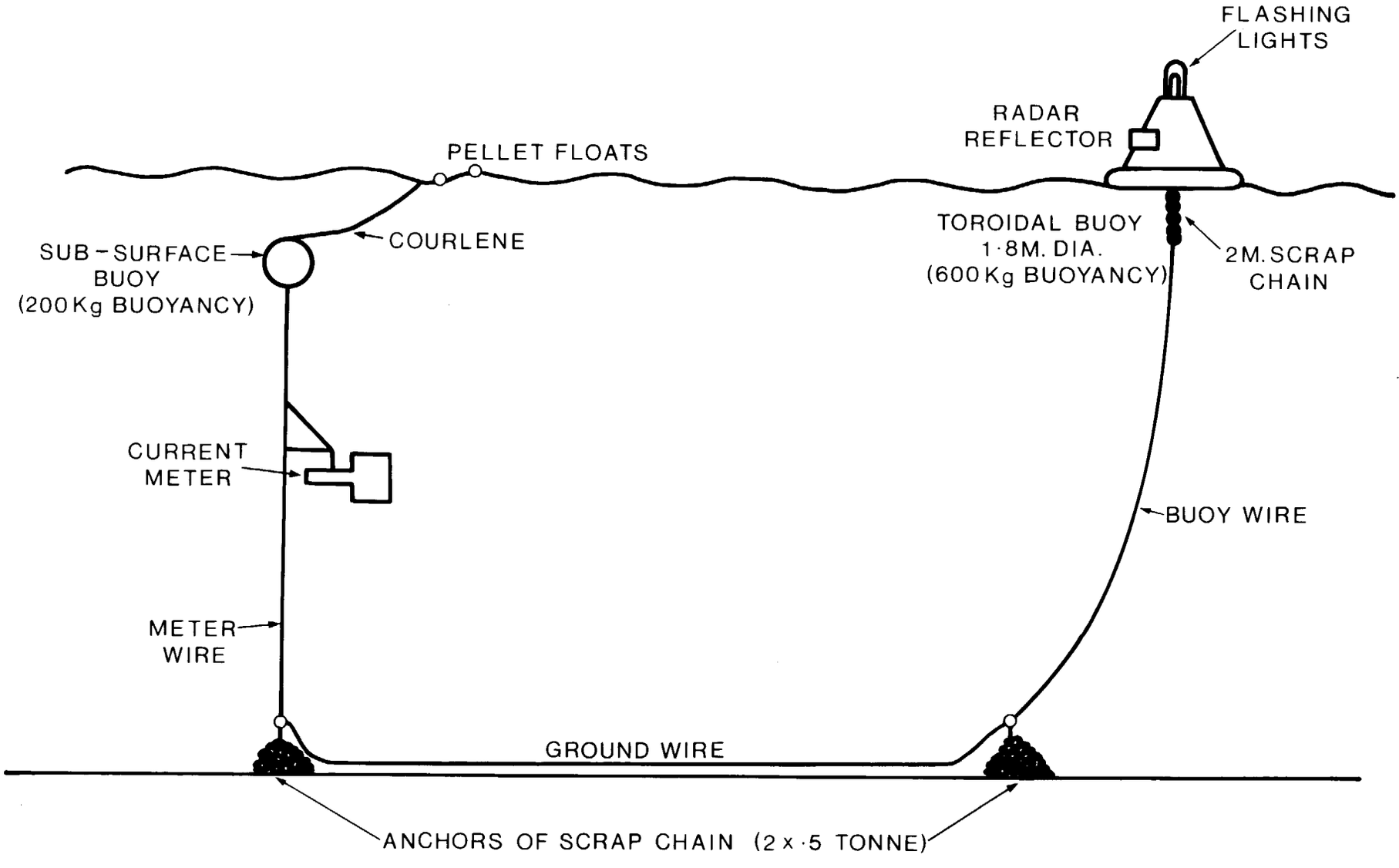

Figure 6 IOS recording current meter mooring of type used in the Sizewell-Dunwich Banks area.

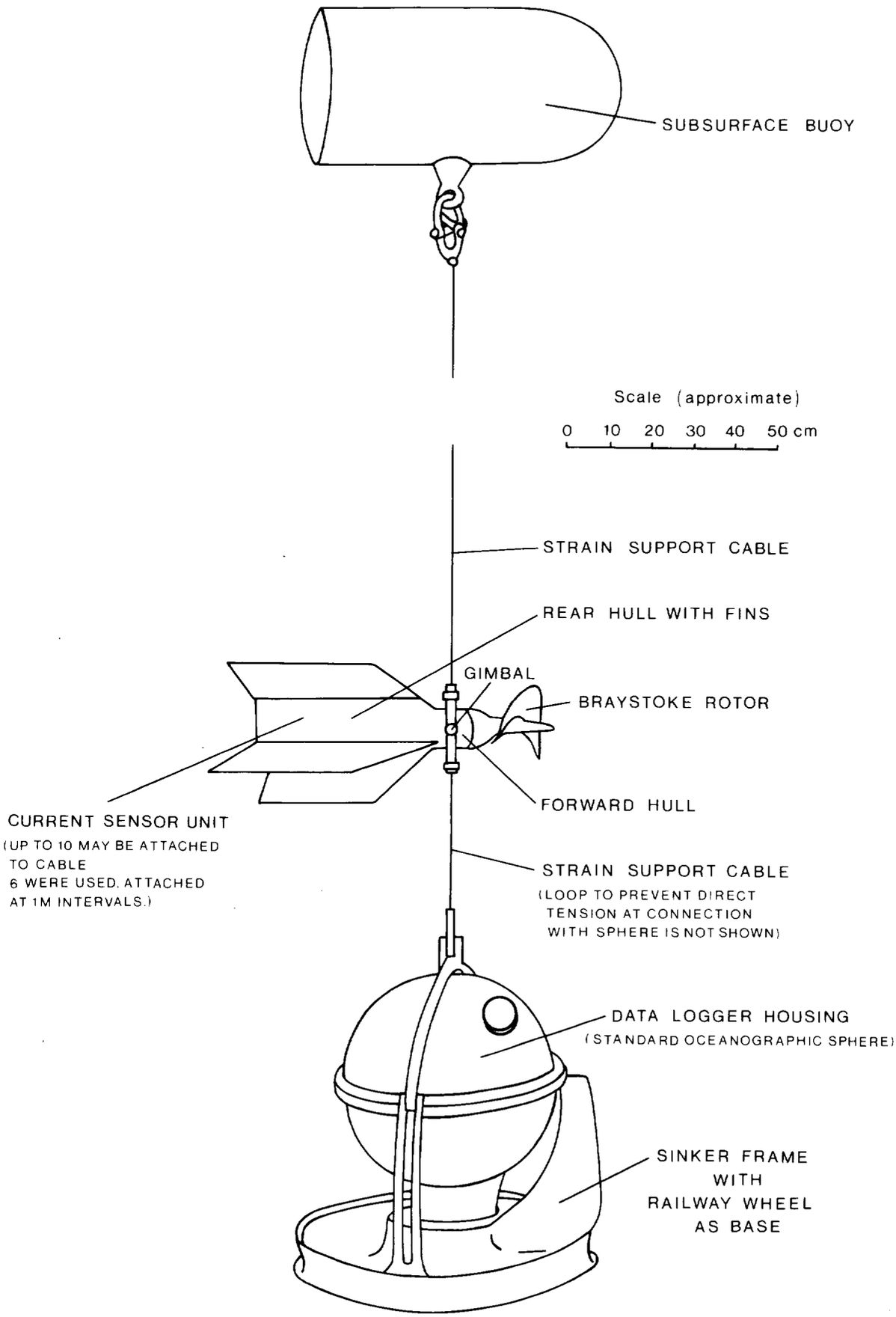

Figure 7 Marconi current meter system

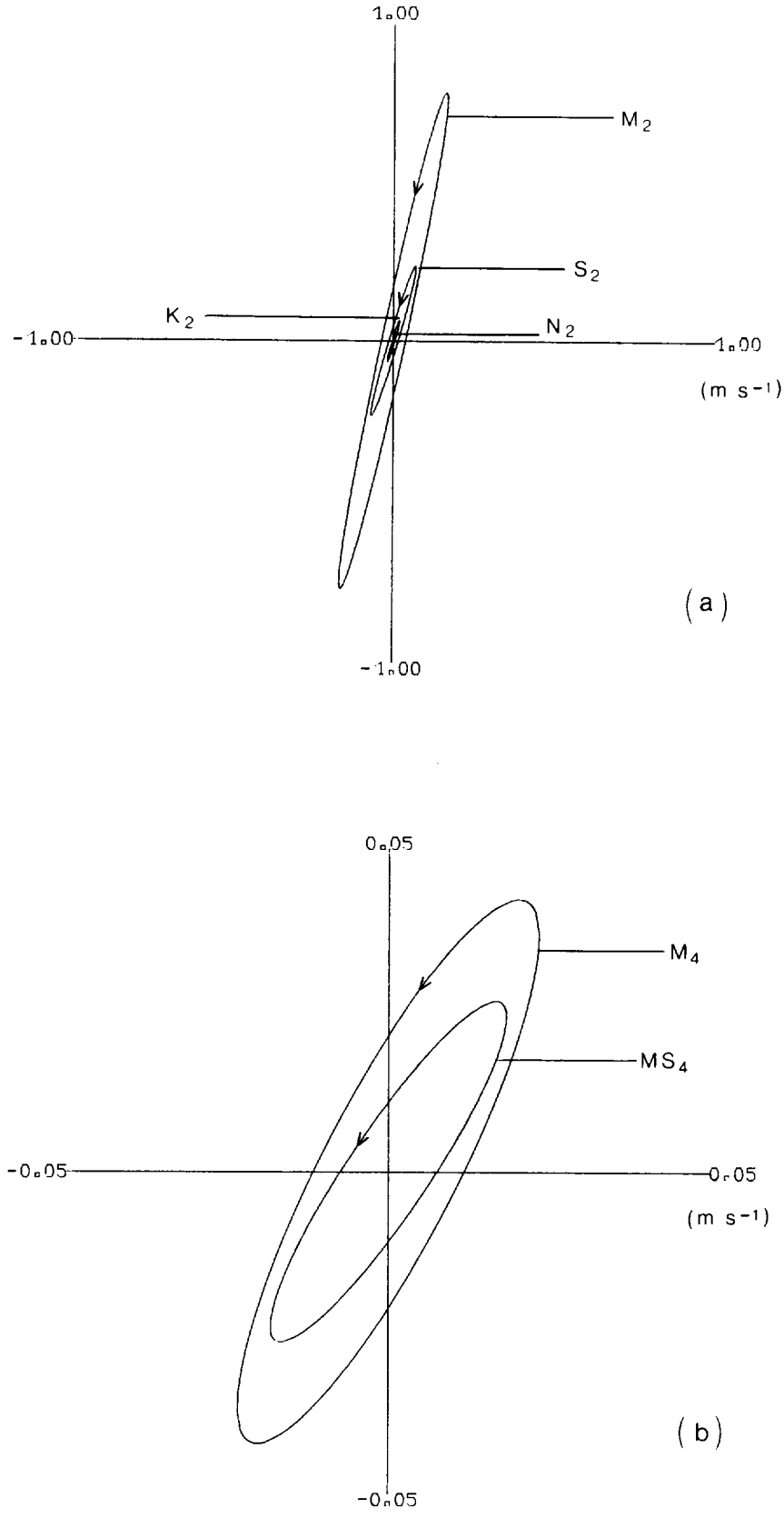

Figure 8 Tidal ellipses for the principal semi-diurnal (a) and quarter-diurnal (b) in the mid-depth currents Station A in the Sizewell-Dunwich Banks area (record 238H6).

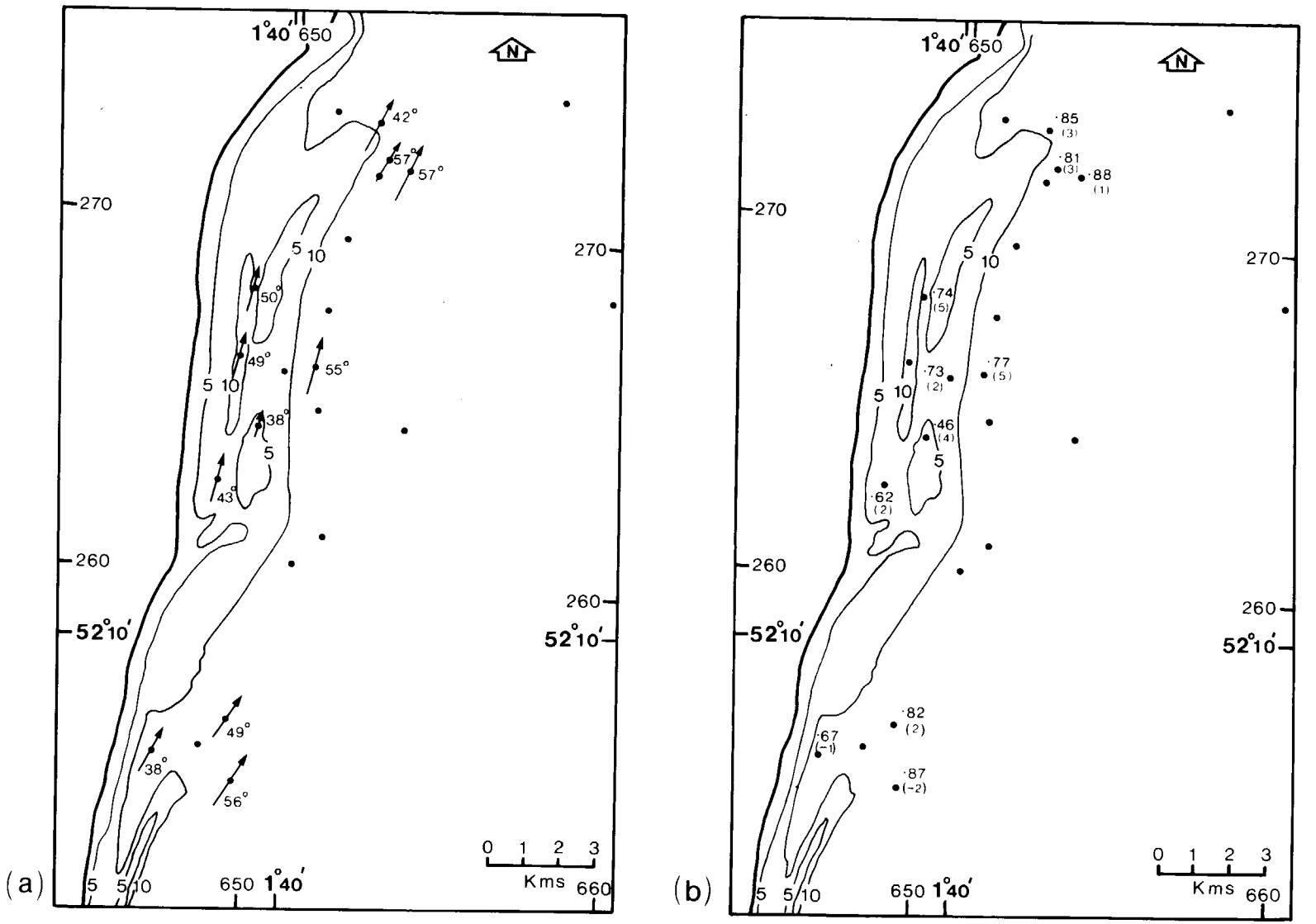

Figure 9 M_2 tidal current, ellipse data: (a) orientation with arrow indicating direction of flow corresponding to given phases, shown in degrees relative to the equilibrium tide at Greenwich (direction shown corresponds to the ebb tide); (b) M_2 tidal stream amplitudes ($m\ s^{-1}$) and, in brackets, the ellipticities expressed as a percentage. Positive and negative values correspond to anticlockwise and clockwise rotations respectively.

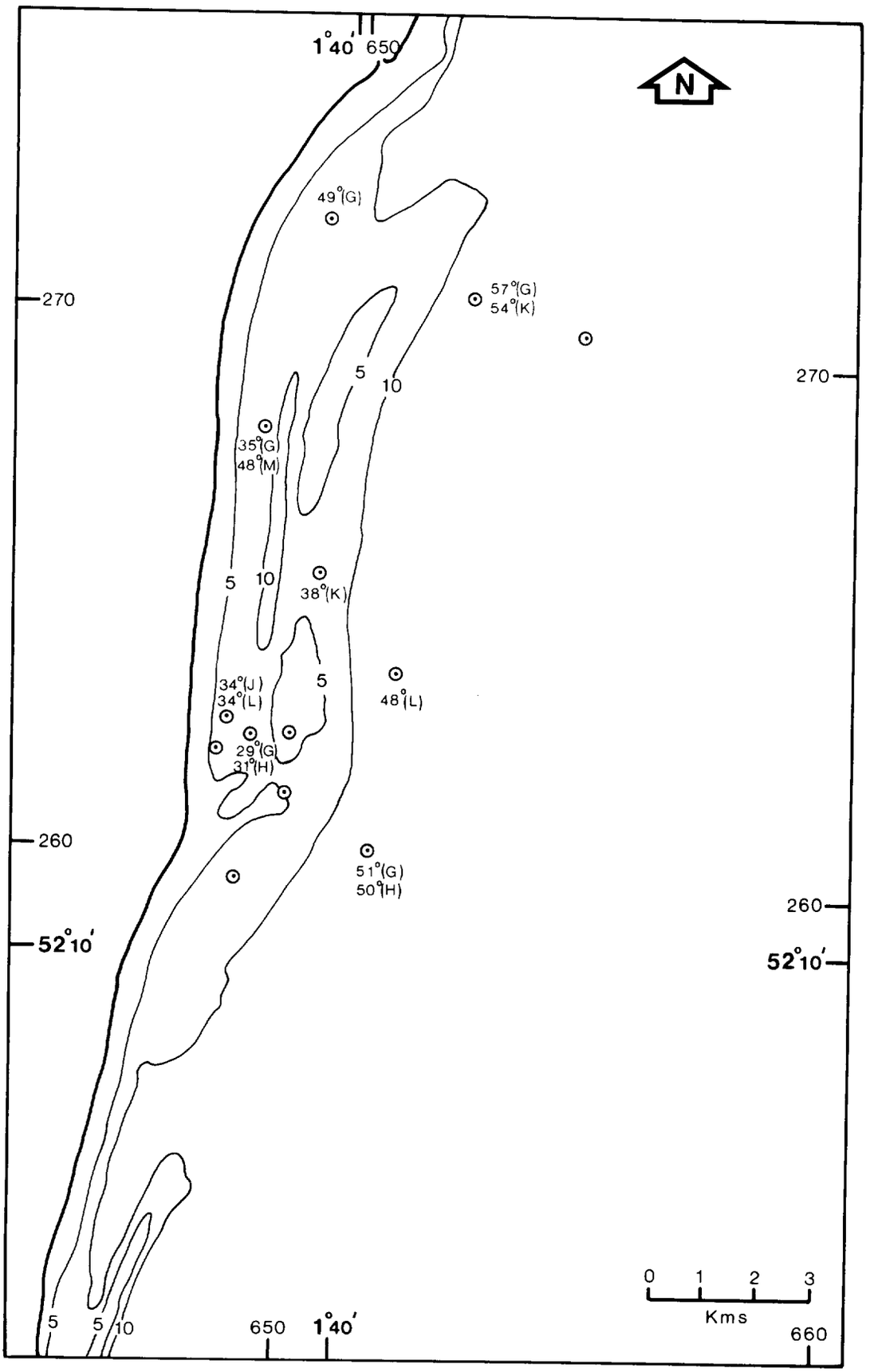

Figure 10 M_2 tidal current phases, for north flowing component only, after Macqueen and Parker (1979). Phases are in degrees relative to the equilibrium tide at Greenwich and the letters in brackets indicate the month of the year in which the measurements were made (see Table 1).

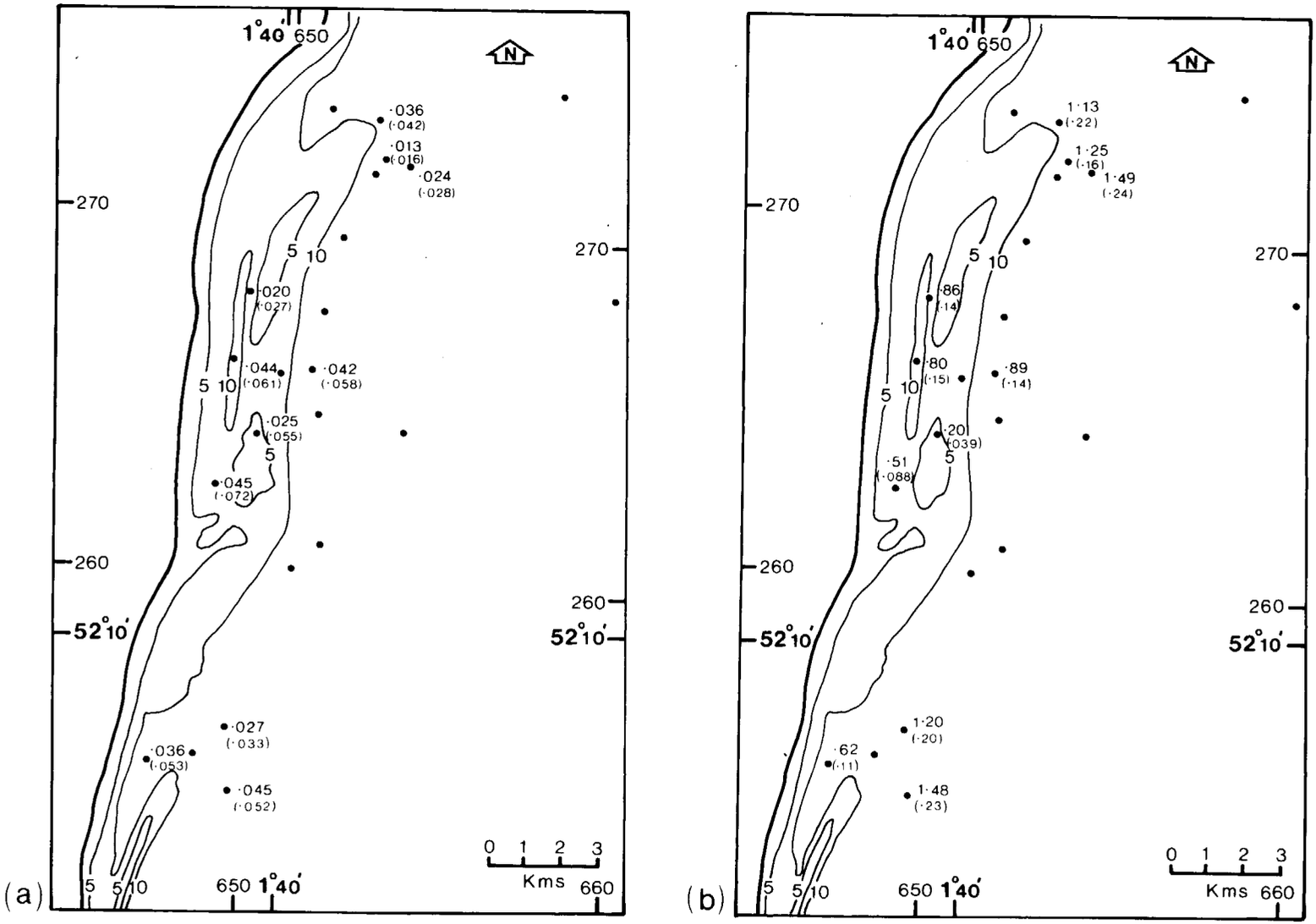

Figure 11 (a) Amplitude of M_4 tidal currents (m s^{-1}) and in brackets M_4/M_2 tidal current ratio; (b) Tidal stream amplitude cubed at Springs, ie $(M_2 + S_2)^3$ and, in brackets, at Neaps, ie $(M_2 - S_2)^3$.

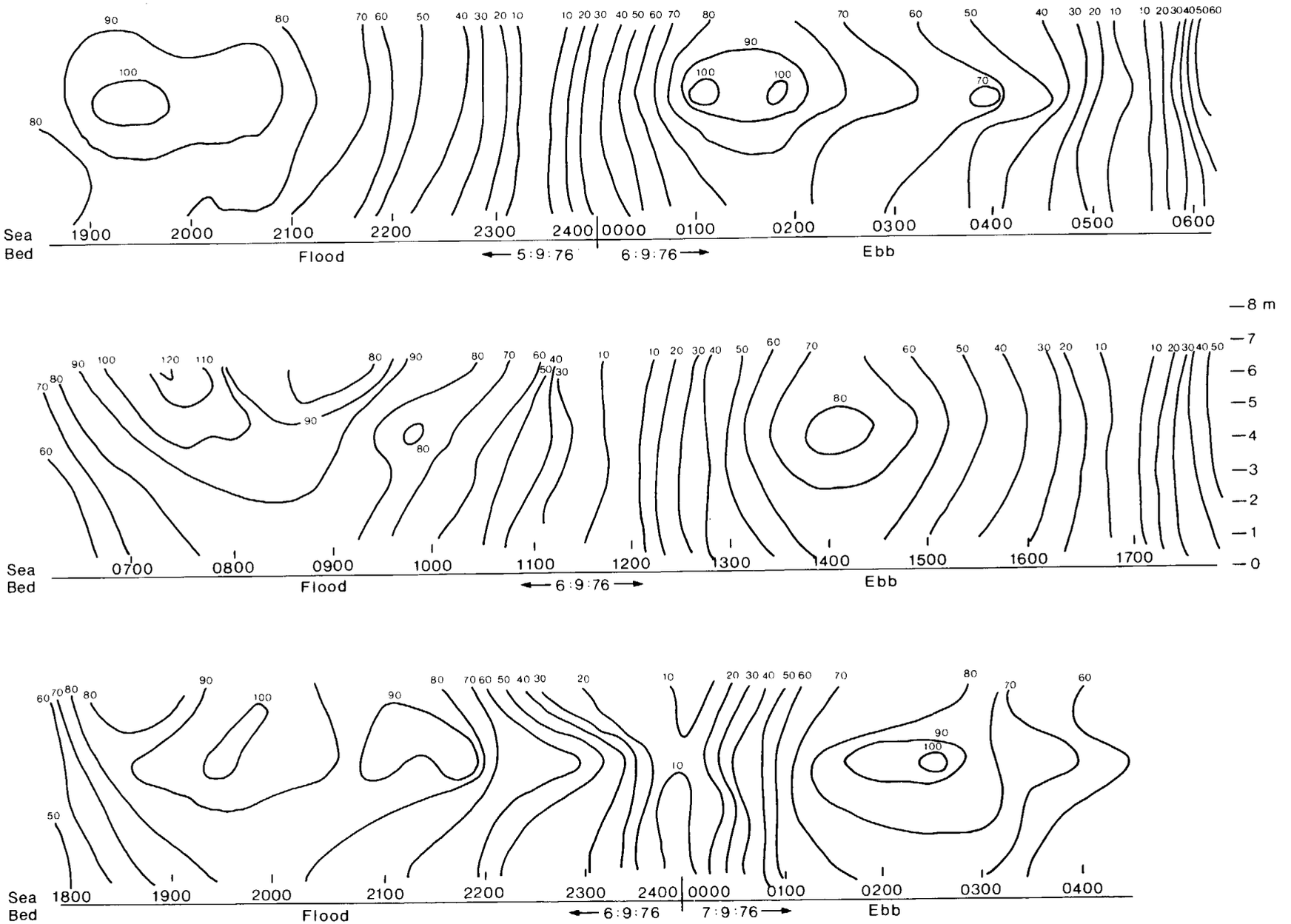

Figure 12 Variation in the velocity structure of tidal currents inshore of the Dunwich Bank (Figure 3) from the Marconi current meter mooring. Isopleths are in cm s^{-1}.

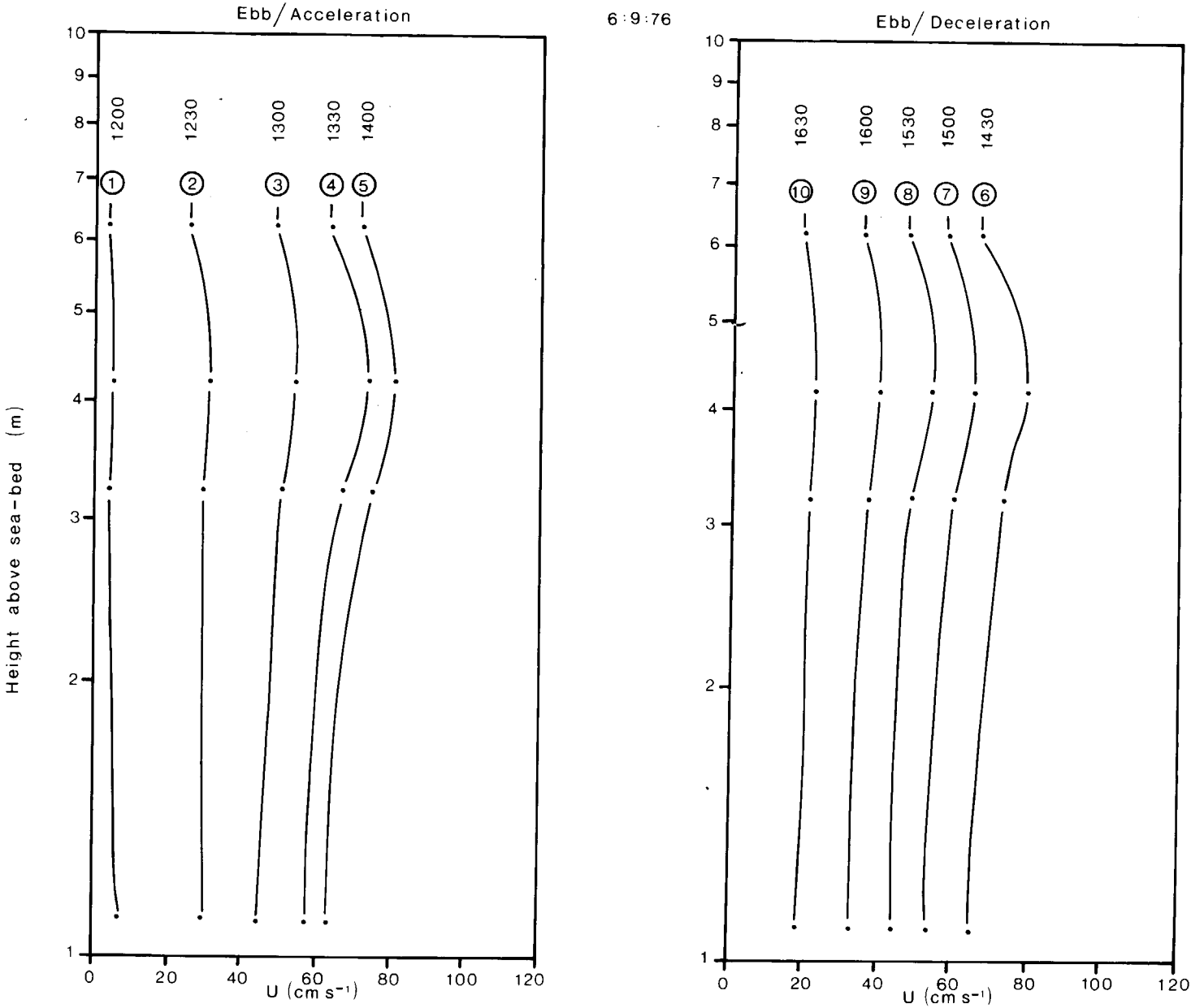

Figure 13 Velocity profiles during the accelerating and decelerating phases of the ebb tide, inshore of the Dunwich Bank (Figure 3), from the Marconi current meter mooring.

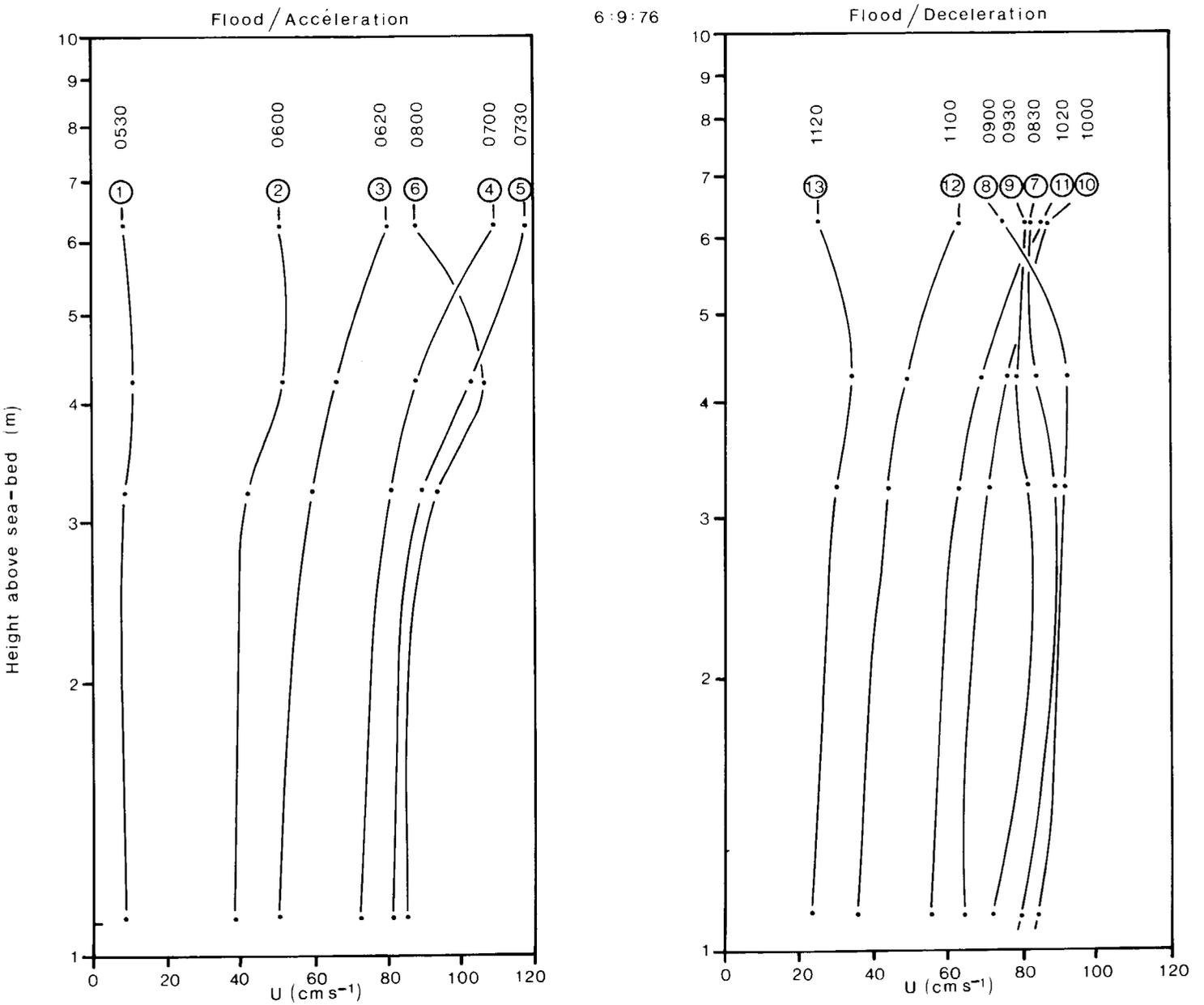

Figure 14 Velocity profiles during the accelerating and decelerating phases of the flood tide, inshore of the Dunwich Bank (Figure 3), from the Marconi current meter mooring.

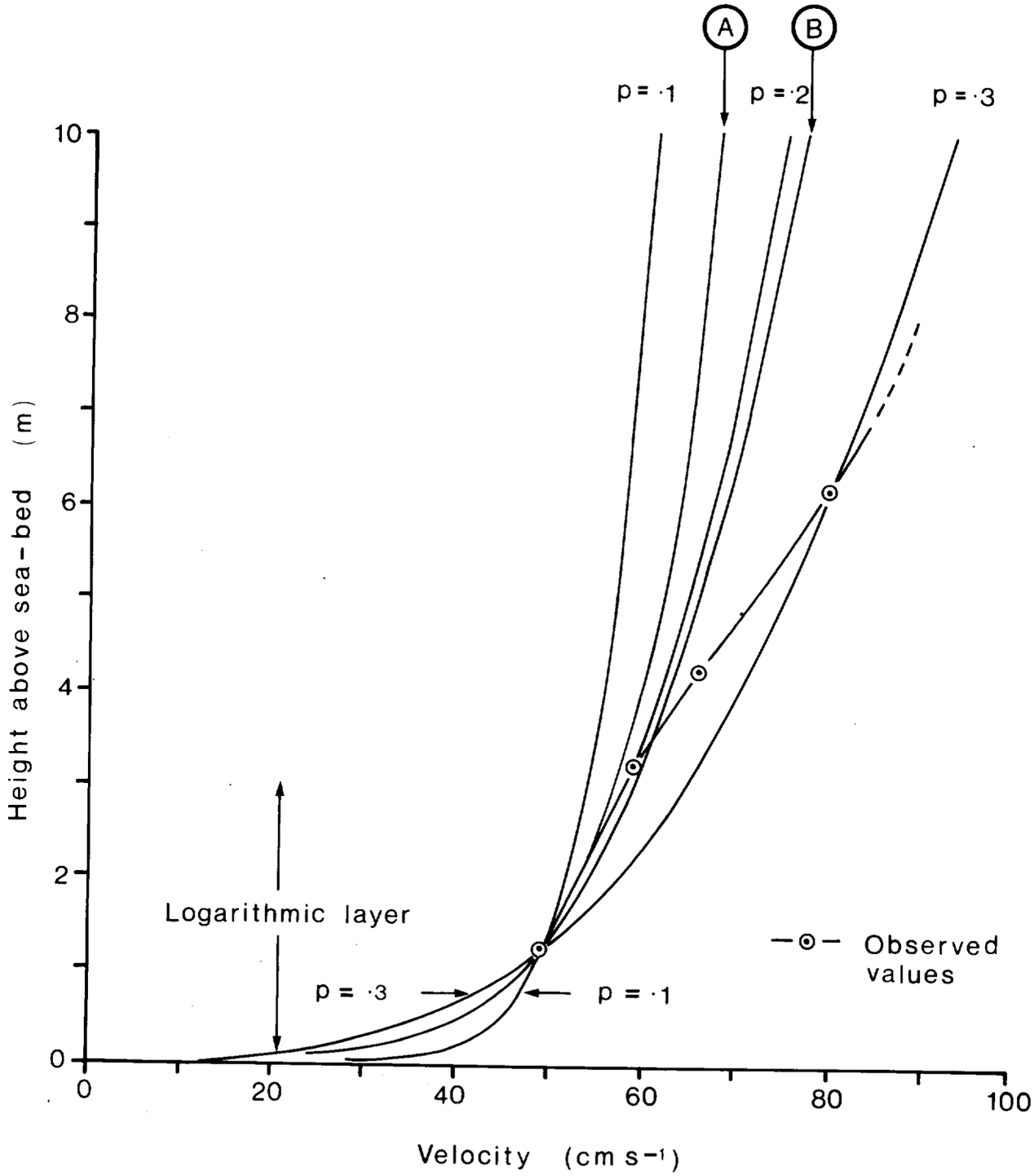

Figure 15 Power law velocity profiles for exponent values (Equation 13) of p = .1, .2 and .3. Also shown are (A) a logarithmic velocity profile (Equation 12) and velocity profile (B) given by Cole's Wake law (Equation 14). For clarity the power law profile for p = .2 is not shown below 1 m and curves(A) and (B) are coincident.

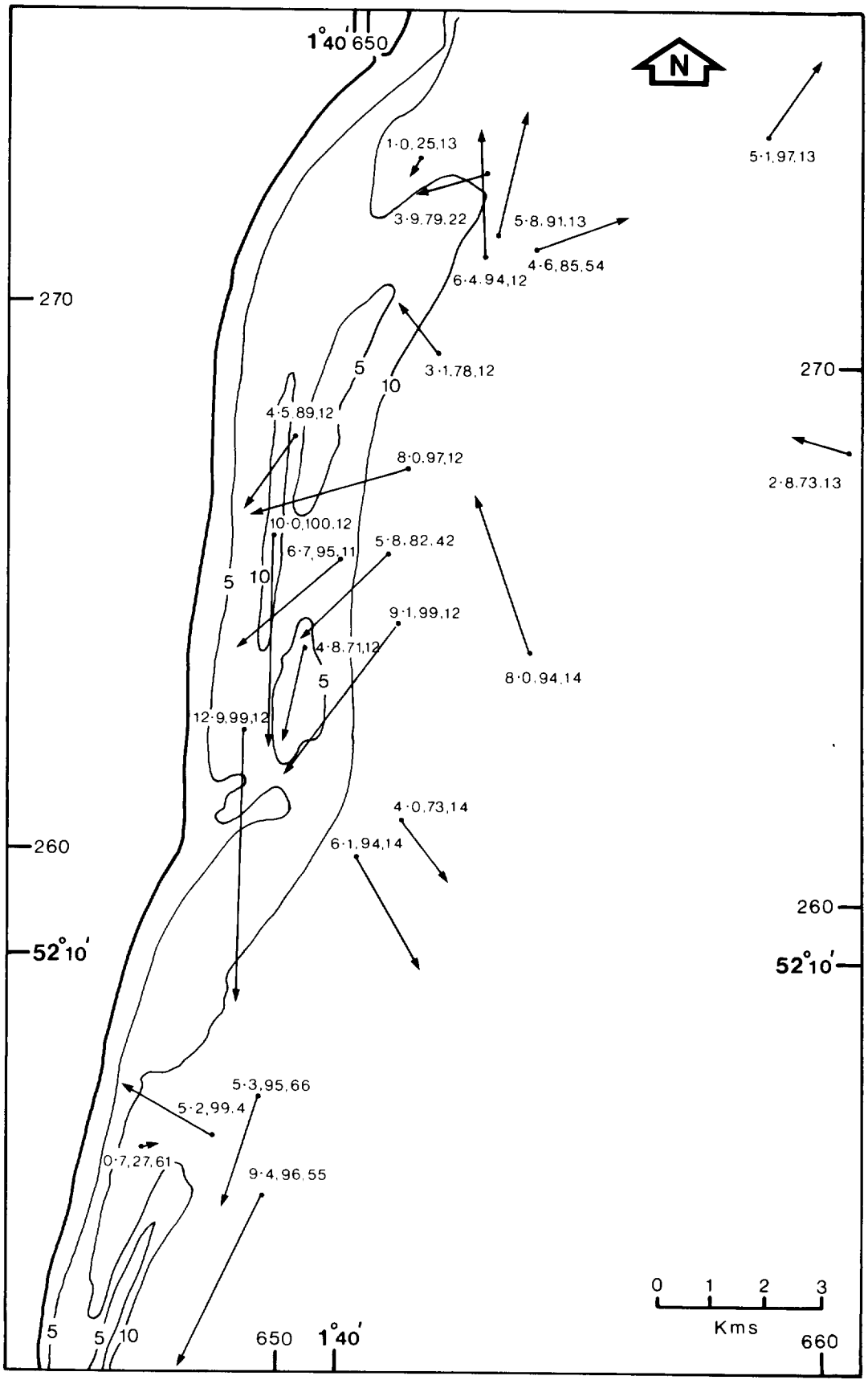

Figure 16 Summary of mid-depth tidally induced residuals. Residual flow data have been presented in the manner suggested by Ramster et al (1978) and each set of figures shows; the residual flow speed in cm s^{-1}; the steadiness factor as a percentage; the length of the record in days (in that order).
NB: These data are not synoptic.

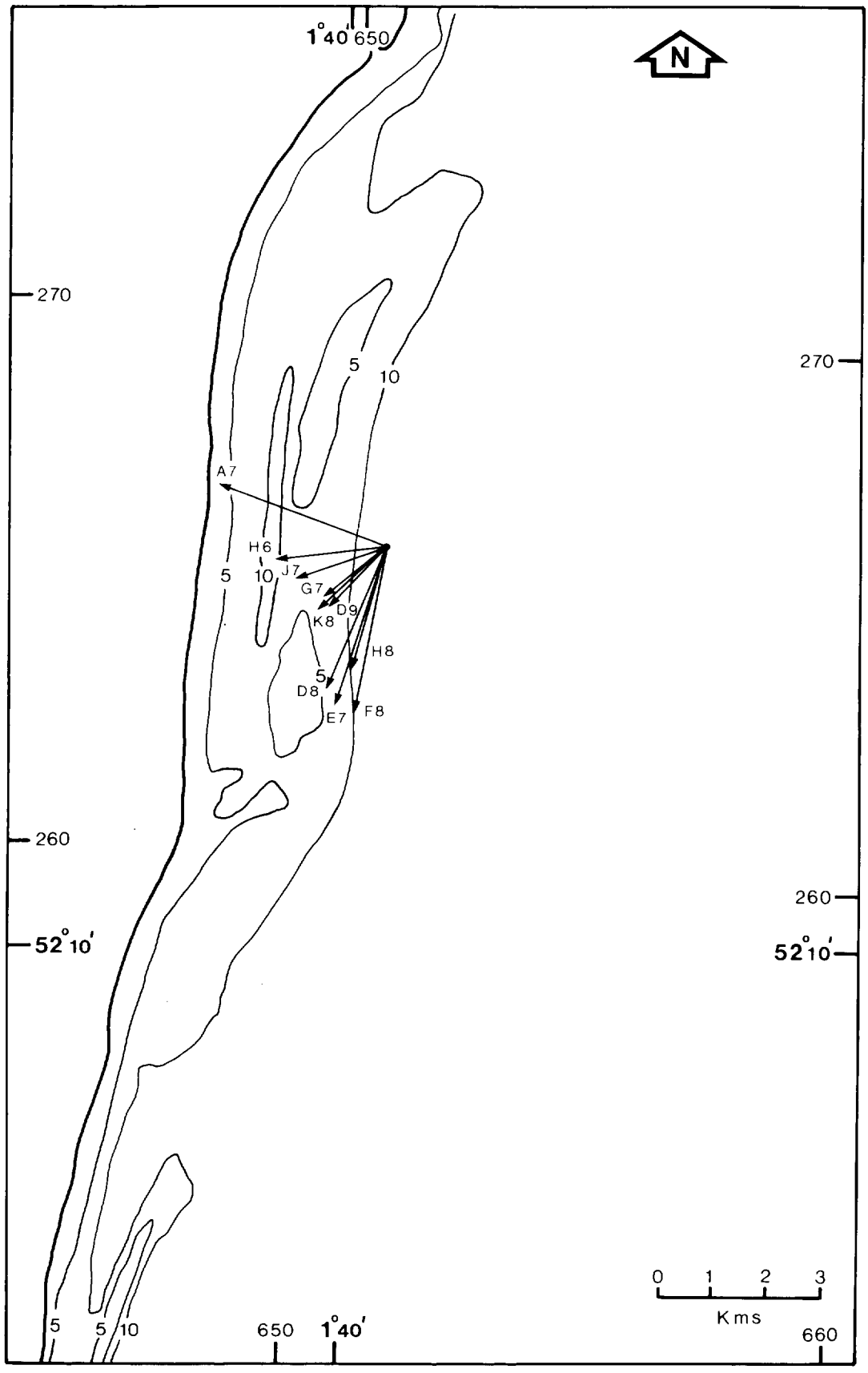

Figure 17 Mid-depth residual flow measurements at Station A. For clarity record K6 has been omitted; details of this and other records are given in Table 1.

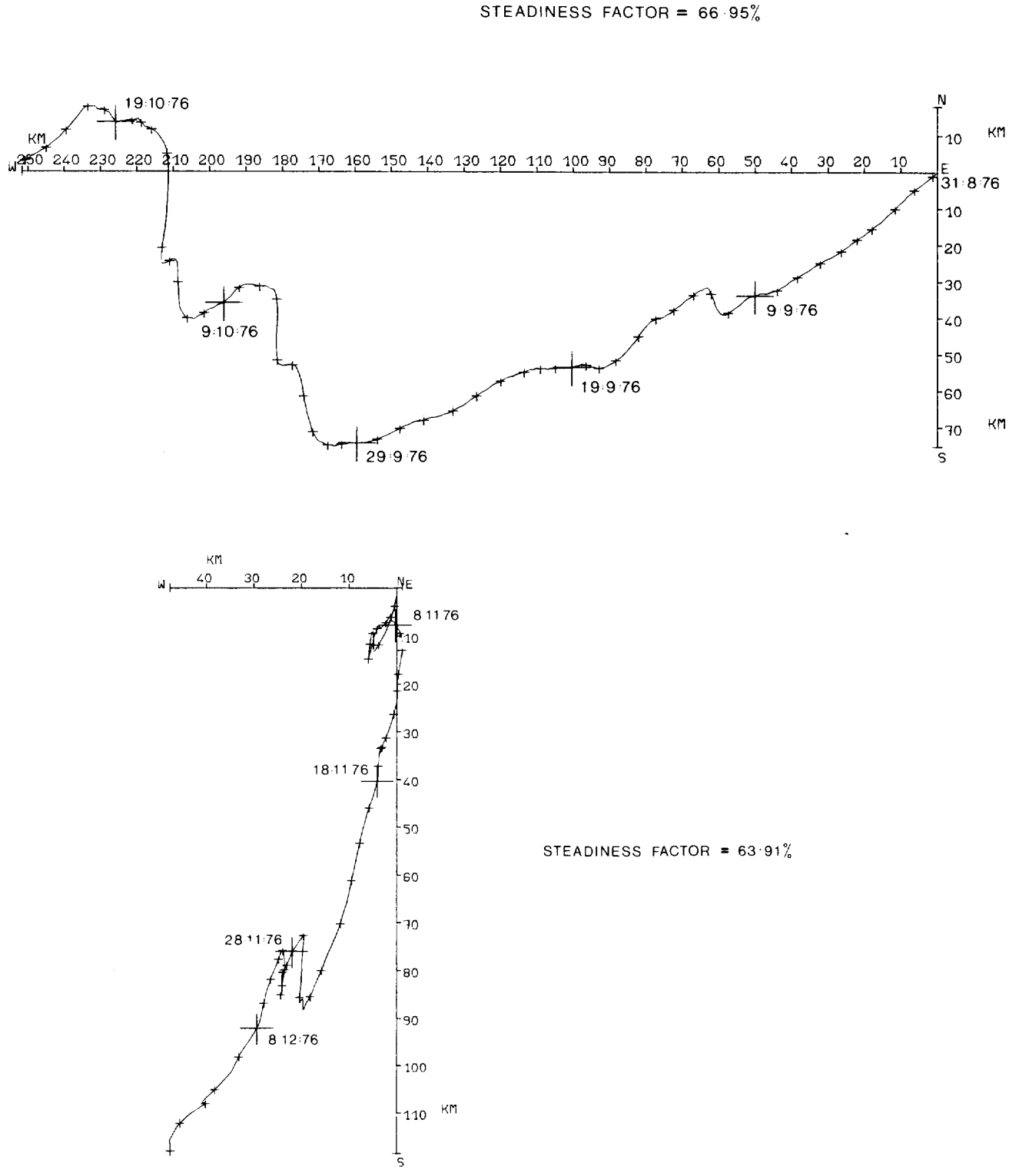

Figure 18 Progressive vector plots from Station A showing the residual flow at 6 m above the seabed during September and October 1976 (top) and October and November 1976 (bottom).

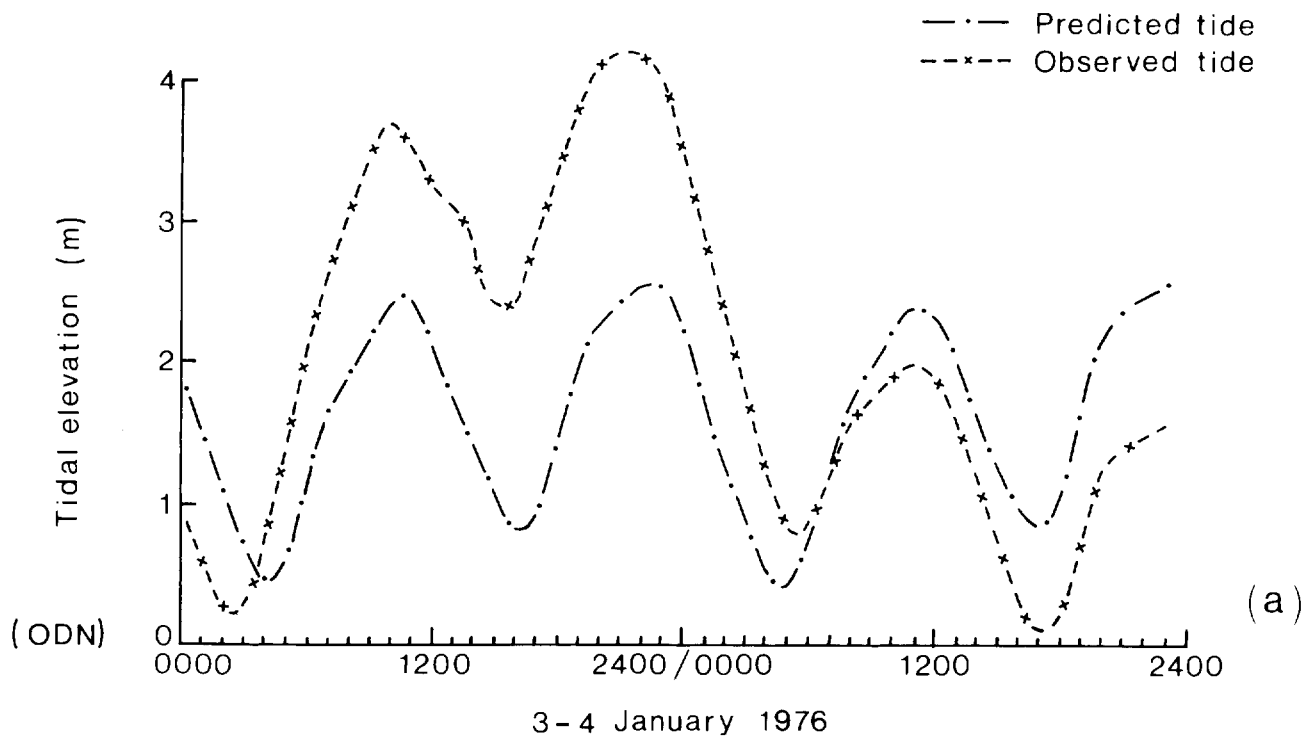

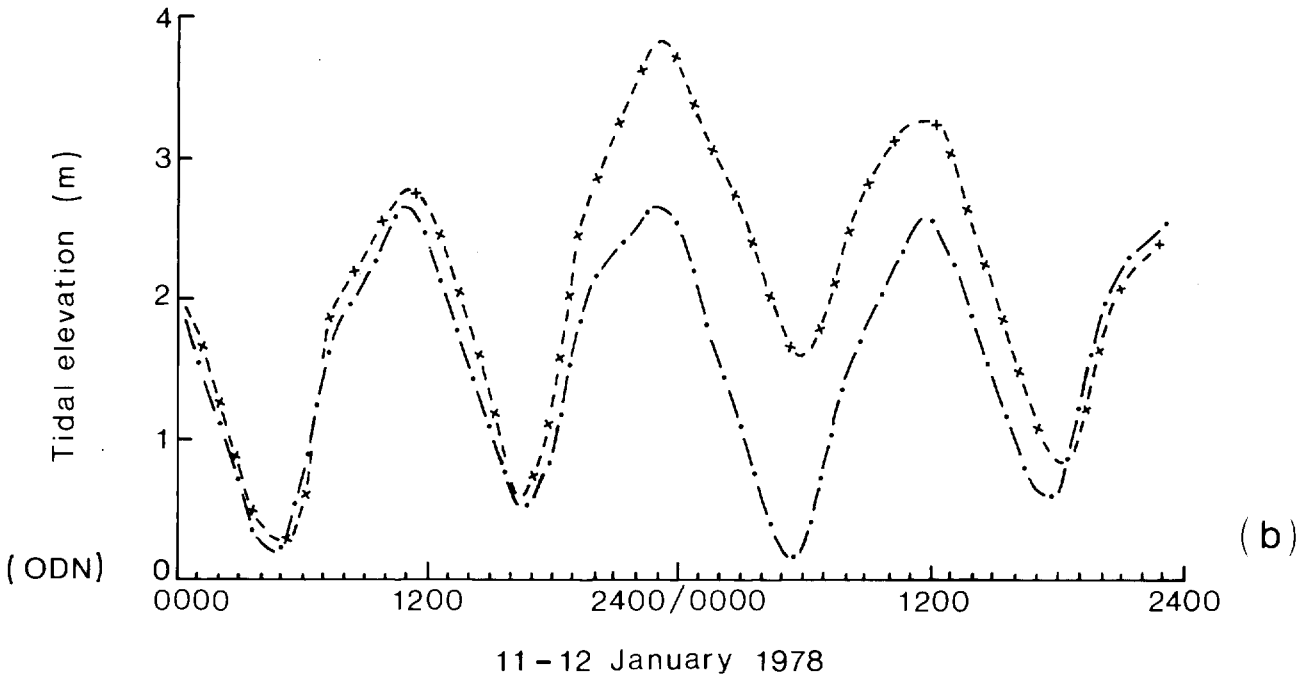

Figure 19 Observed and predicted tides at Lowestoft during storm surges in January 1976 and January 1978.

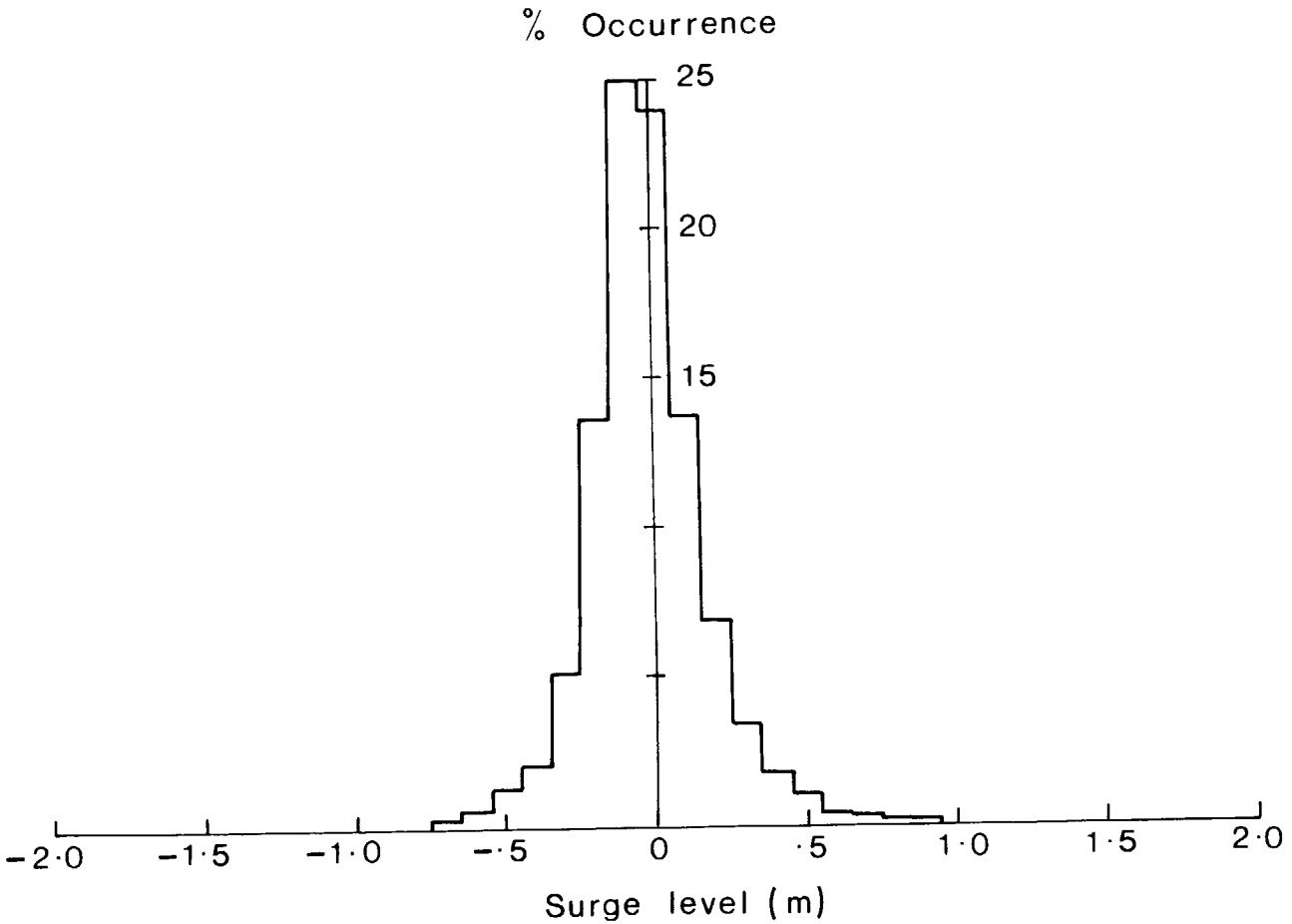

Figure 20 Analysis of hourly differences between observed and predicted tides at Lowestoft for the years 1975-1979.

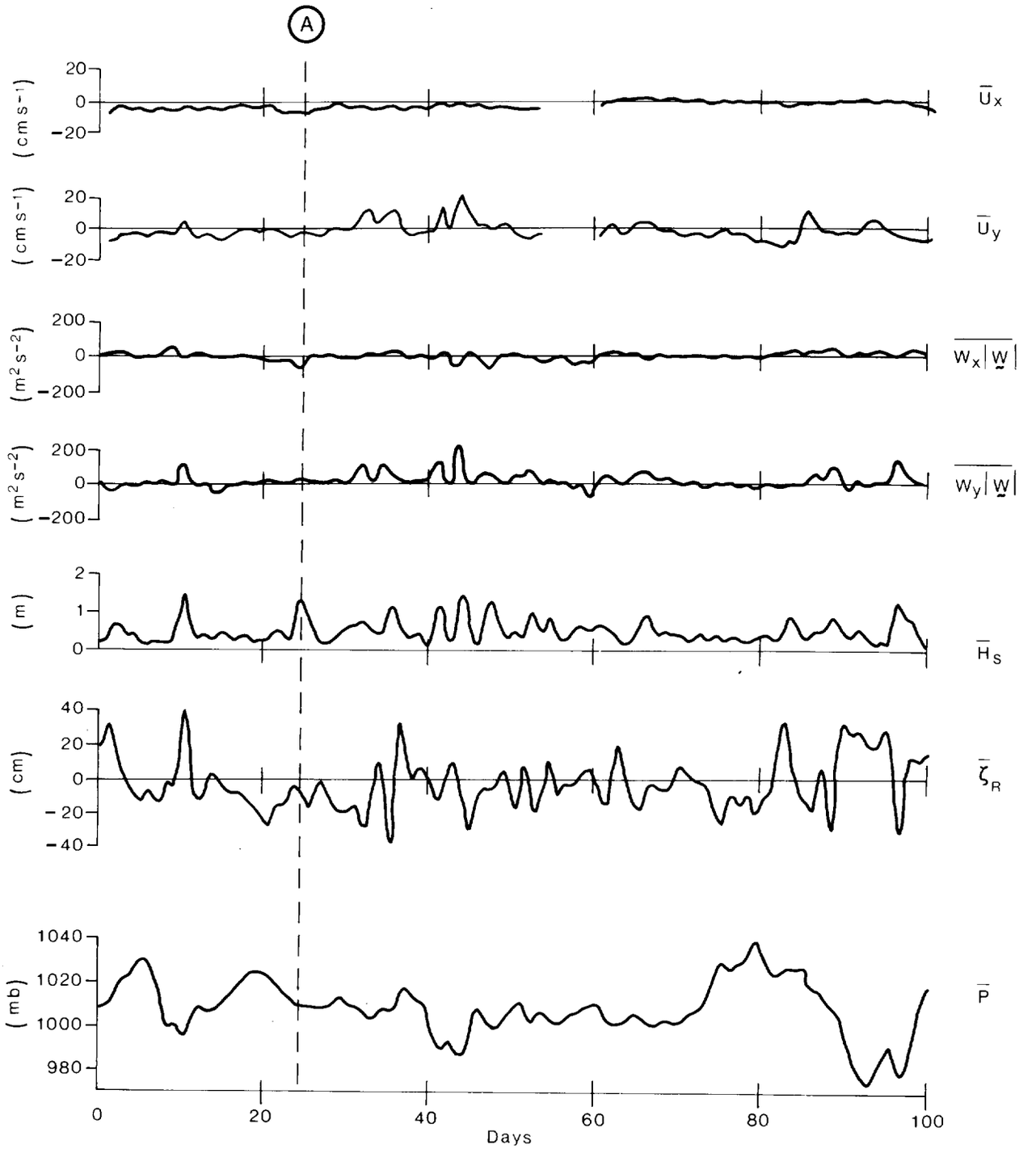

Figure 21 Daily means of the offshore and alongshore components of the tidal residuals ($\bar{U}_x$, $\bar{U}_y$) and the wind stress (as $\overline{W_x|\underline{W}|}$, $\overline{W_y|\underline{W}|}$). Also shown are daily means of the significant wave height ($\bar{H}_S$), from a Waverider outside the Dunwich Bank (Figure 3), the residual tidal elevations ($\bar{\zeta}_R$) at Lowestoft (observed tide minus predicted tide) and atmospheric pressure ($\bar{P}$) at Gorleston. Residual currents were measured at Station A and (A) marks a low wind stress event with high waves having no effect on the residual currents. Data correspond to the period September-December 1976.

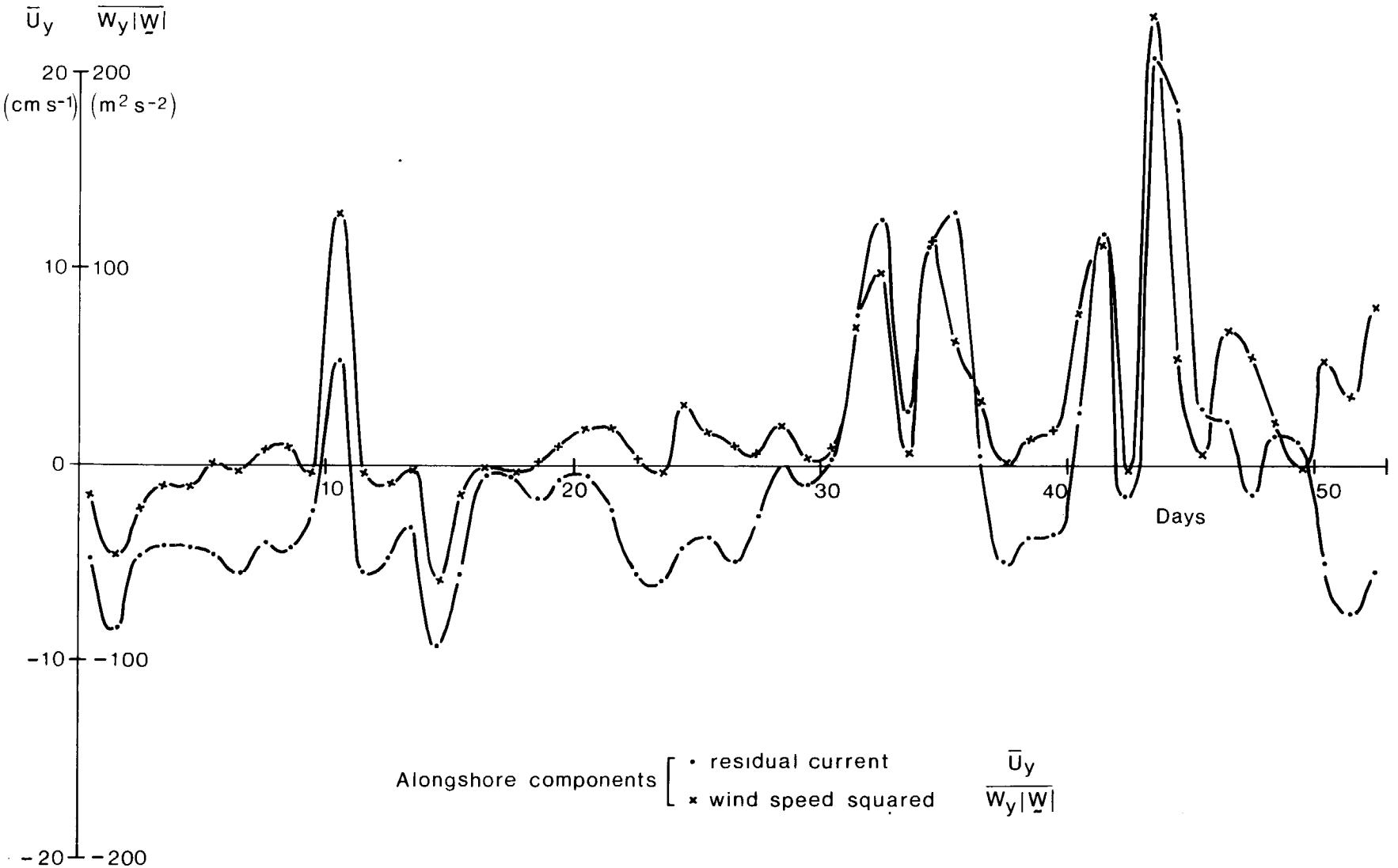

Figure 22 53 day data set illustrating the correlation between daily mean values of the alongshore residual currents ($\bar{u}_y$) and the wind stress (as $\overline{W_y|\underline{W}|}$). Residual currents were measured at Station A and these results correspond to the first 53 days of data shown in Figure 21.

APPENDIX A

Smoothed progressive vector diagrams for residual water movements in the Sizewell-Dunwich Banks area. B is the steadiness factor expressed as a percentage. See also Table 13 and Figure 16.

Figure	Station
A1-9	A
A10	B
A11	C
A12-13	D
A14	E
A15	F
A16	G
A17	H
A18	J
A19	K
A20	L
A21	M
A22	N
A23	P
A24	Q
A25	R
A26	S
A27	T
A28	V
A29	W
A30	X
A31	Y
A32	Z

Note: the header code on each diagram indicates the following:

eg 238 : File name

12 1 7 : Date record starts

SD : Area (eg Sizewell-Dunwich Bank)

A : Station

6 M : Height above seabed

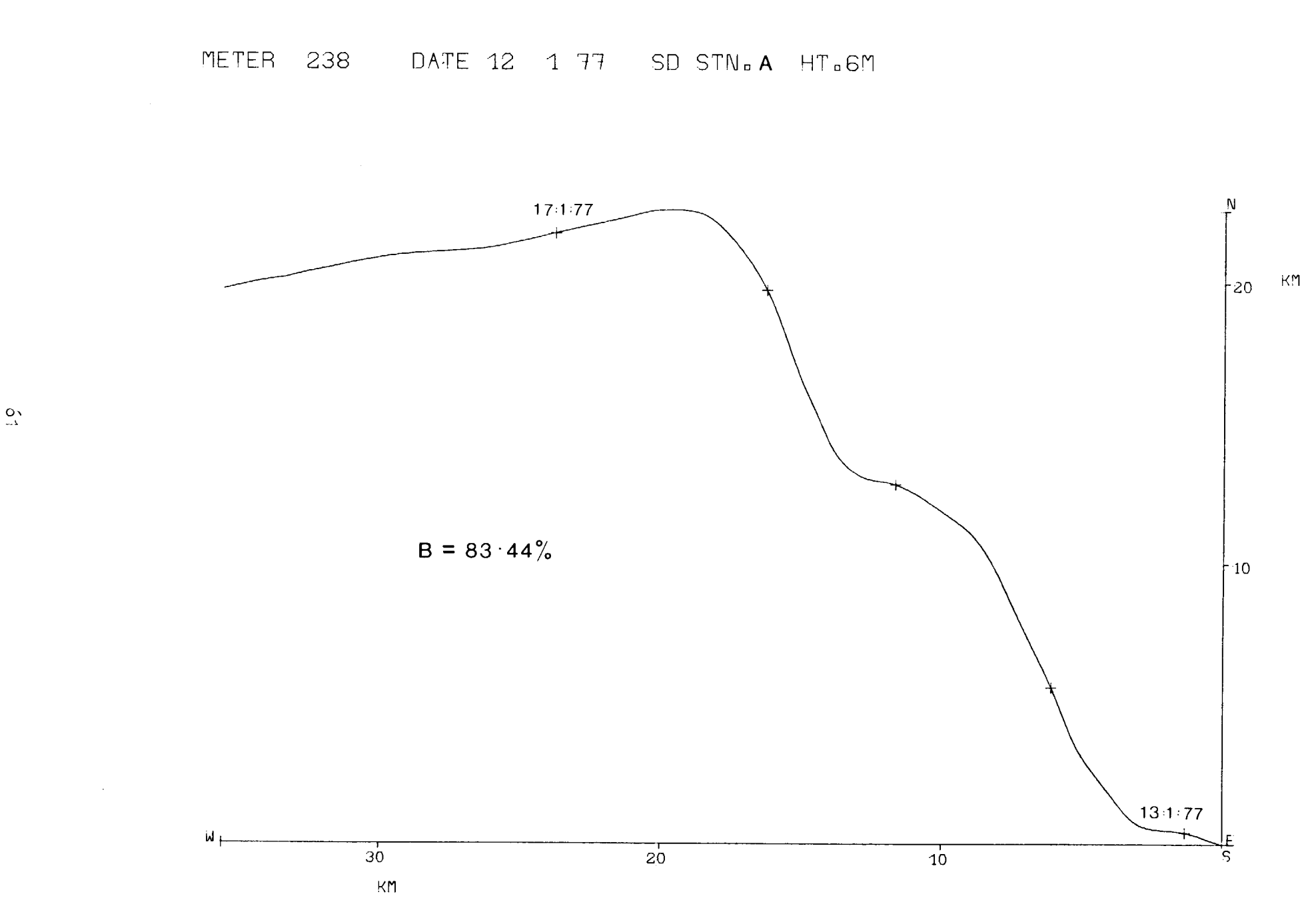
METER 238 DATE 12 1 77 SD STN. A HT. 6M
17:1:77
B = 83·44%
13:1:77
N
20
KM
10
W
30
20
10
S
E
KM

Figure A1

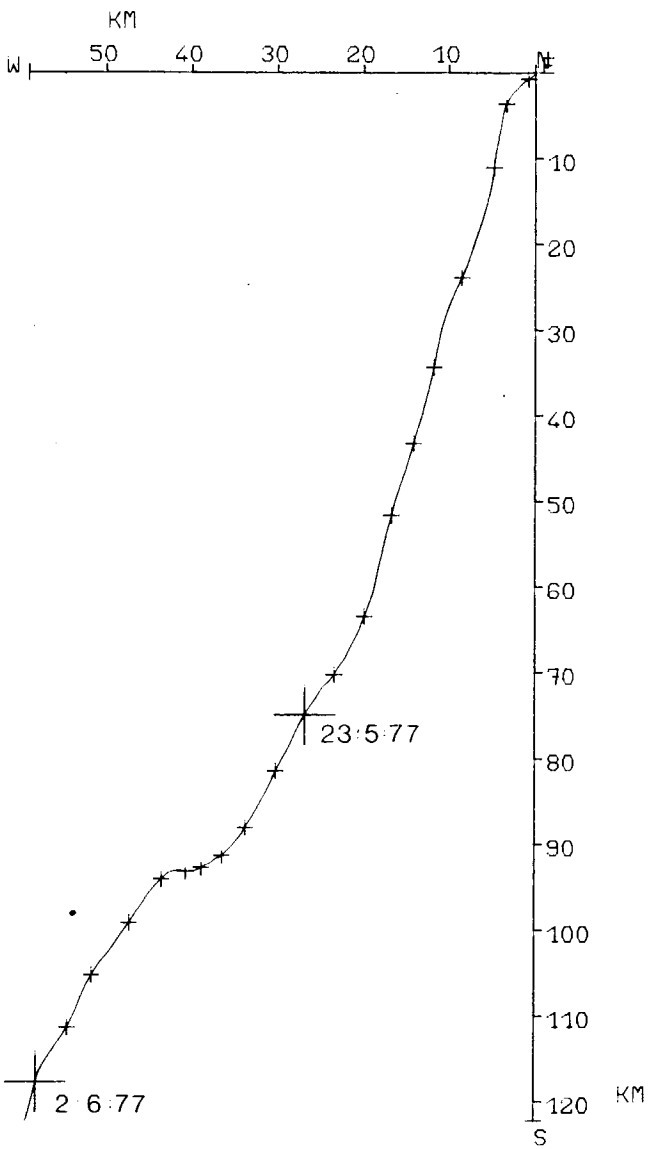

B = 97·23%

Figure A2

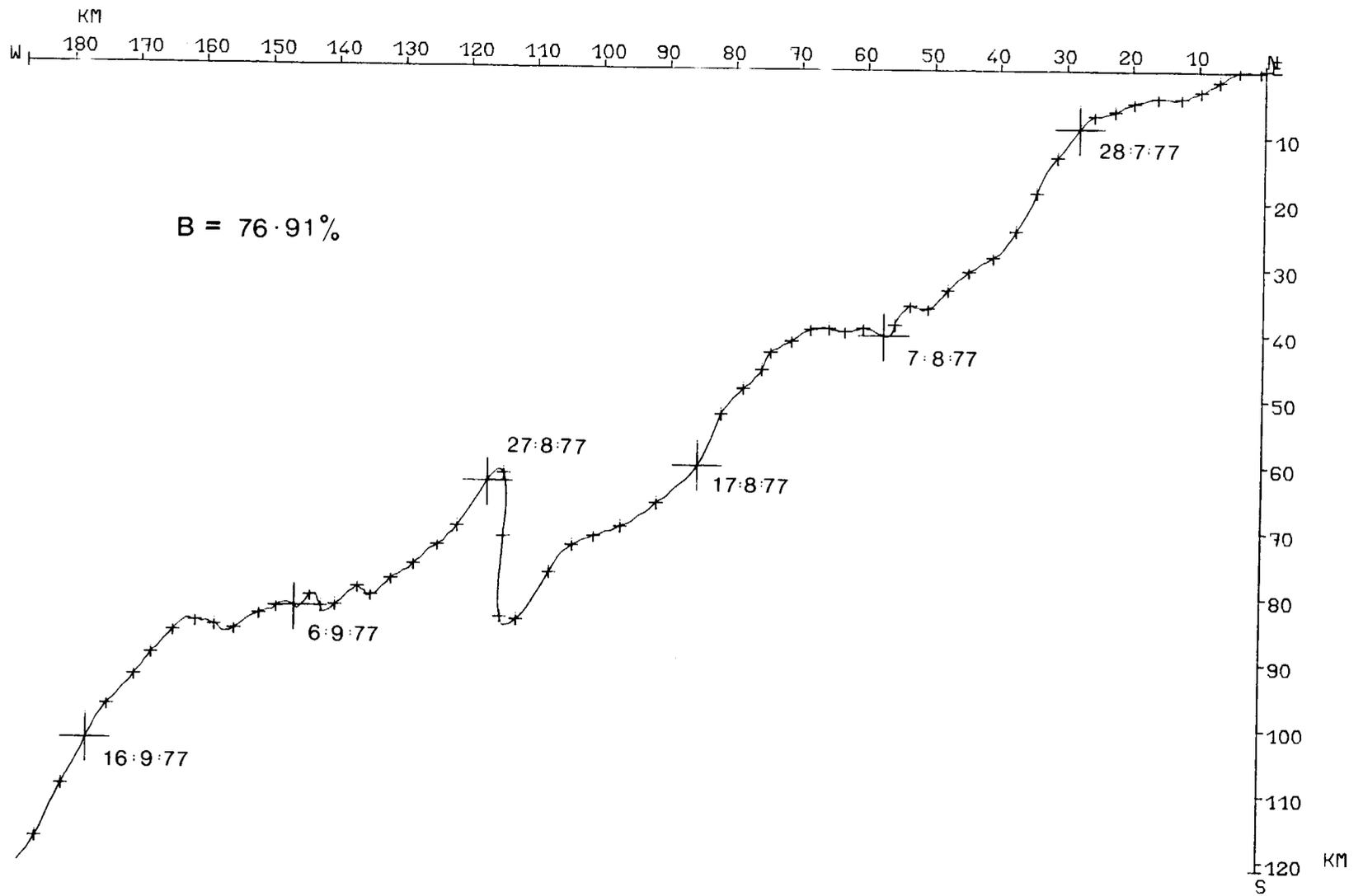
METER 238 DATE 18 7 77 SD STN. A HT. 6M
KM
W
180 170 160 150 140 130 120 110 100 90 80 70 60 50 40 30 20 10
N
B = 76·91%
28:7:77
7:8:77
17:8:77
27:8:77
6:9:77
16:9:77
10 20 30 40 50 60 70 80 90 100 110 120
KM
S

Figure A3

METER 629 DATE 19 9 77 SD STN. A HT. 6M

B = 72·42%

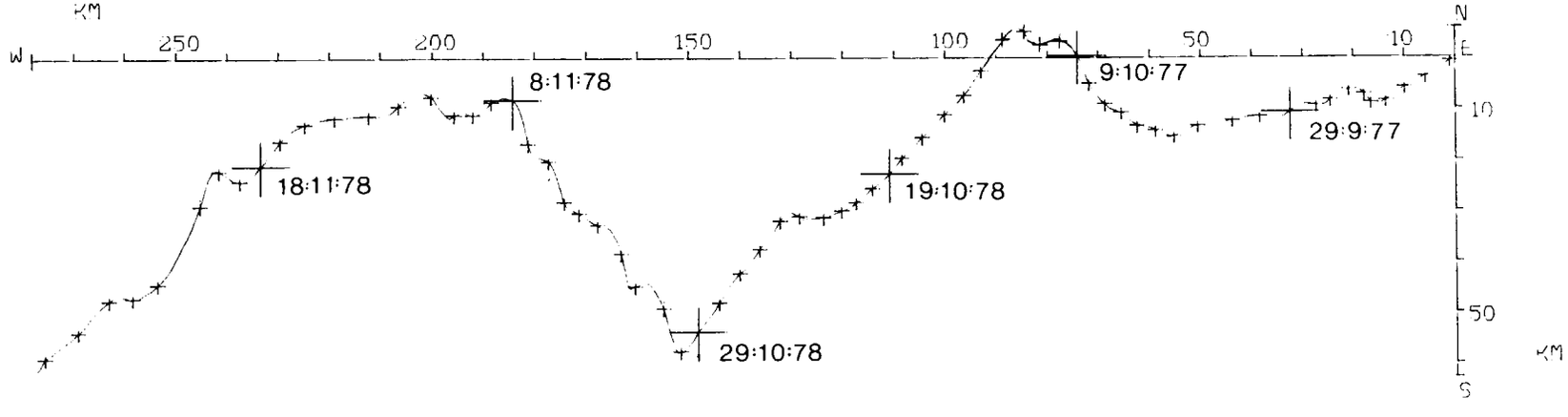

Figure A4

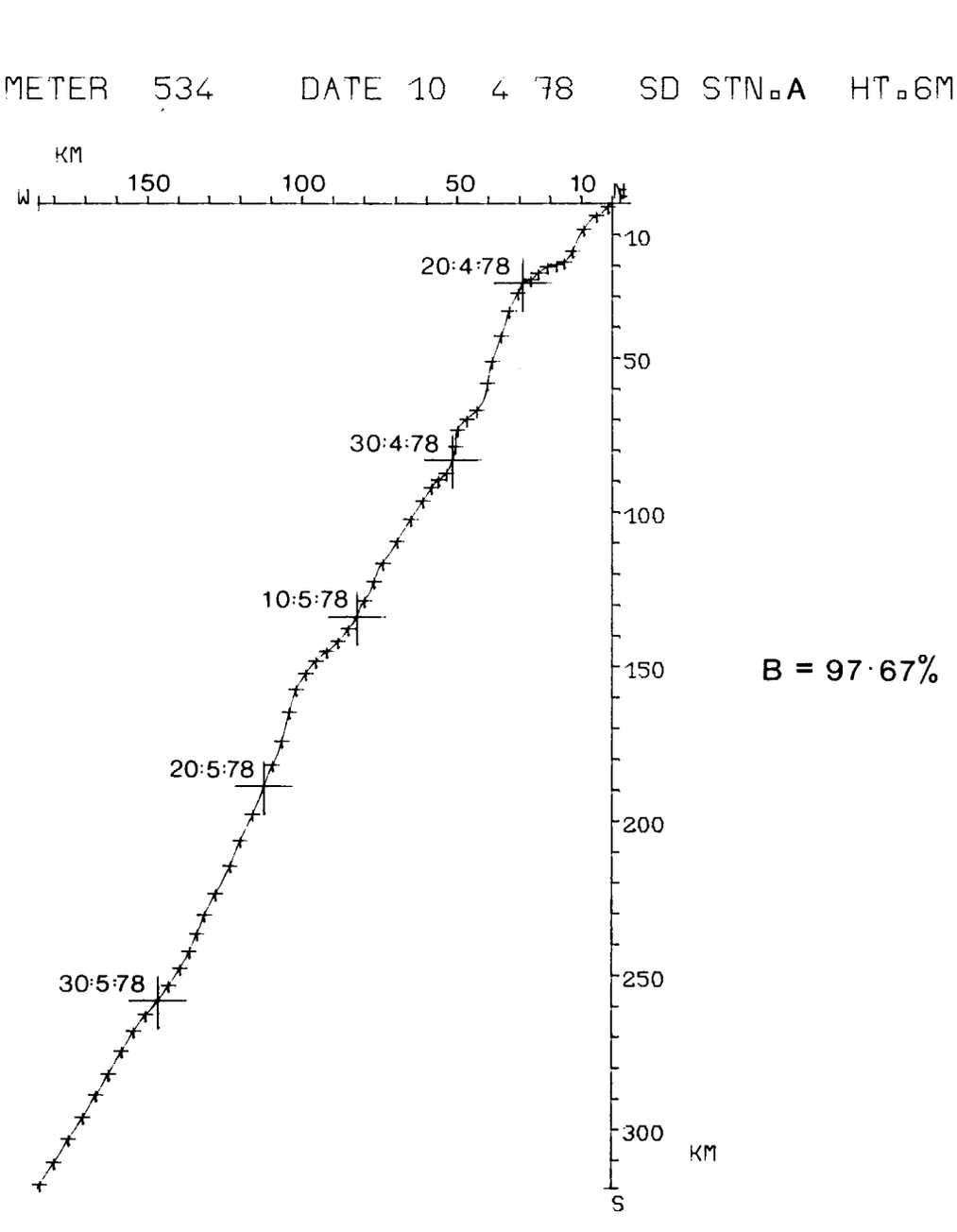
METER 534 DATE 10 4 78 SD STN. A HT. 6M
KM
W
150
100
50
10
N
10
50
100
150
200
250
300
KM
S
20:4:78
30:4:78
10:5:78
20:5:78
30:5:78
B = 97·67%

Figure A5

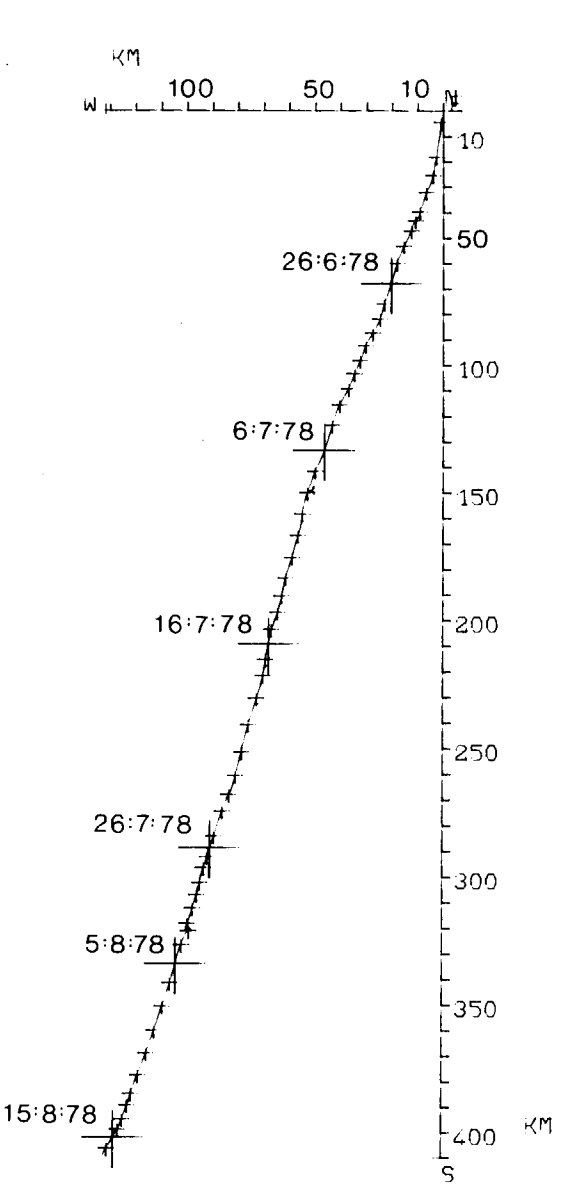

B = 98·41%

Figure A6

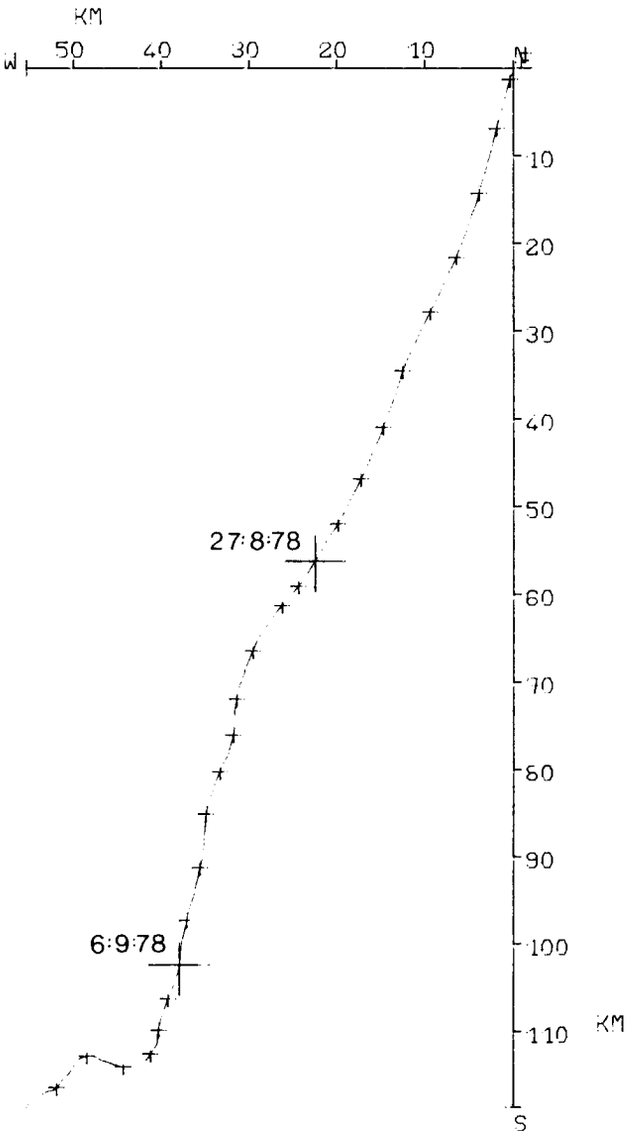

B = 95·69%

Figure A7

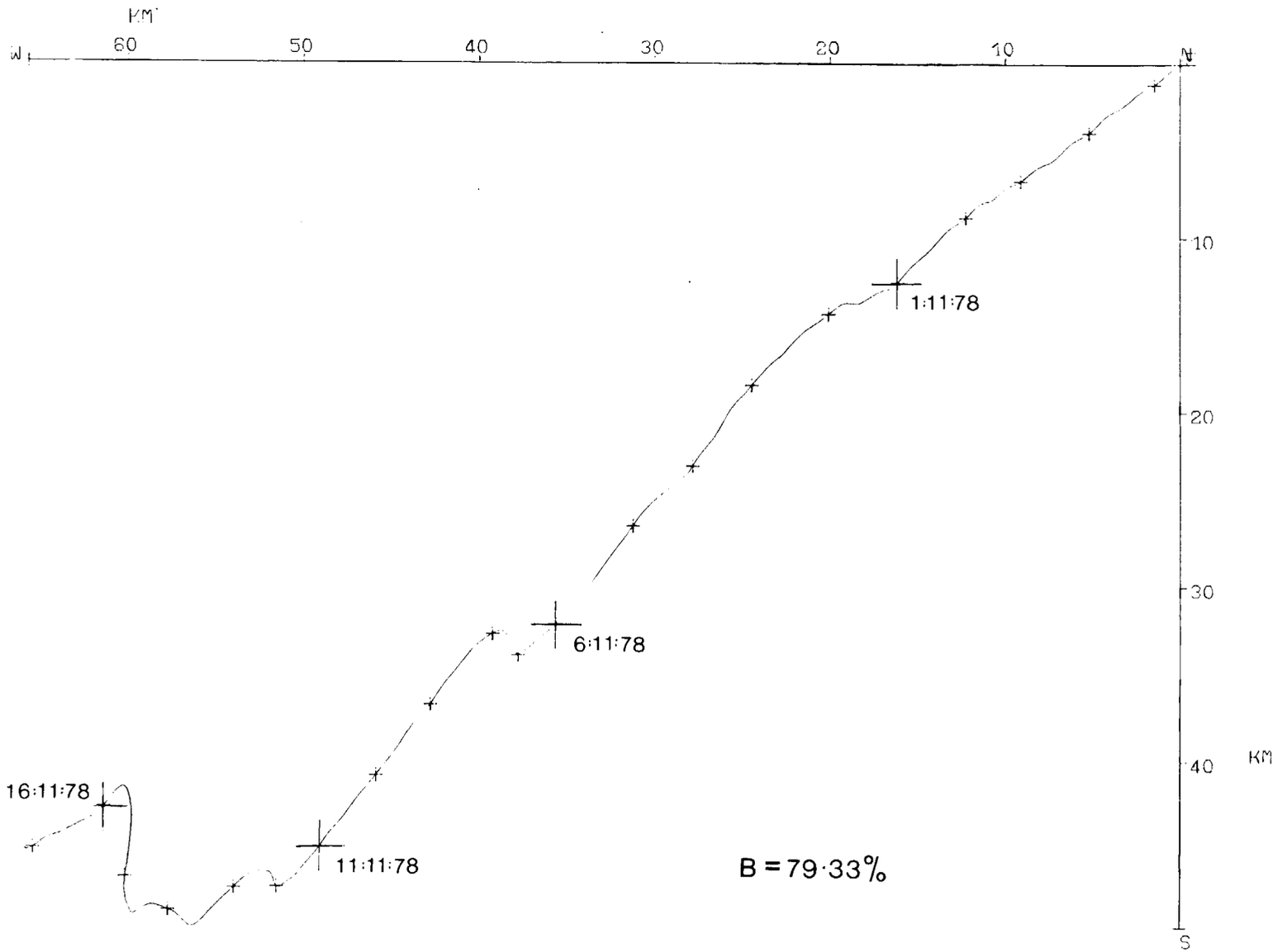
METER 560 DATE 27 10 78 SD STN. A HT. 6M
KM
60
50
40
30
20
10
W
N
S
10
20
30
40
KM
1:11:78
6:11:78
11:11:78
16:11:78
B = 79·33%

Figure A8

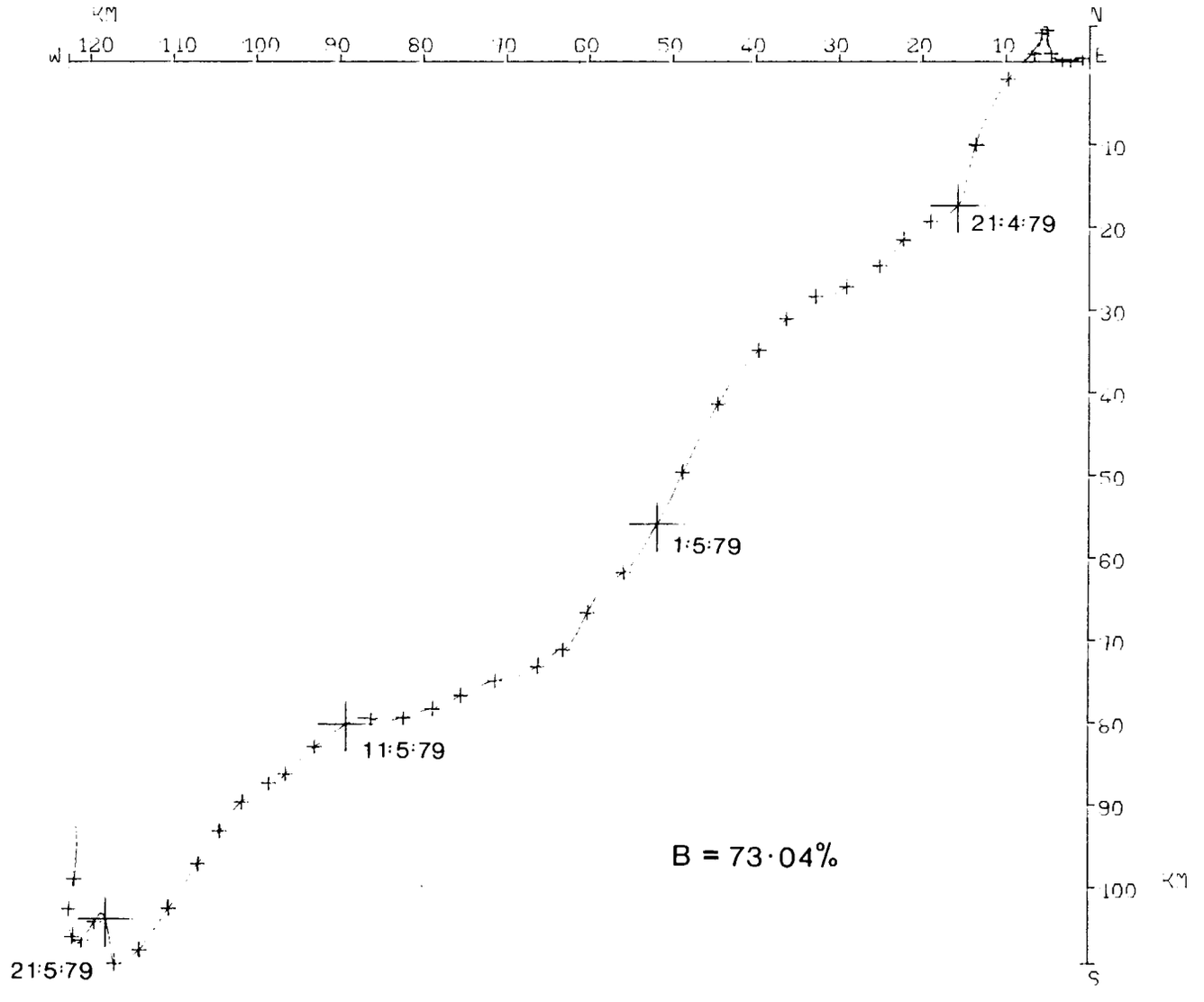
METER 534 DATE 11 4 79 SD STN.A HT.6M
KM
W 120 110 100 90 80 70 60 50 40 30 20 10 E
N
10
20
30
40
50
60
70
80
90
100
KM
S
21:4:79
1:5:79
11:5:79
21:5:79
B = 73·04%

Figure A9

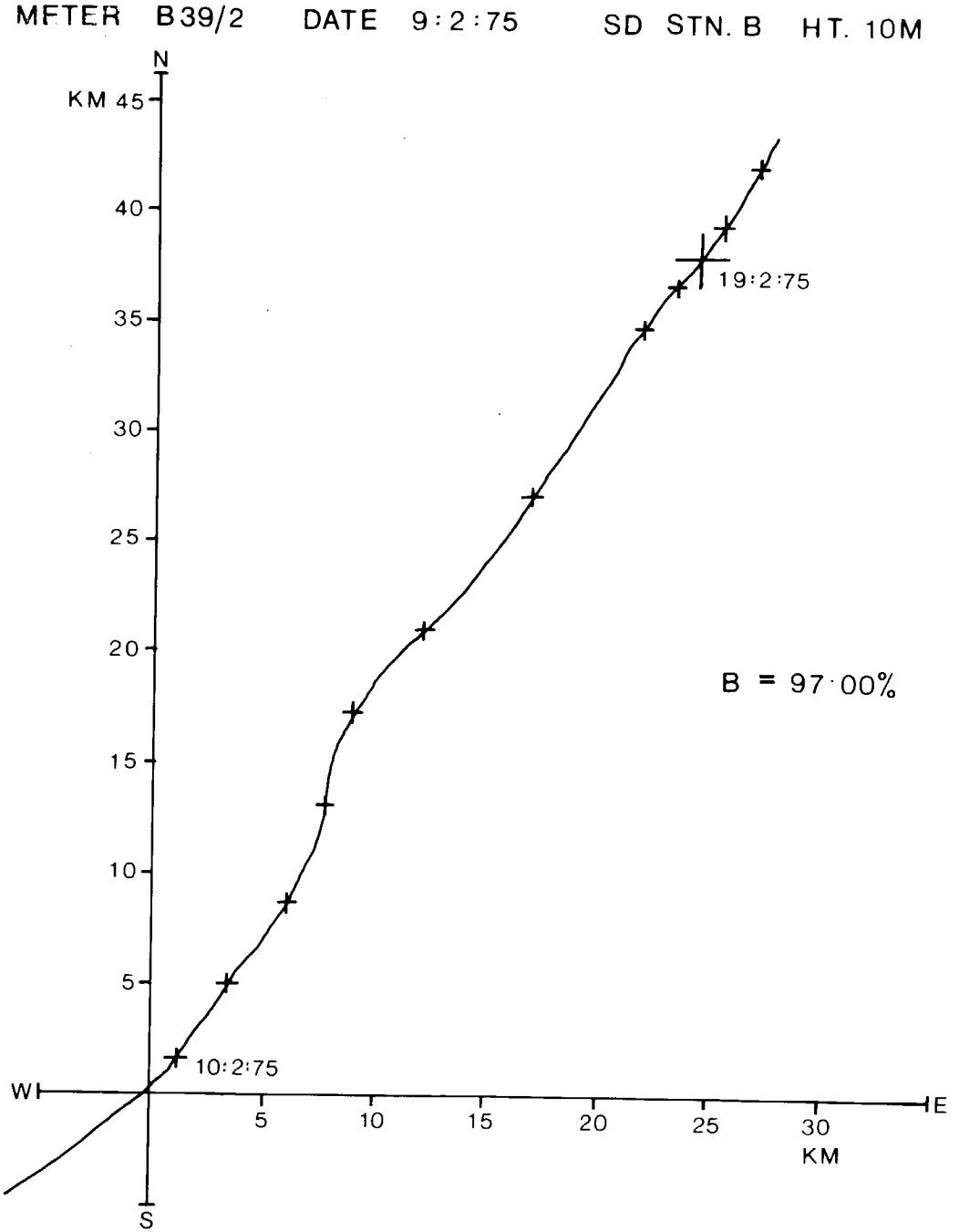
METER B39/2 DATE 9:2:75 SD STN. B HT. 10M
N
KM 45
40
35
30
25
20
15
10
5
19:2:75
B = 97·00%
10:2:75
W
E
S
5
10
15
20
25
30
KM

Figure A10

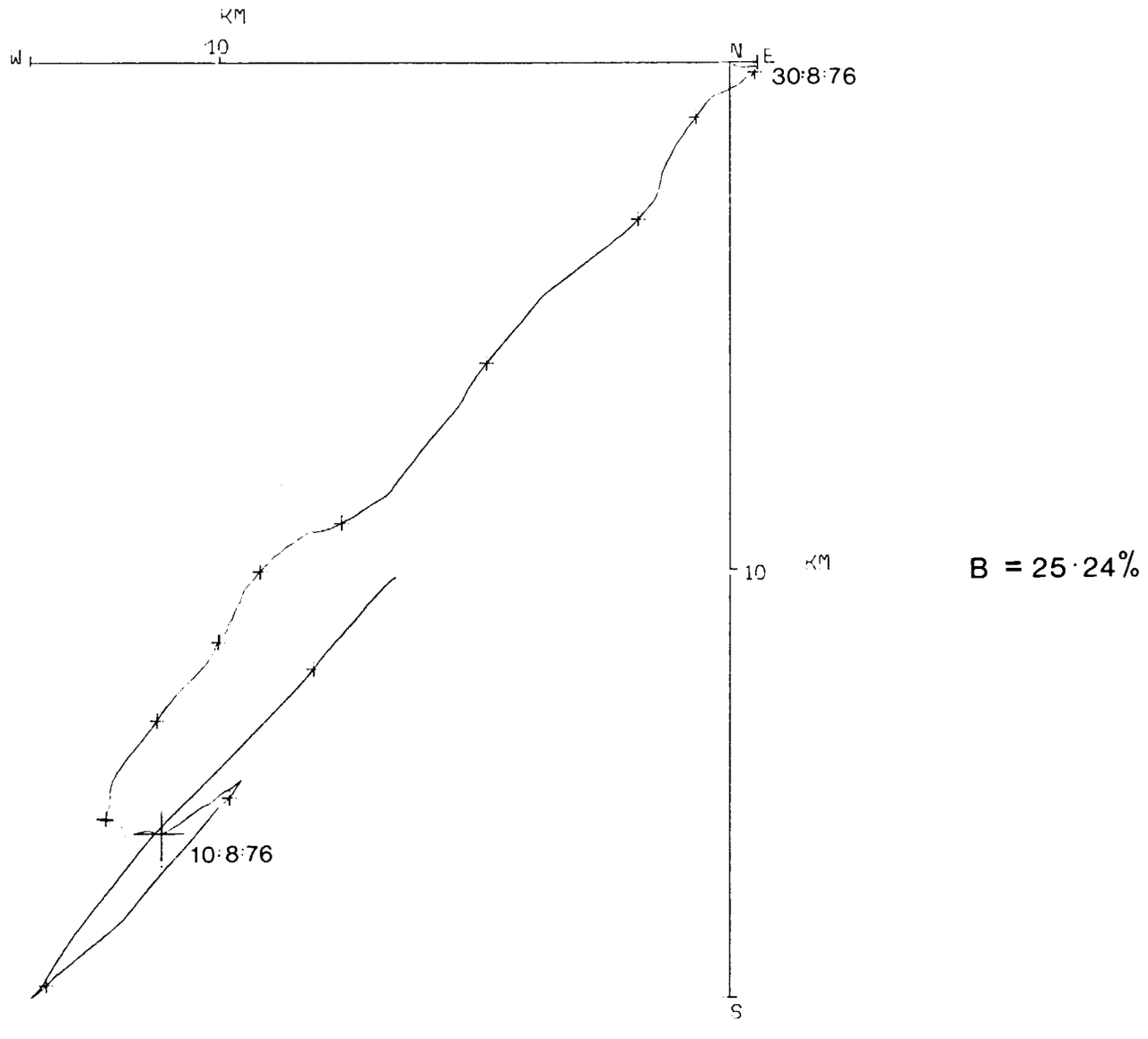

B = 25·24%

Figure A11

METER 669 DATE 17 8 78 SD STN. D HT. GM (PART A)

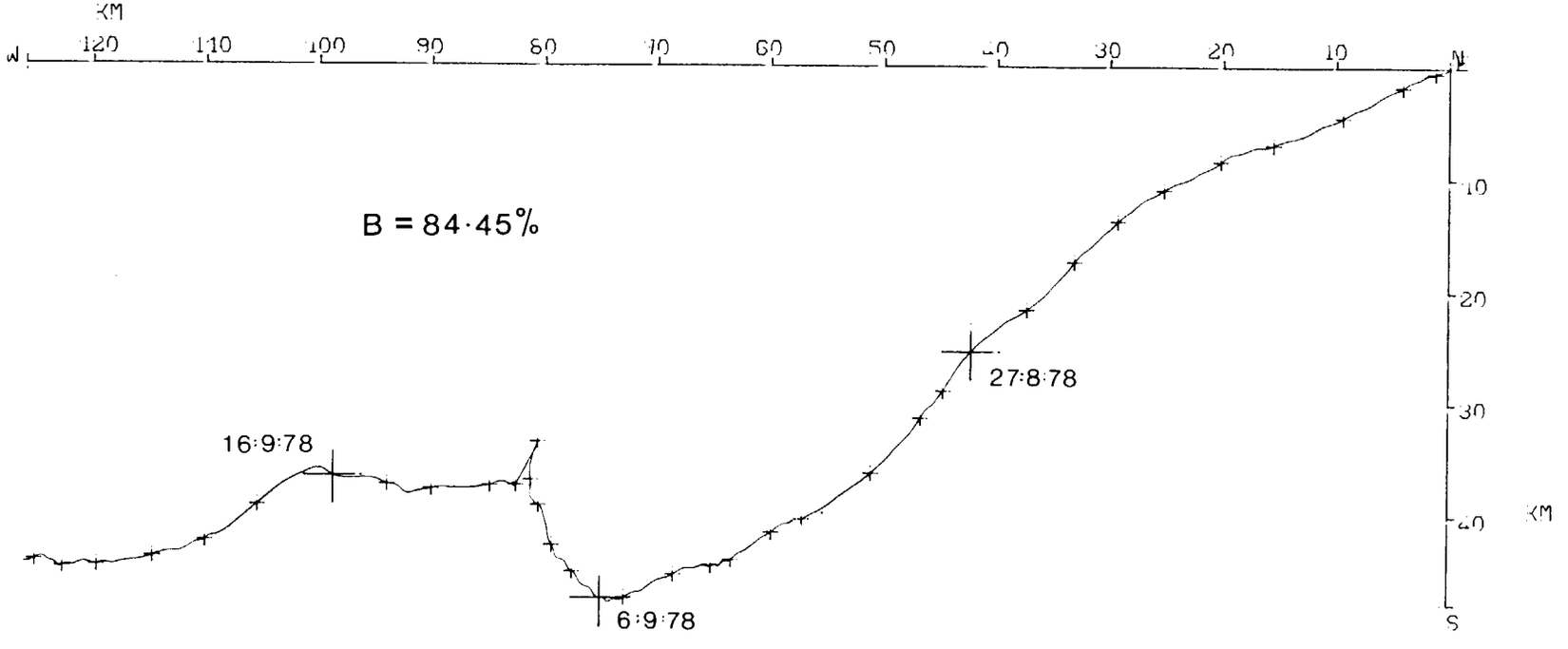

Figure A12

METER 669 DATE 1 10 78 SD STN.D HT.6M (PART B)

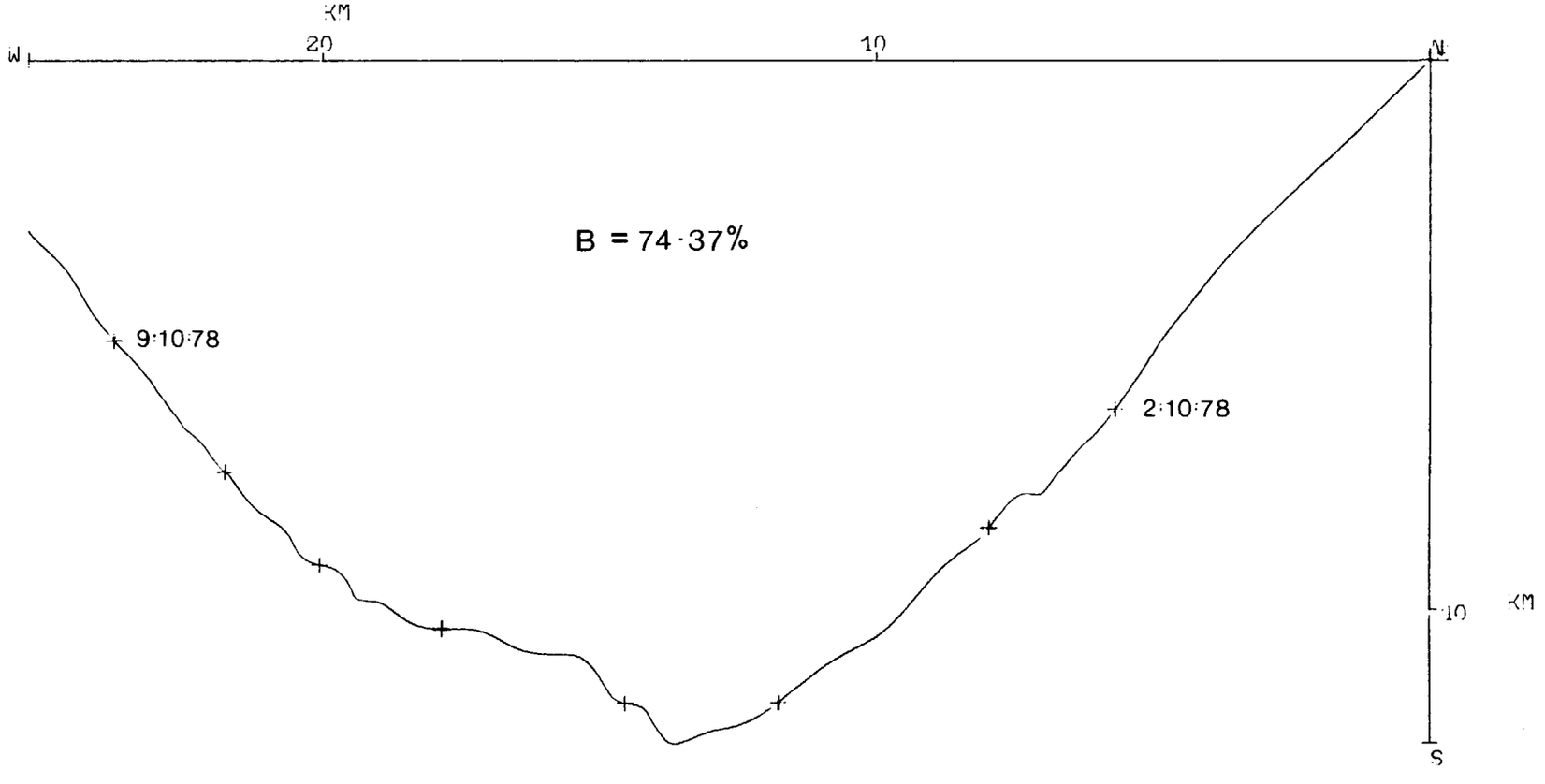

Figure A13

METER 667 DATE 29 8 76 SD STN. E HT. 7M

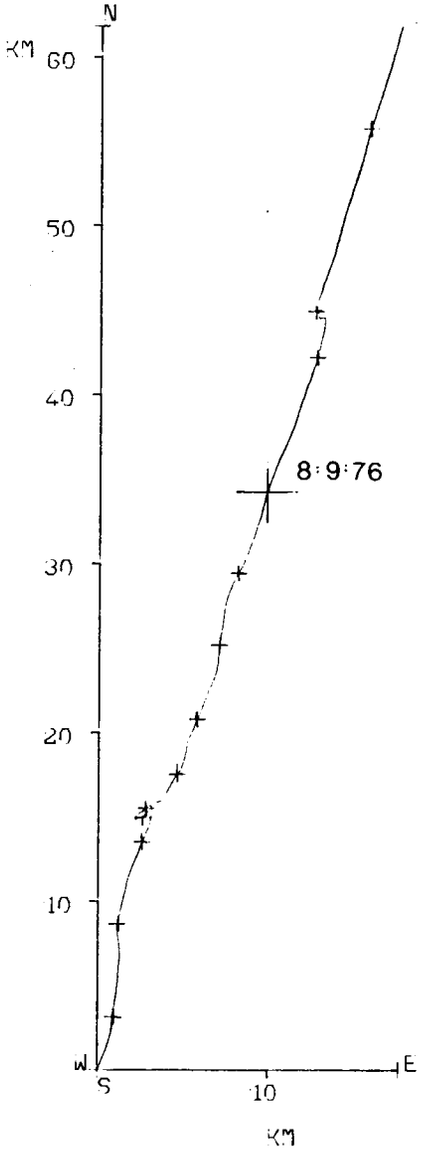

B = 91·43%

Figure A1.4

METER 232 DATE 17 7 77 SD STN. F HT. 8M

B = 85·19%

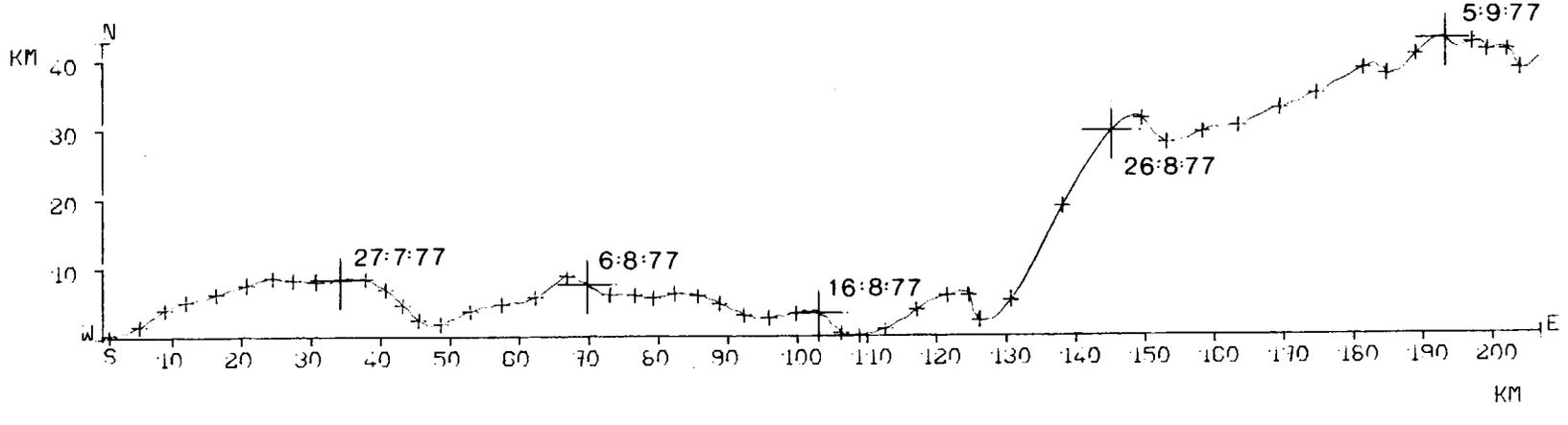

Figure A15

METER 534 DATE 19:4:75 SD STN.G HT. 6M

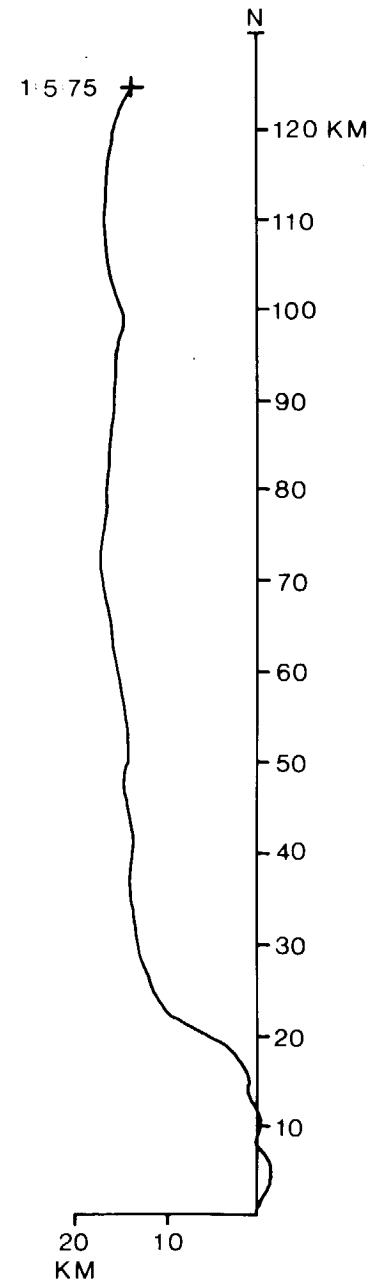

B = 94·00%

Figure A16


METER 680 DATE 19:4:75 SD STN. H HT. 6M
1:5:75
N
60 KM
50
40
30
20
10
B = 78·00%
W
30
20
10
KM

Figure A17

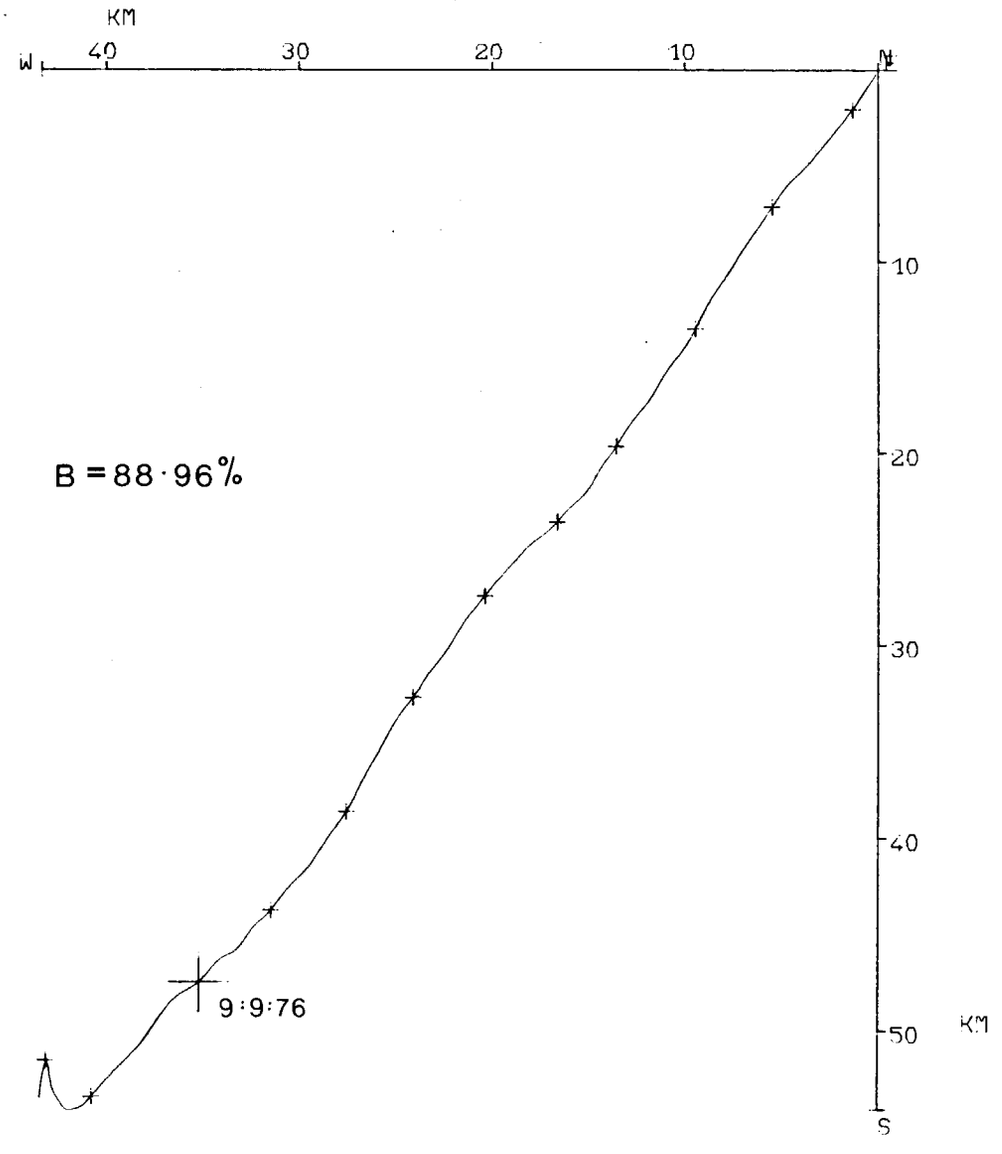
METER 626 DATE 30 8 76 SD STN. J HT. 4. 5M
KM
W
40
30
20
10
N
10
20
30
40
50
KM
S
B = 88·96%
9:9:76

Figure A18

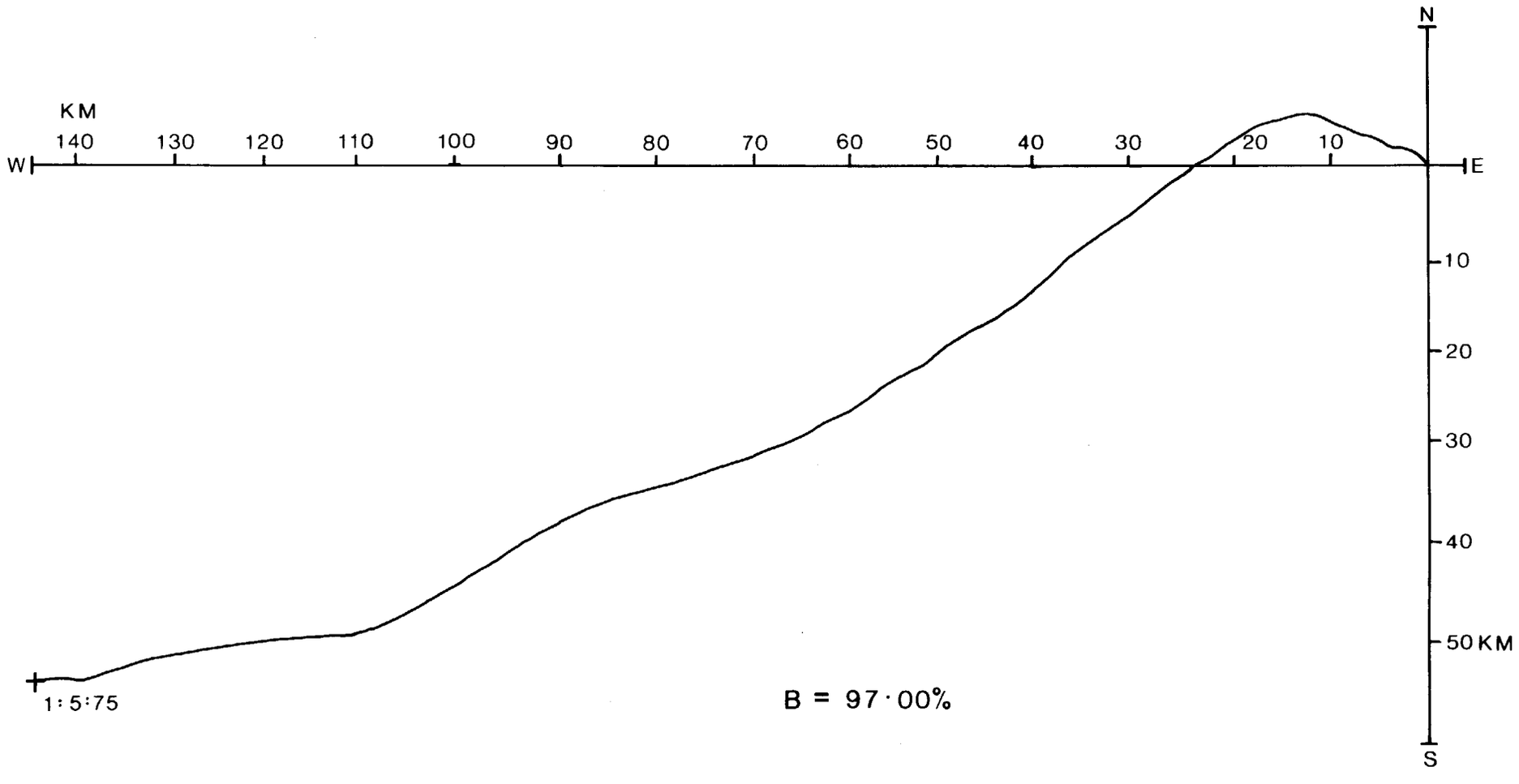
METER 556 DATE 19:4:75 SD STN.K HT. 6M
KM
140 130 120 110 100 90 80 70 60 50 40 30 20 10
W
E
N
S
10
20
30
40
50 KM
1:5:75
B = 97·00%

Figure A19

METER 295/C DATE 9:2:75 SD STN. L HT. 10M

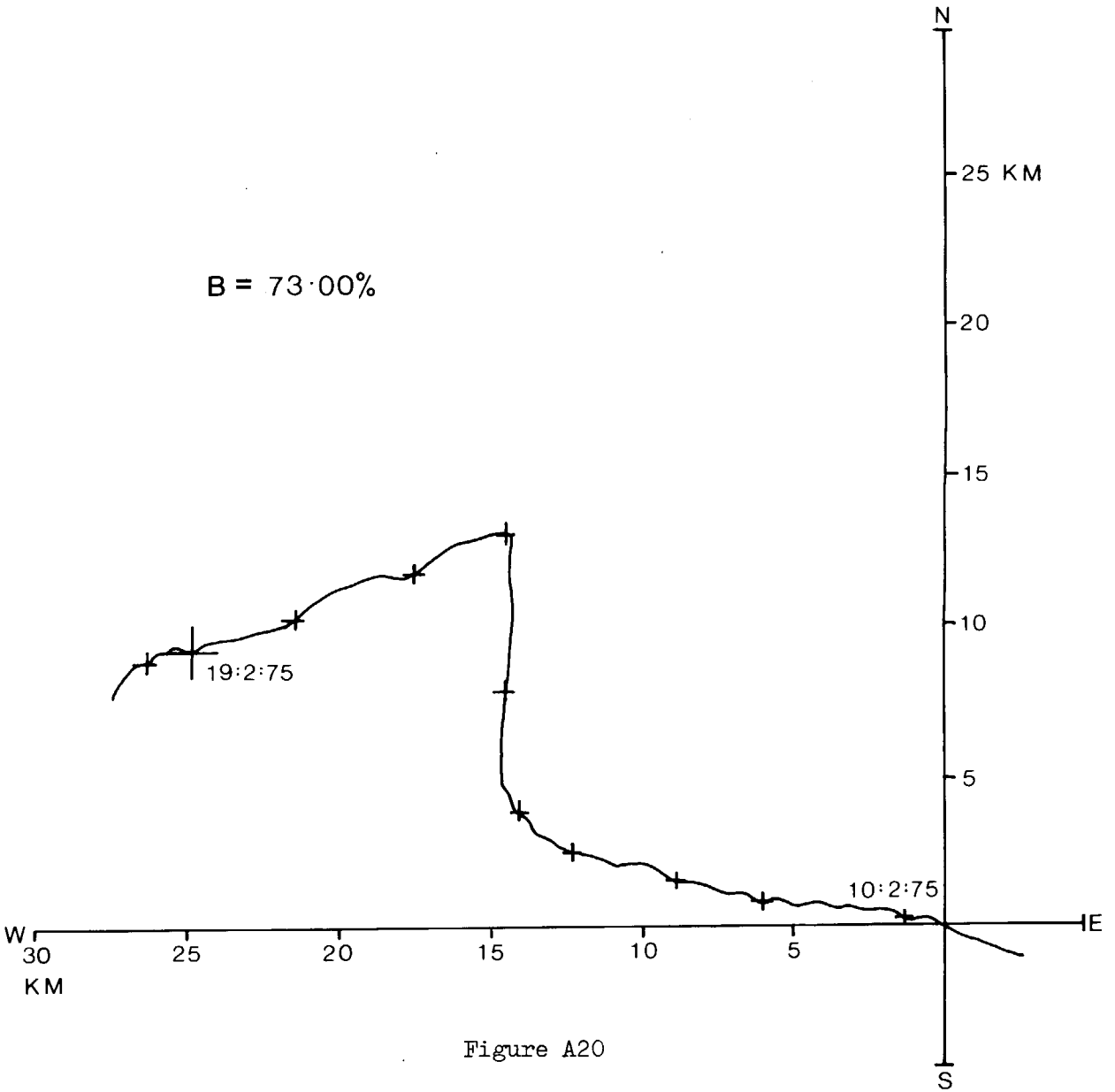

Figure A20

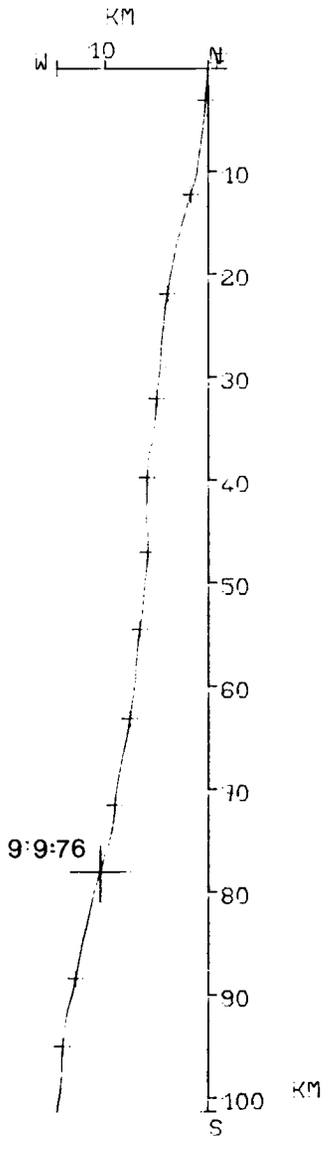

B = 99·56%

Figure A21

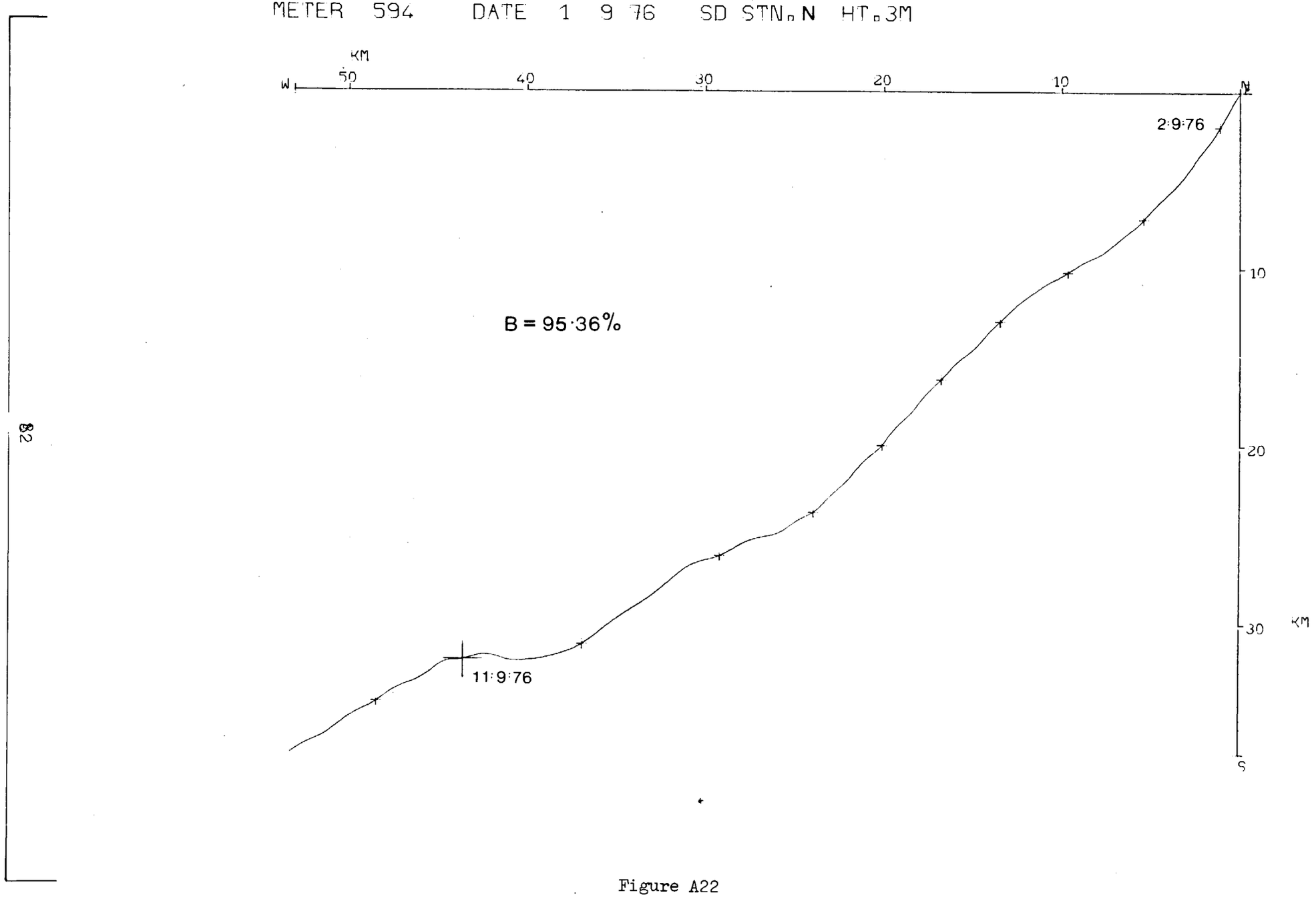
METER 594 DATE 1 9 76 SD STN. N HT. 3M
KM
W
50
40
30
20
10
N
2·9·76
B = 95·36%
11·9·76
10
20
30
KM
S
82

Figure A22

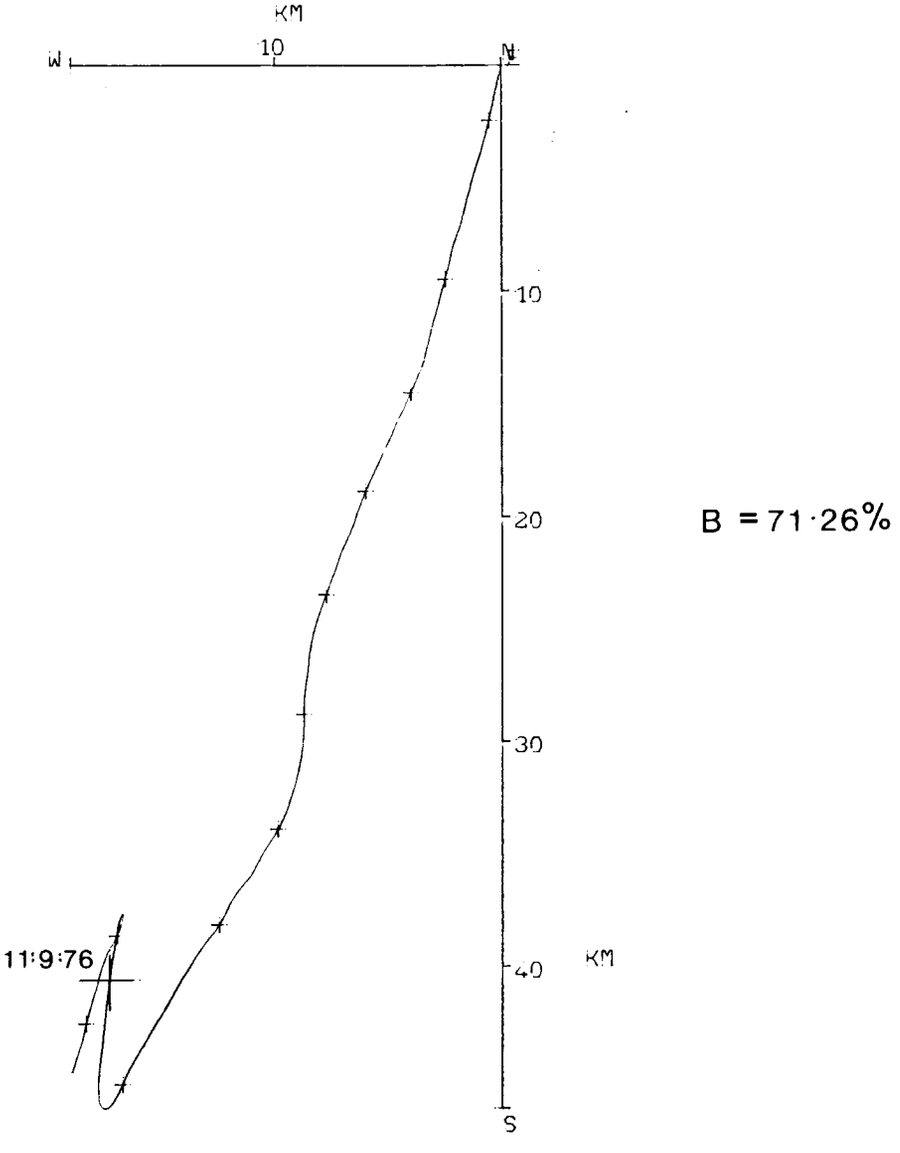

B = 71·26%

Figure A23

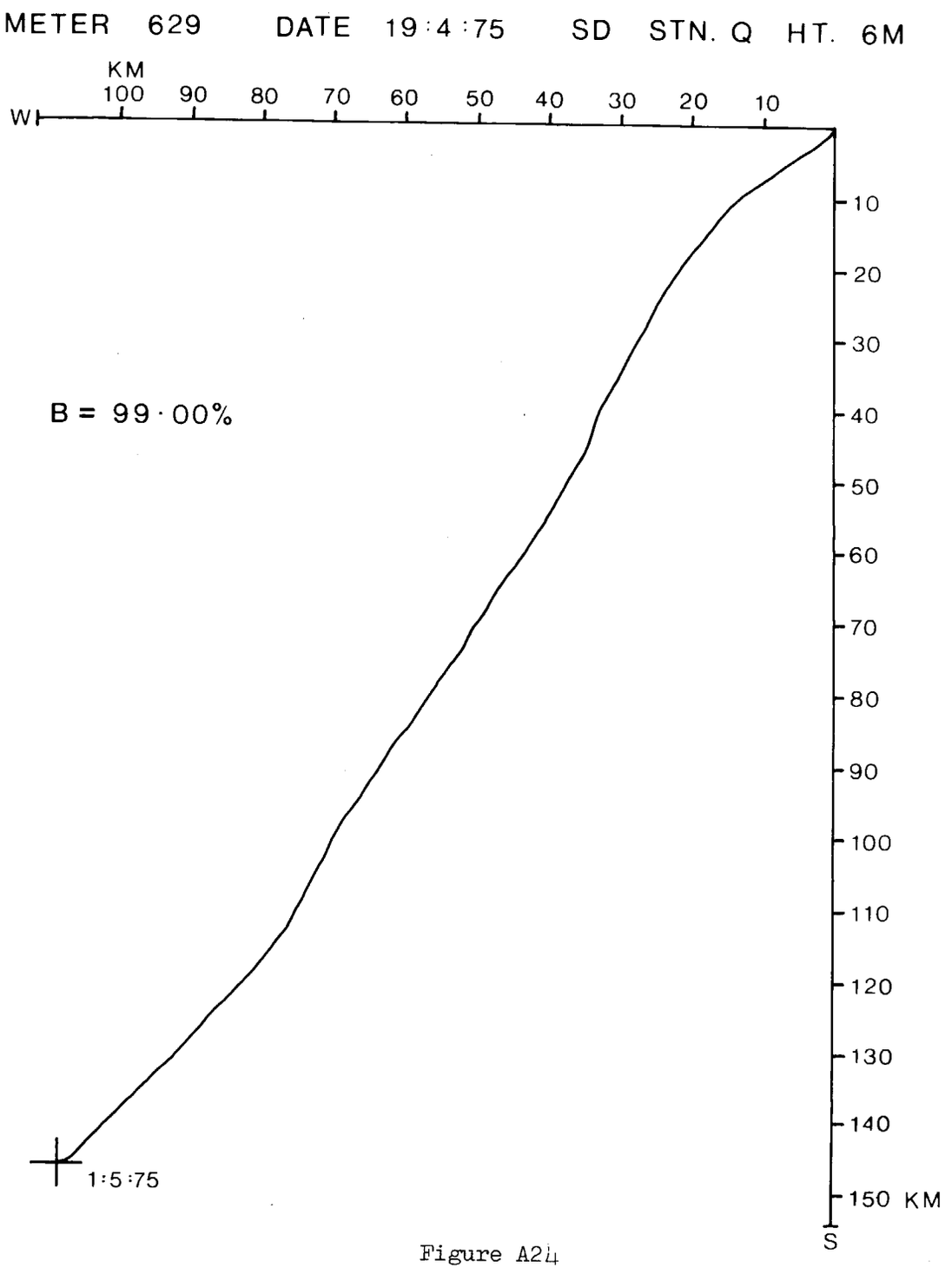
METER 629 DATE 19:4:75 SD STN. Q HT. 6M
KM
100 90 80 70 60 50 40 30 20 10
W
10 20 30 40 50 60 70 80 90 100 110 120 130 140 150 KM
S
B = 99·00%
1:5:75

Figure A2.4

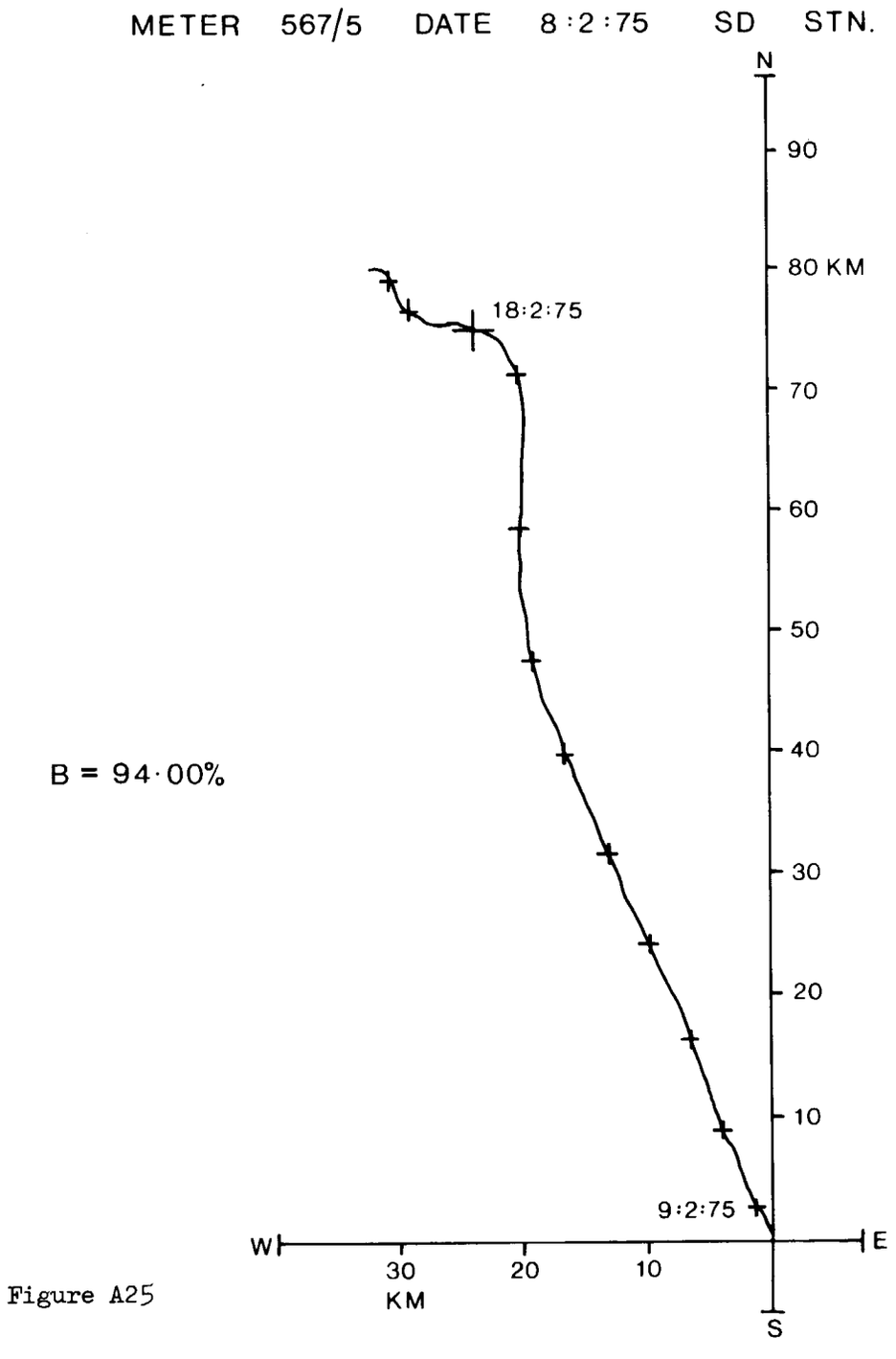
METER 567/5 DATE 8:2:75 SD STN. R HT. 10M
N
90
80 KM
70
60
50
40
30
20
10
18:2:75
9:2:75
B = 94·00%
W
E
S
30
20
10
KM

Figure A25

METER 232 DATE 30 8 76 SD STN. S HT. 6M

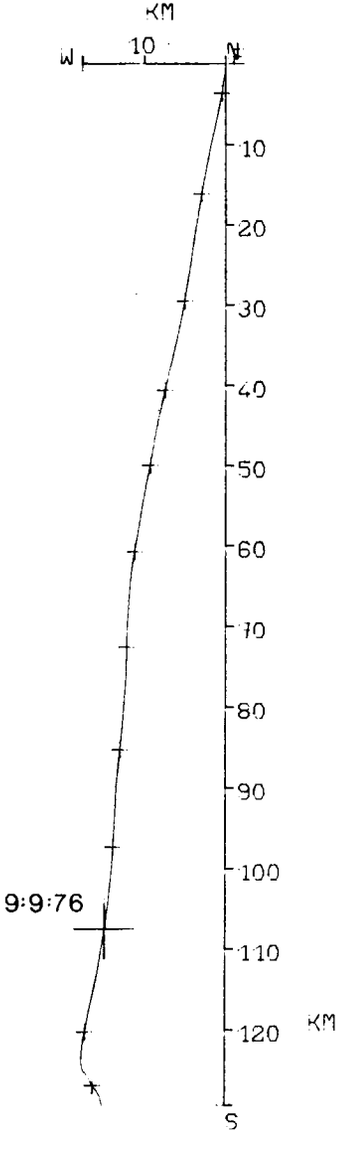

B = 99·21%

Figure A26

METER 570/6 DATE 8 : 2 : 75 SD STN. T HT. 10M

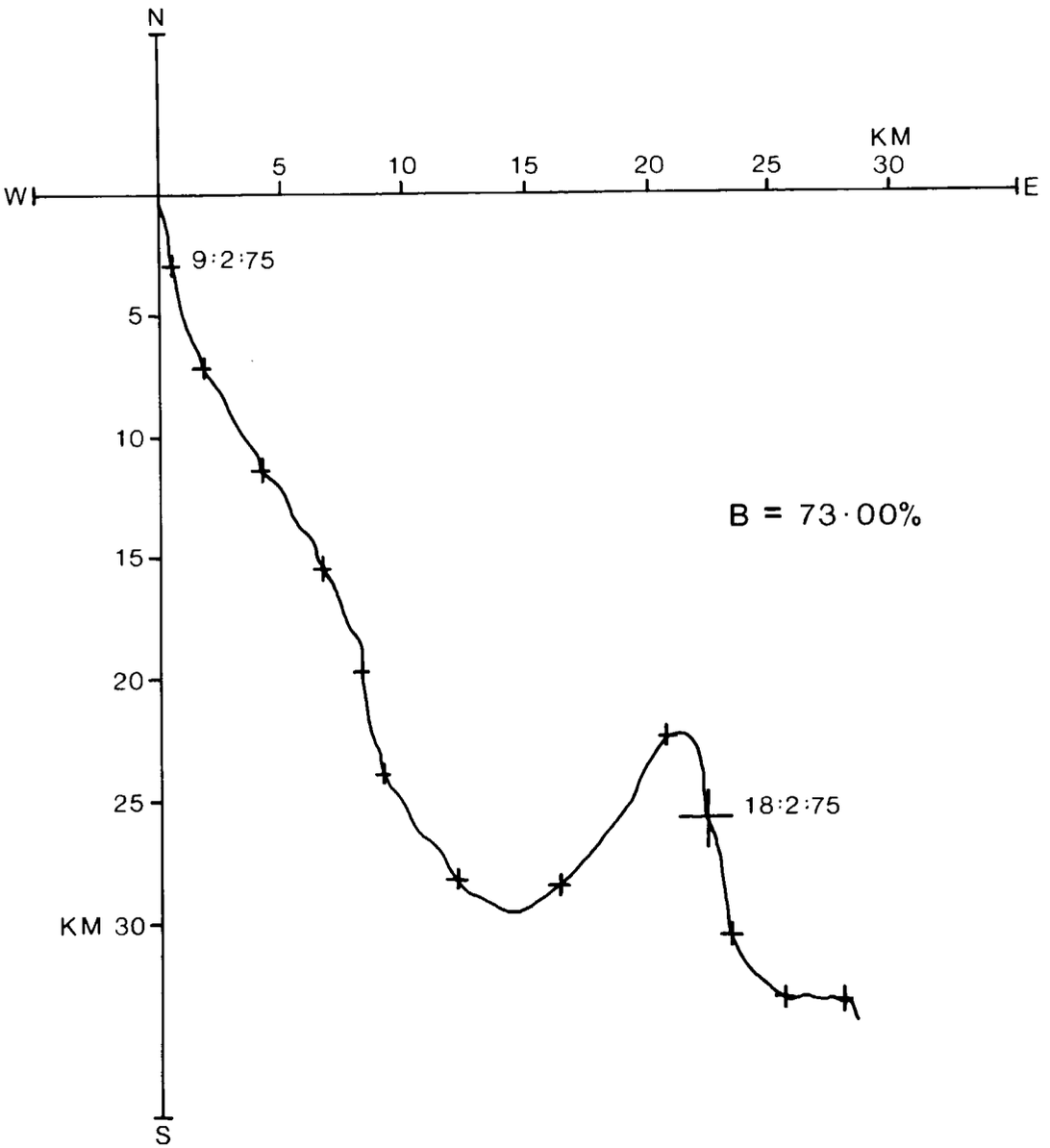

Figure A27

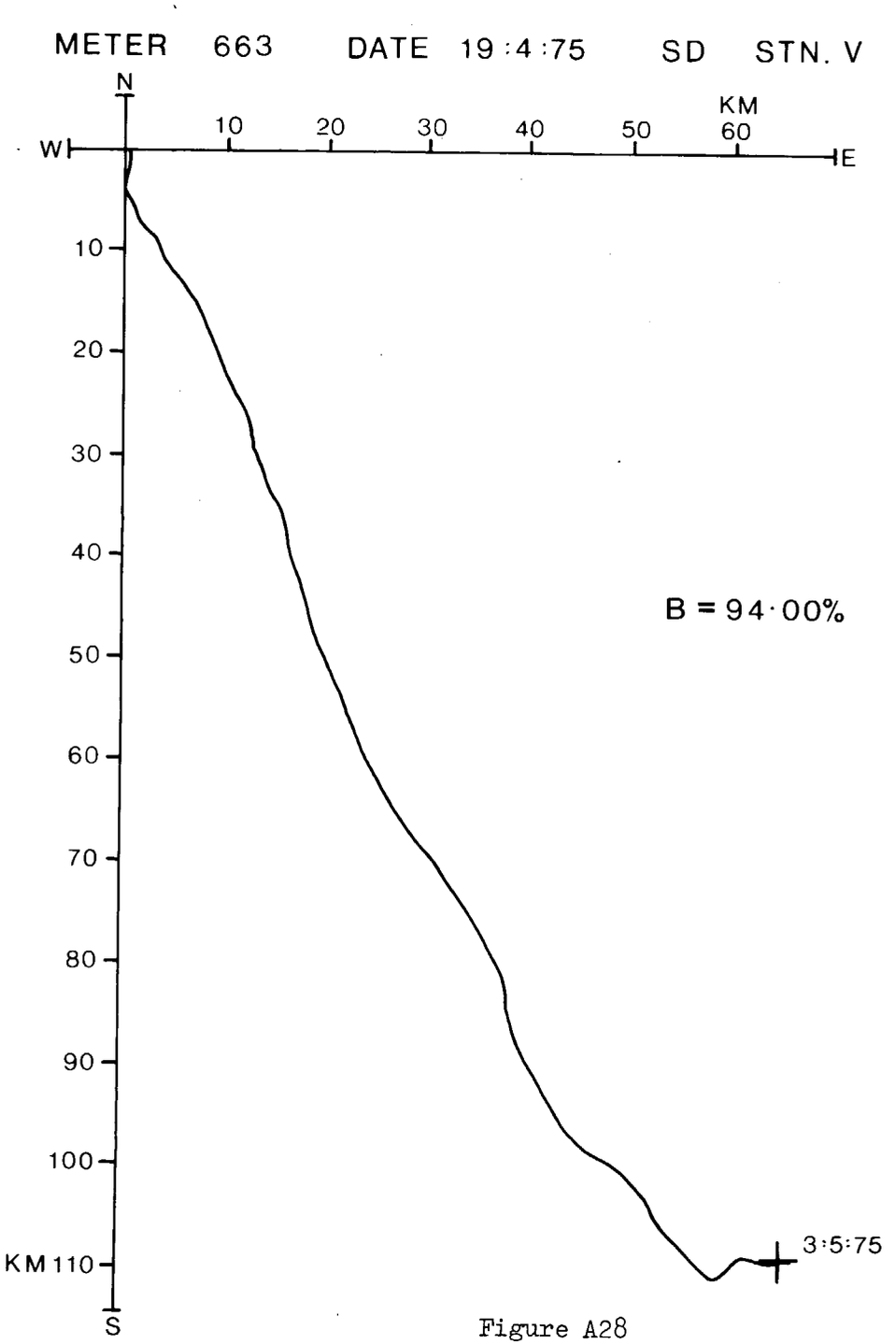
METER 663 DATE 19:4:75 SD STN. V HT. 6M
N
W
E
S
10
20
30
40
50
60
KM
10
20
30
40
50
60
70
80
90
100
KM 110
B = 94·00%
3:5:75

Figure A28

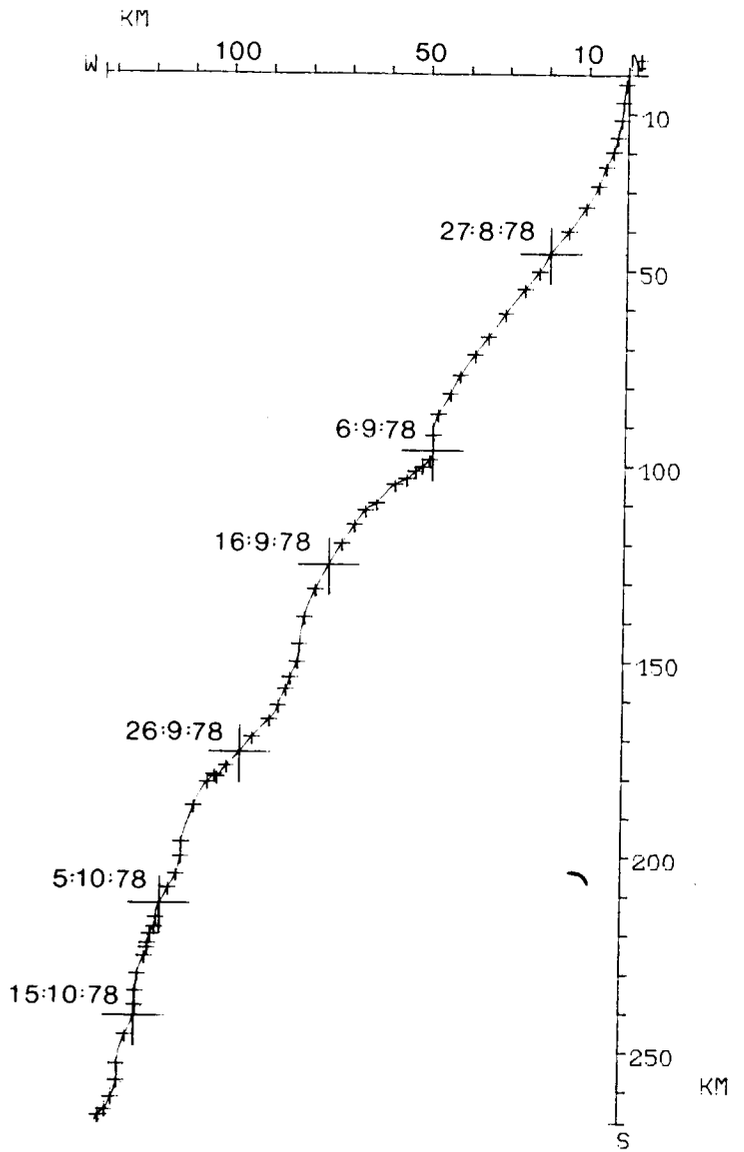

B = 95·29%

Figure A29

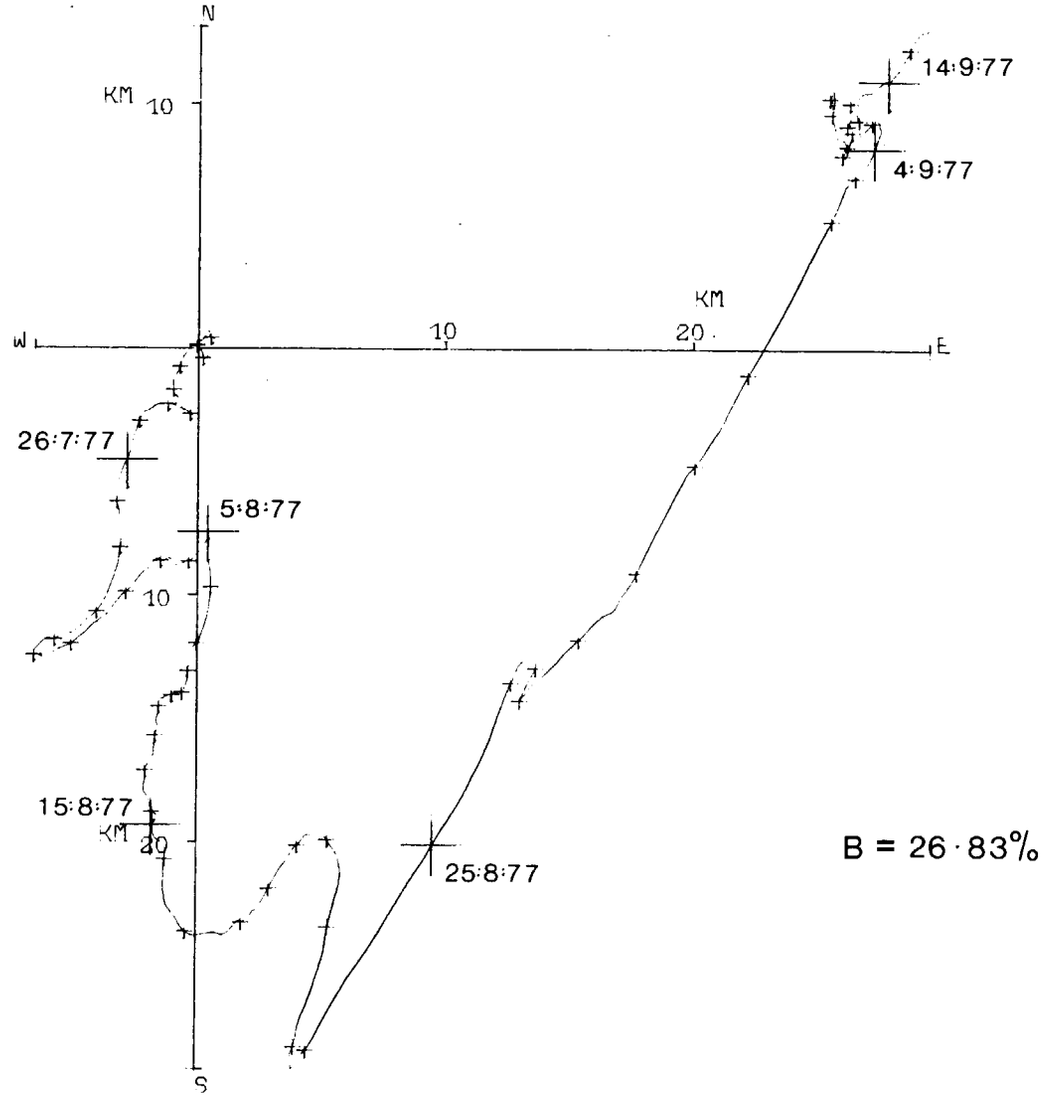
METER 560 DATE 16 7 77 SD STN. X HT. 6M
N
KM 10
W
10
KM
20
E
S
14:9:77
4:9:77
26:7:77
5:8:77
10
15:8:77
KM 20
25:8:77
B = 26·83%

Figure A30

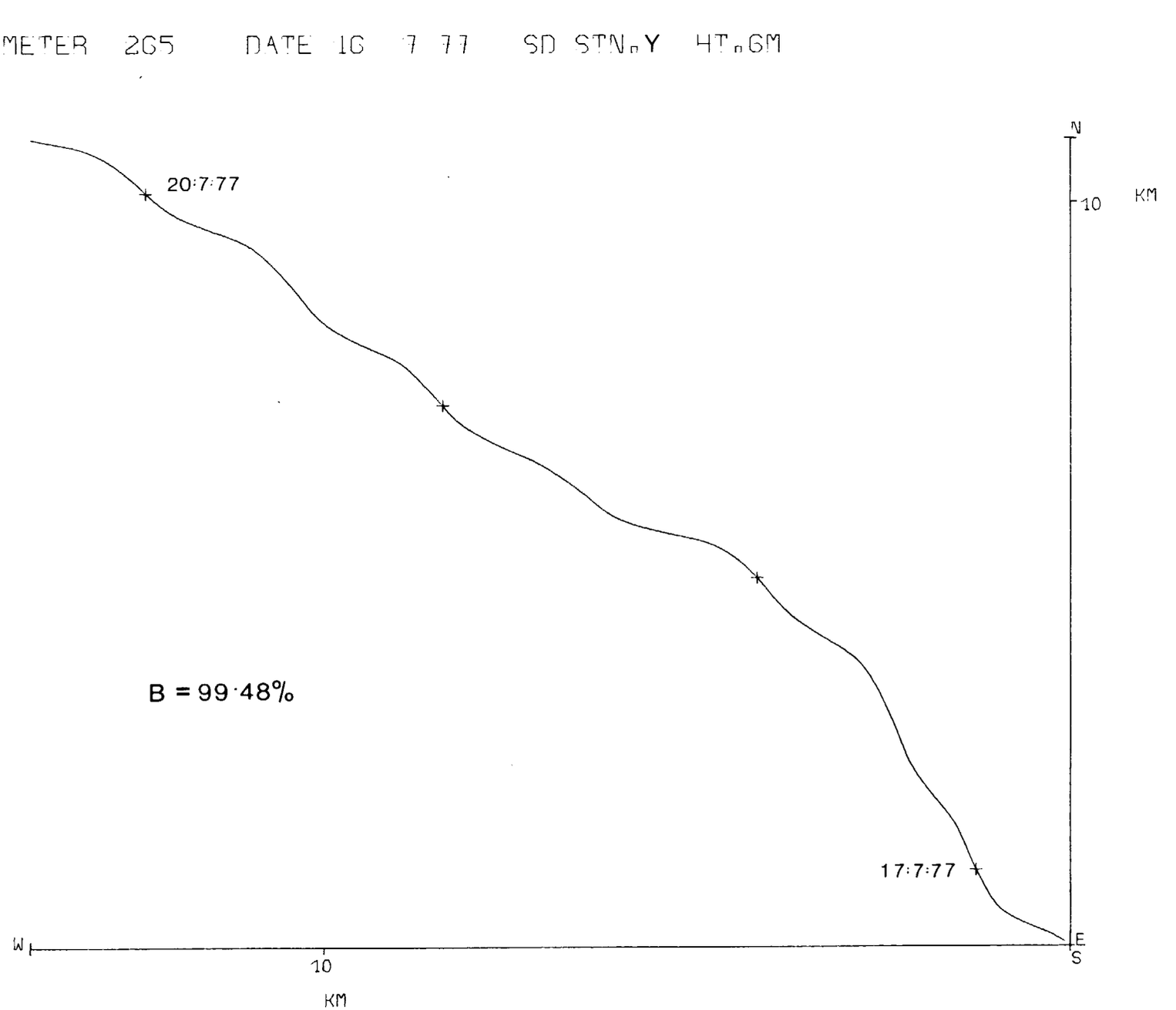
METER 265 DATE 16 7 77 SD STN. Y HT. 6M
N
10
KM
20:7:77
B = 99·48%
17:7:77
W
E
S
10
KM

Figure A31

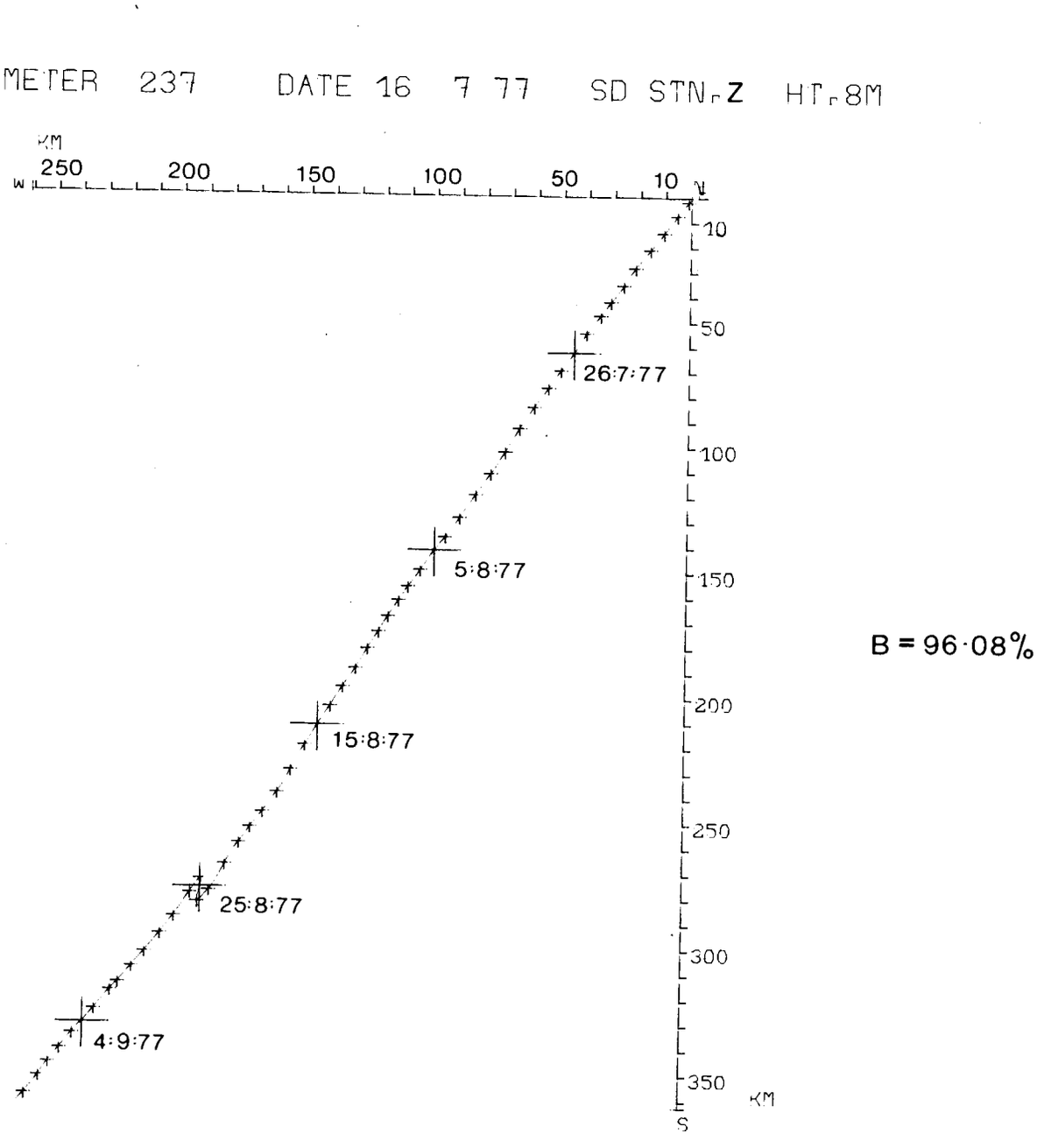

B = 96·08%

Figure A32